INFORMATION TO USERS

This manuscript has been reproduced from the microfilm master. UMI films the text directly from the original or copy submitted. Thus, some thesis and dissertation copies are in typewriter face, while others may be from any type of computer printer.

The quality of this reproduction is dependent upon the quality of the copy submitted. Broken or indistinct print, colored or poor quality illustrations and photographs, print bleedthrough, substandard margins, and improper alignment can adversely affect reproduction.

In the unlikely event that the author did not send UMI a complete manuscript and there are missing pages, these will be noted. Also, if unauthorized copyright material had to be removed, a note will indicate the deletion.

Oversize materials (e.g., maps, drawings, charts) are reproduced by sectioning the original, beginning at the upper left-hand corner and continuing from left to right in equal sections with small overlaps.

ProQuest Information and Learning
300 North Zeeb Road, Ann Arbor, MI 48106-1346 USA
800-521-0600

INTERACTIONS BETWEEN TWO DIFFERENT SURFACTANTS IN MIXED MONOLAYERS AT VARIOUS INTERFACES AND IN MIXED MICELLES

by

QIONG ZHOU

A dissertation submitted to the Graduate Faculty in Chemistry
in partial fulfillment of the requirements for the degree of

Doctor of Philosophy

The City University of New York

2003

UMI Number: 3083723

ProQuest Information and Learning Company
300 North Zeeb Road
P.O. Box 1346
Ann Arbor, MI 48106-1346

This manuscript has been read and accepted for the Graduate Faculty in Chemistry in satisfaction of the dissertation requirement for the degree of Doctor of Philosophy.

4/14/03
Data

Chair of Examining Committee

4/14/03
Date

Executive Officer

Alexander Green

David C. Locke

Supervisory Committee

The City University of New York

ABSTRACT

Interactions Between Two Different Surfactants in Mixed Monolayers at Various Interfaces and in Mixed Micelles

by

Qiong Zhou

Advisor: *Professor Milton J. Rosen*

The relationship between the interaction between the same two surfactants in a mixed monolayer at the air/aqueous solution interface (β^{σ}) and their interaction in a mixed micelle in the aqueous phase (β^{M}) was investigated. It is shown that the relative strengths of the interactions at the interface and in the micelle in the anionic – polyoxyethylene (POE) nonionic surfactant mixtures are determined by the branching and bulkiness of the hydrophobic and hydrophilic groups of the surfactants in the mixture. Interaction in the mixed micelle is reduced by branching in the hydrophobic group in either surfactant of the mixture. Branching close to the hydrophilic group of the anionic surfactant in the mixture reduces the interactions both in the mixed micelle (β^{M}) and in the mixed monolayer. Interaction in the anionic – POE nonionic mixed micelle is sharply enhanced by an increase of the oxyethylene units in the POE group of the nonionic surfactant of the mixture.

Regular solution theory has been used to explain the values of surfactant molecular interaction (β) parameters observed in mixed monolayers and mixed

micelles. Reduction in electrostatic self-repulsion interaction energy of the ionic surfactant, due to the dilution effect upon mixing, is suggested as a major contributor to the negative β values observed for mixed monolayers and mixed micelles. Steric effects appear when surfactant molecular structure varies in the size of the head groups and in the branching of the hydrophobic groups. Bulkiness due to branching in the hydrophobic group of the ionic surfactant decreases electrostatic self-repulsion before mixing with a nonionic surfactant having a linear hydrophobic group. Branching in the hydrophobic group of a POE nonionic surfactant results in slightly more negative β^{σ} values upon mixing with an anionic surfactant with a linear hydrophobic group, than with the corresponding linear hydrophobic chain nonionic surfactant.

Molecular interactions at the solid/aqueous solution interface (β_{SL}^{σ}) were also investigated. It is suggested that the observed spreading enhancement from mixed solutions on hydrophobic polyethylene film resulted from the stronger attractive interactions at the polyethylene / aqueous solution interface, as indicated by the negative β_{SL}^{σ} values, than that at the air / aqueous solution interface, as indicated by the small negative β_{LA}^{σ} values. Lower dynamic contact angles of the mixture than either of the components on hydrophobic polyethylene film, caused by adsorption enhancement and faster adsorption at the solid / aqueous solution interface after mixing, imply spreading enhancement for the mixture.

ACKNOWLEDGEMENTS

I wish to thank the members of my committee, Professor Alexander Greer for his kind advice and support during the course of my doctoral studies, Professor David Locke and Professor Zhen Huang for their valuable time and helpful suggestions to my research work.

Professor Milton J. Rosen served as my mentor and taught me invaluable lessons, both scientific and philosophic. He guided me through my whole doctoral studies, the enlightening conversations with him always inspired me and made me grow professionally. His dedication and enthusiasm has made deep impact in my future career. Professor Rosen, I can't thank you more.

Also, I would like to thank all the friendly people and co-workers in the Chemistry Department of Brooklyn College, for their generous help and support over the years.

TABLE OF CONTENTS

LIST OF TABLES

LIST OF FIGURES

Chapter 1

Introduction

1.1 Surfactants in Aqueous Solution

1.1.1 Surfactant's unique structure. Surfactants, as one of the most versatile products of the chemical industry, are often used for better performance, including: additives in cosmetics, enhanced oil recovery[1-6], industrial cleaning or laundry detergents, mineral flotation[7-11], environmental remediation[12-15] and medical applications via liposomes. The unique amphipathic molecular structure (Figure 1) is characteristic for all kinds of surfactants: one or more hydrophobic tails, either a long-chain hydrocarbon residue or a halogenated or oxygenated hydrocarbon or polysiloxane chain, and one or more hydrophilic head groups, either ionic or highly polar.

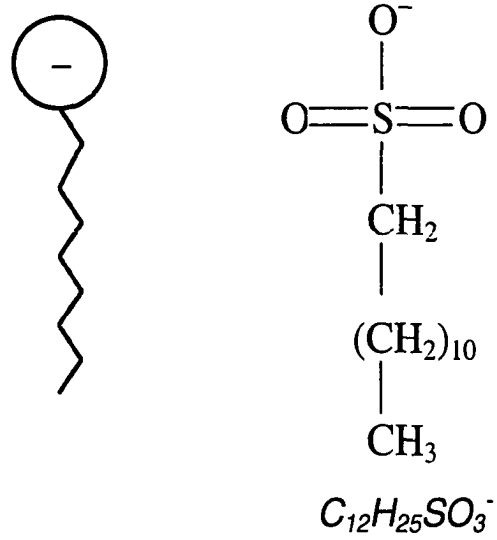

Figure 1. Characteristic molecular structure of surfactant

1.1.2 Surfactant's applications. Surfactant applications originate from the enhancement or modification of the desired properties in the solution or at the interface with the presence of surfactant molecules. Applications include: wetting and waterproofing[16-24], foaming and defoaming[25-30], emulsification and demulsification[31-34], dispersion, flocculation and adhesion[35,36], which are achieved by surfactant adsorption onto air/aqueous solution, liquid/aqueous solution or solid/aqueous solution interfaces; solubilization[37-41], microemulsion formation[42-49], and viscosity increase, which are achieved through the formation of micelles by surfactant aggregation in solution. Also, there are other applications, such as detergency, which require the modification of both the air/aqueous solution or solid/aqueous solution interfaces and of the bulk solution phase.

As early as 1806, Laplace suggested that the molecules within a liquid exert a more or less uniform attraction for each other, whereas the molecules at the surface are attracted uniformly downward and sideways, but are attracted upward much less strongly because of the smaller number of molecules in the vapor phase. The pressure difference across a curved interface due to the surface or interfacial tension of the solution is quantitatively described by the Laplace equation:

$$\Delta P = \gamma(\frac{1}{R_1} + \frac{1}{R_2}) \qquad (1)$$

where R_1 and R_2 are the radii of curvature of the interface. This equation has been used to account for many familiar phenomena at the boundary surface: the

existence of a meniscus, the rise or fall of a liquid in a vertical capillary tube, and the tendency of a drop of liquid to assume a spherical form.

1.1.3 Surfactant adsorption at air/aqueous solution interface. Surfactants (a contraction of surface-active-agent) when dissolved in a solvent (most often H_2O), usually decrease the surface tension in a dramatic manner. Why is surface tension decreased with the addition of surfactants? When surfactant molecules are dissolved in water, due to the presence of their hydrophobic tails, there exists some distortion of the iceberg structure of the water caused by contact with the hydrophobic groups. This distortion increases the free energy of the system. To minimize the distortion and the free energy increase, surfactant molecules will be arranged in two different ways at low concentrations. (1) Surfactant molecules migrate to the interface and orient their hydrophobic groups away from solvent water, avoiding contact between water molecules and surfactant hydrophobic groups. This is the process of adsorption. At higher concentrations, (2) surfactant molecules aggregate to form micelles or vesicles, the process of micellization (Figure 2). With the free energy decrease resulting from spontaneous adsorption, less work is needed to bring surfactant molecules to the surface, therefore, less work is needed to create unit area of surface (lower surface tension).

The dependence of surface or interfacial tension on the amount of surfactant in the solution phase is described by the Gibbs adsorption equation[50]:

$$d\gamma = -\sum_i \Gamma_i d\mu_i$$

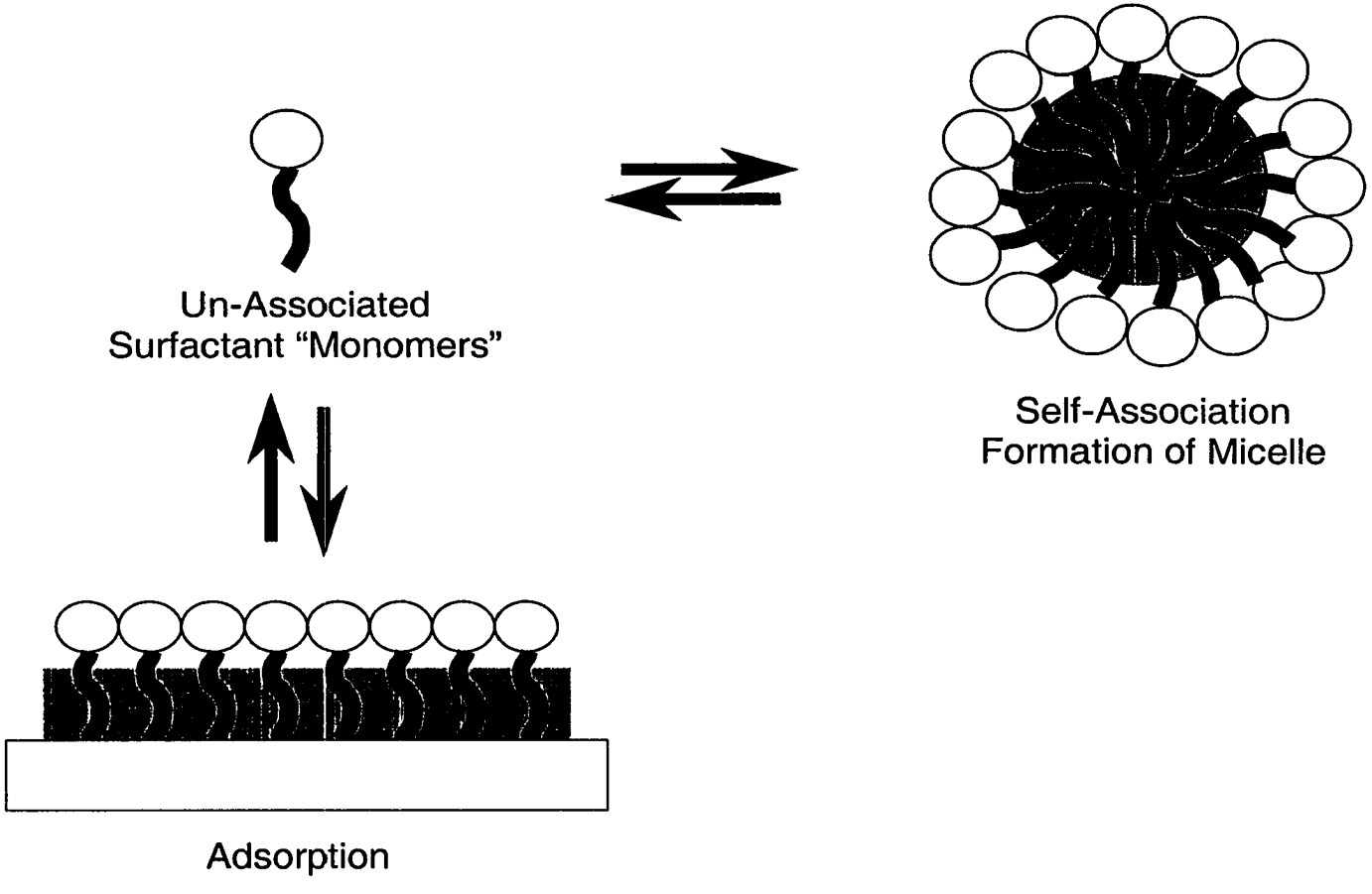

Figure 2. Scheme of three different ways to minimize distortion between water molecule and dissolved surfactants.

where $d\gamma$ = the change in surface or interfacial tension of the solvent,

Γ_i = the surface excess concentration of any component of the system,

$d\mu_i$ = the change in chemical potential of any component of the system.

At equilibrium between the interfacial and bulk phase concentrations, $d\mu_i = RTd\ln a_i$, where a_i is the activity of any component in the bulk (liquid) phase, R is gas constant, and T is the absolute temperature.

A typical equilibrium surface tension (γ) versus log bulk surfactant molar concentration (C) plot is shown in Figure 3. From this curve, several key surfactant properties can be determined. The break point in the curve indicates the concentration at which surfactant molecules begin to aggregate and form colloidal-sized clusters known as micelles. This special concentration is called the critical micelle concentration (CMC) of the surfactant. The corresponding surface tension at this concentration, symbolized by γ_{CMC}, indicates the effectiveness of surface tension reduction by this surfactant. The concentration at which surface tension has been reduced by 20 mN/m, compared to pure solvent, is called C_{20}. When the surface tension is decreased by 20, the air/aqueous solution interface would normally be 80% to 100% covered by surfactant molecules. Thus C_{20} indicates the efficiency of surface tension reduction by this surfactant. Surface excess concentrations (Γ) in mol/cm^2 and minimum area per molecule (A_{min}) in Å^2 at the air/aqueous solution interface are calculated from equations 2 and 3,[51a]

$$\Gamma_{max} = -\frac{1}{2.303nRT}\left(\frac{\partial\gamma}{\partial \log C}\right)_{T,max} \qquad (2)$$

$$A_{min} = \frac{10^{16}}{N\Gamma} \qquad (3)$$

where $(\partial\gamma/\partial \log C)_{T,max}$ is the maximal slope in the γ vs. log C plot; T is the absolute temperature, R=8.314 $J \bullet mol^{-1} \bullet K^{-1}$, and N is Avogadro's number. For solutions containing a single surfactant, n is the number of species whose interfacial concentration changes with change in the bulk phase concentration of the surfactant.

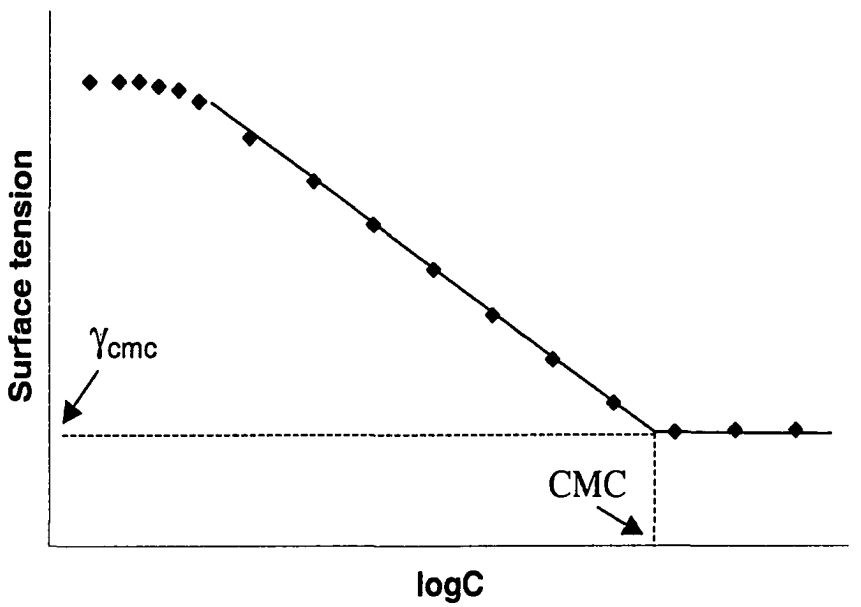

Figure 3. Plot of surface tension versus log of the bulk phase concentration for an aqueous solution of a surfactant.

From Figure 3, we notice that even when the maximal surface excess concentrations (Γ_{max}), as calculated from the slope of the curve, have been reached (and Γ_{max} usually indicates a complete monolayer coverage of the air /

aqueous solution interface by surfactant molecules), the surface tension of the surfactant solution keeps decreasing. This has been ascribed to the increase in the activity of the surfactant in the solution phase (when the solution is dilute, it is equal to its molar concentration). When the surfactant concentration is high enough, surfactant molecules aggregate to form micelles. Since at that concentration the surfactant monomeric concentration does not increase significantly, the surface tension reaches its minimum value around the CMC and doesn't decrease significantly with the increase of surfactant concentration. Monolayer adsorption is common in surfactant adsorption at the air/aqueous solution interface, and in surfactant adsorption onto the solid / aqueous solution interface, when the solid has a nonpolar, hydrophobic surface, such as hydrophobic carbon and polyethylene or polypropylene. The corresponding adsorption isotherms for this kind of surfactant adsorption are of the Langmuir type, as shown in Figure 4.

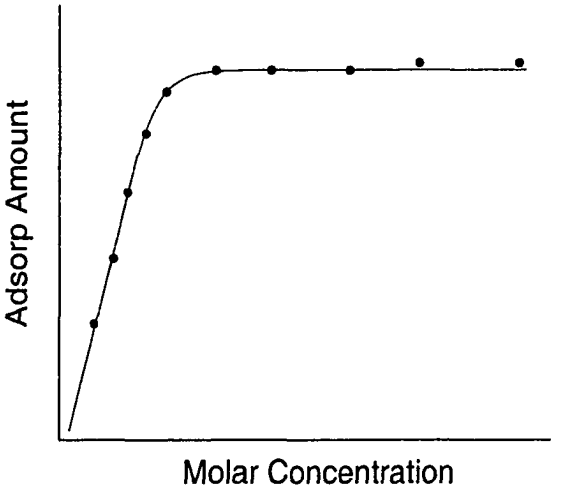

Figure 4. Langmuir-type adsorption isotherm of surfactant on a nonpolar, hydrophobic surface.

1.1.4 Langmuir adsorption at solid/aqueous solution interface. The Langmuir-type isotherm (Langmuir, 1918) is expressed by

$$\Gamma_{SL} = \frac{C_{eq}}{C_{eq} + a}\Gamma_{SL}^{m} \qquad (4)$$

where Γ_{SL} = the surface concentration of the surfactant, in units of mol/cm^2,

Γ_{SL}^{m} = the maximum surface concentration of the surfactant, in units of mol/cm^2, at monolayer adsorption,

C_{eq} = the concentration of the surfactant in the liquid phase at adsorption equilibrium, in units of mol/L,

a = a constant $[= 55.3\exp(\Delta G^0 / RT)]$, in units of mol/L, at absolute temperature T, and ΔG^0 is the adsorption free energy at infinite dilution.

This type of adsorption is valid in theory only under the following conditions:

1. The adsorbent is of homogeneous surface energy.
2. Both solute and solvent have equal molar surface areas.
3. Both surface and bulk phase exhibit ideal behavior, e.g., no solute-solute or solvent-solvent interactions in either phase.
4. The adsorption film is a monolayer.

Many surfactant solutions show Langmuir-type behavior, even when these restrictions are not met[51b].

1.1.5 Modern instrumental approach to surfactants. Modern instruments have more and more often been utilized in the investigation of surfactants, even though properties of surfactants are still well studied by some traditional

methods, such as surface/interfacial tension, phase diagrams, electrical conductivity, light scattering, etc. NMR chemical shift change due to the formation of micelles[52-61], can be used to check critical micelle concentrations by applying the pseudophase separation model for micellization. Surfactant aggregation number can be calculated from the NMR chemical shift change by applying the mass action model for micellization. Also, NMR has been used to study surfactant solution phase behavior and molecular conformation in the micelle. FTIR has been used in study surfactant adsorption at the solid/liquid interface, and surfactant solubilization by regular or reverse micelles[62-67]. Also, it has been utilized to check the CMC and to study surfactant solution phase behavior. Both steady state and time-resolved fluorescence spectroscopy[68-73], and small-angle neutron scattering[74-79] have been used to measure surfactant aggregation number.

1.2 Molecular Interaction in Mixed Monolayers at the Air / Aqueous Interface and in Mixed Micelles in Aqueous Solution

1.2.1 Molecular interaction parameters (β). Surfactant systems used for practical applications consist of mixtures of surfactants, either because commercial surfactants are always mixtures due to the raw materials used and method of manufacture, or because mixtures of surfactants often show better performance properties than those of individual ones.[80-84] Because of this, there has been considerable research on the molecular interactions between different surfactants in their binary mixtures, particularly as it relates to the existence of synergy between them. Several molecular – thermodynamic theories have been

developed recently by different investigators, for predicting properties of and interactions in binary surfactant systems.[85-88] However, use of these theories involves knowledge or calculation of the values of various physical – chemical parameters, some of which are not readily obtained. As a result, molecular interactions between two surfactants at an interface or in micelles are commonly measured by the so-called beta parameters,[89-95] which are conveniently obtained from surface (or interfacial) tension or from critical micelle concentration data by use of equations 5 – 8.

Equilibrium surface tension (γ) versus log bulk surfactant molar concentration (C) plots for some ionic – nonionic binary surfactant systems and their individual surfactants are shown in Figure 5. Surface excess concentrations (Γ) in mol/cm^2 and minimum area per molecule (A_{min}) in Å^2 at the air/aqueous solution interface for both individual surfactants and surfactant mixtures were calculated from equations 2 and 3. For solutions containing a single surfactant, n in equation 2 is the number of species whose interfacial concentration changes with change in the bulk phase concentration of the surfactant. For the surfactant mixtures, $n = n_1X_1 + n_2X_2$, where n_1 and n_2 are the number of species of surfactant 1 and 2, respectively, whose interfacial concentration changes with the change in surfactant bulk phase concentration; X_1 and X_2 are the molar fractions (on a surfactant only basis) of surfactants 1 and 2, respectively, at the interface. The value of n is 1 in all cases here because of the swamping amount of NaCl used (0.1 M). The standard deviation for experimental A_{min} is normally within 1 percentage when determined in this manner.[96]

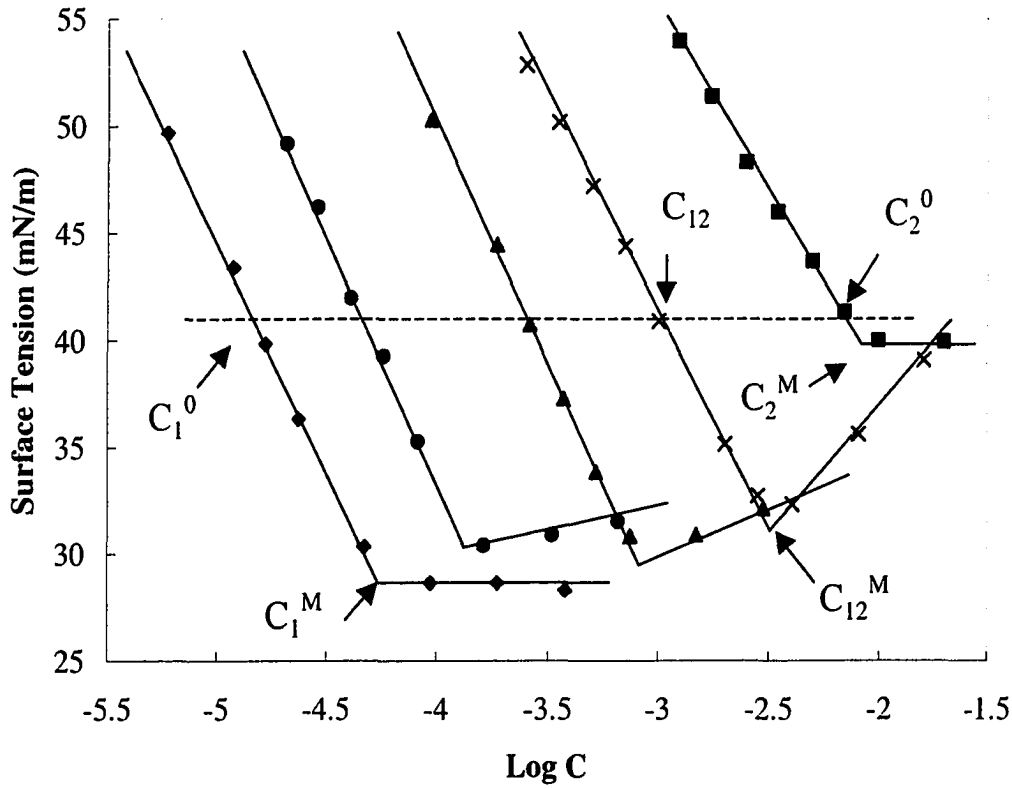

Figure 5. Surface tension vs. log C plots of $C_{12}EO_4$ and its mixtures with ionic surfactants in 0.1M NaCl at 25°C. ◆: $C_{12}EO_4$; ●: $C_{12}EO_4/C_{12}E_2S$ (α_{non} = 0.149); ▲: $C_{12}EO_4/C_{12}SO_3Na$ (α_{non} = 0.0254); ×: $C_{12}EO_4/C_{12}TAC$ (α_{non} = 0.00793); ■: $C_{12}TAC$. α_{non} : the molar fraction of nonionic surfactant in the bulk solution.

One of the best ways of improving the surface or interfacial properties of a surfactant is to add to it another surfactant with which it can interact to obtain synergy between them. Synergy[51c] is defined here as the condition in which the properties of the mixture at some ratio of the two surfactants are better than those attainable with the individual components by themselves. Synergy can be predicted from the molecular interaction between the two surfactants and relevant properties of the individual surfactants by themselves.[51d] Molecular interactions (designated by the so-called beta parameters, β^{σ} and β^{M}) in binary mixture systems involving conventional surfactants[97-99] and the recently developed gemini surfactants[100] have been of academic and industrial interest for some time now.

1.2.2 Calculation of interaction parameters. The nature and the strength of the interaction between two surfactants in their mixed monolayer at the air/aqueous solution interface (β^{σ}), can be determined by calculating the value of their β parameter, from surface tension (γ) vs. concentration (C) plots of aqueous solutions of the individual surfactants and at least one mixture of them, as illustrated in Figure 5. The interaction, β^{σ}, is calculated by use of equations 5 and 6,[51e,101]

$$\frac{X_1^2 \ln(\alpha_1 C_{12} / X_1 C_1^0)}{(1-X_1)^2 \ln[(1-\alpha_1)C_{12}/(1-X_1)C_2^0]} = 1 \qquad (5)$$

$$\beta^{\sigma} = \frac{\ln(\alpha_1 C_{12} / X_1 C_1^0)}{(1-X_1)^2} \qquad (6)$$

where X_1 is the mole fraction of surfactant 1 in the total mixed monolayer (on a surfactant-only basis); C_1^0, C_2^0, and C_{12} are the molar concentrations in the solution phase of surfactant 1, surfactant 2, and their mixture, respectively, at the mole fraction α_1 of surfactant 1 (on a surfactant-only basis), required to produce a given surface or interfacial tension, γ, value. Equation 5 is solved numerically for X_1, which is then substituted into equation 6 to calculate β^σ.

The value of β^M, the interaction parameter for mixed micelle formation in an aqueous medium, is calculated from equations 7 and 8,[51e,102]

$$\frac{(X_1^M)^2 \ln(\alpha_1 C_{12}^M / X_1^M C_1^M)}{(1-X_1^M)^2 \ln[(1-\alpha_1)C_{12}^M /(1-X_1^M)C_2^M]} = 1 \qquad (7)$$

$$\beta^M = \frac{\ln(\alpha_1 C_{12}^M / X_1^M C_1^M)}{(1-X_1^M)^2} \qquad (8)$$

where X_1^M is the mole fraction of surfactant 1 in the total surfactant in the mixed micelle and C_1^M, C_2^M, and C_{12}^M are the critical micelle concentrations (CMC) for surfactant 1, surfactant 2, and their mixture, respectively, at the mole fraction α_1.

In order to obtain valid β^σ or β^M parameters, several conditions must be met: 1) the surfactants used must be molecularly homogeneous and free of surface-active impurities; 2) for mixtures of ionic and nonionic surfactants, the ionic strength of aqueous solutions of the components of the system and all mixtures of them must be kept constant and, since in the derivation of the equations[101,102] electrical effects are ignored, it is advisable to use a swamping amount of electrolyte in all solutions; 3) because the quantity $(X_1)^2/(1-X_1)^2$ or $(X_1^M)^2/(1-X_1^M)^2$

in equations 1 or 3, respectively, is subject to a large error as X_1 or X_1^M approaches either 0 or 1, it is advisable to use values of X_1 or X_1^M between 0.2 and 0.8; 4) the common value of γ used in equation 1 should be as low as possible to ensure that the slopes of the γ – logC plots are constant in the regions where C_1, C_2 and C_{12} are taken; 5) when molecular interactions are strong ($|\beta|$ > 6), the change in the average area/molecule at the interface must be taken into account.[20] Under these conditions, the values of β^σ and β^M are essentially constant with change in the values of X_1 and X_1^M. These conditions are often ignored by investigators.

Table 10 of Chapter 4 lists beta values in the mixed monolayer at the air/aqueous solution interface and in the mixed micelle in aqueous media for some ionic – ionic and some ionic – nonionic mixtures, almost all of which have linear hydrophobes. As illustrated in Figure 6, for all the ionic – nonionic mixture systems studied, both the β^σ and β^M values stay essentially the same when the mixture composition at the air/aqueous solution interface (X_1) or at the micelle surface (X_M) changes in the valid range of 0.2 – 0.8. This has also been observed in many other mixed systems in 0.1M NaCl or 0.1M NaBr medium.[98,101,103]

1.2.3 Properties of interaction parameters (β). Since the value of the β parameter is proportional to the free energy of mixing of the system[51f], a negative value of β means that the attractive interaction between the two different surfactants after mixing is stronger than the attractive interaction of the two individual surfactants with themselves before mixing, or that the repulsive

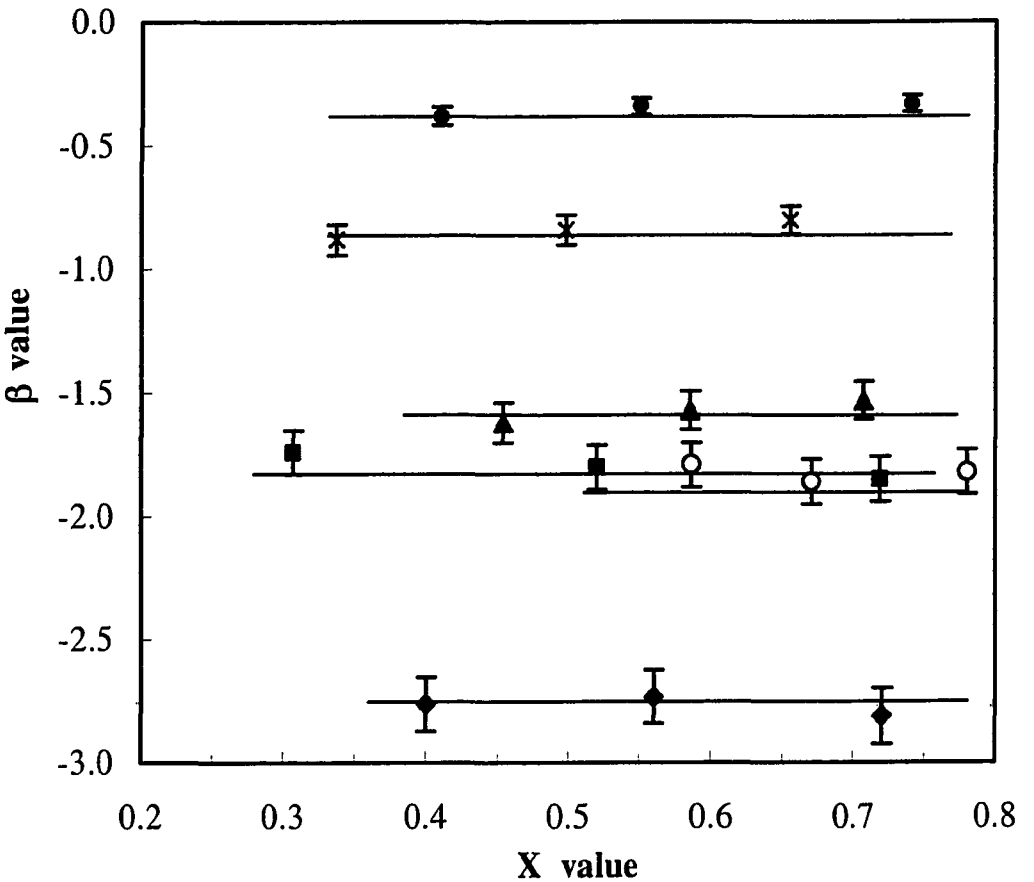

Figure 6. Effect of mixture composition on β values in 0.1M NaCl at 25°C. $C_{12}GA$ / $C_{12}SO_3Na$ ◆ : β^{σ}, ■ : β^{M}; $C_{12}EO_4$ / $C_{12}SO_3Na$ ▲ : β^{σ}, × : β^{M}; $C_{12}EO_4$ / $C_{12}TAC$ ○ : β^{σ}, ● : β^{M}.

interaction between the two different surfactants after mixing is weaker than the self-repulsion of the two individual surfactants before mixing. A positive value of β means that the attractive interaction of the two different surfactants with each other after mixing is weaker than the attractive interaction of the two individual surfactants for themselves before mixing, or that the repulsive interaction between the two different surfactants after mixing is stronger than the self-repulsion of the two individual surfactants before mixing. Repulsive interactions are found in mixtures of hydrocarbon chain and fluorocarbon chain surfactants of the same sign, and in some long chain anionic surfactant – long chain soap mixtures.[104] When the value of the β parameter is close to zero, it indicates almost ideal mixing of the two surfactants.

Usually the interactions, and consequently the values of β parameters, are dominated by electrostatic interaction between the hydrophilic head groups of the two different surfactants.[99] The strength of the interaction between two surfactants in a mixed monolayer at the surface depends on the nature of the surface and the molecular environment, for example, temperature, and ionic strength of the solution phase. From the β parameters, and from relevant properties of the individual surfactant components of the mixture, the existence of synergism can be predicted.

Three kinds of synergy have been investigated[95,105]: synergism in surface tension reduction effectiveness, synergism in surface tension reduction

efficiency, and synergism in mixed micelle formation in aqueous medium. The conditions for the existence of these synergisms are listed as following: 1) synergism in surface tension reduction efficiency: (a) β^{σ} must be negative, (b) $| \beta^{\sigma} | > | \ln(C_1^0/C_2^0) |$; 2) synergism in mixed micelle formation in aqueous medium: (a) β^{M} must be negative, (b) $| \beta^{M} | > | \ln(C_1^M/C_2^M) |$; and 3) synergism in surface tension reduction effectiveness: (a) $\beta^{\sigma} - \beta^{M}$ must be negative, (b) $| \beta^{\sigma} - \beta^{M} | > | \ln((C_1^{0,CMC} * C_2^M) / (C_2^{0,CMC} * C_1^M)) |$; where $C_1^{0,CMC}$, $C_2^{0,CMC}$ are the molar concentrations of surfactant 1 and 2, respectively, required to yield a surface tension equal to that of any mixture at its CMC.

The value of β^{σ} (the interaction parameter for mixed monolayer formation at the air/solution interface) is generally not the same as the value of β^{M} (the interaction in mixed micelle formation in the solution phase) for the same two surfactants under the same conditions. Generally, interaction in the mixed monolayer is stronger than in the mixed micelle, for the same two surfactants under the same conditions. But there are some situations in which there are relatively stronger interactions in the mixed micelle than in the mixed monolayer. The purpose of this study is to determine which factors affect the relative strengths of the molecular interactions in the mixed micelle and in the mixed monolayer in a mixture of the same two surfactants.

The importance of this is that one of the conditions for synergism in surface tension reduction effectiveness (when the surface tension of the mixture at its CMC is lower than that attainable with either surfactant of the mixture by itself) is

that the value of β^{σ} must be more negative than the value of β^{M} (β^{σ}–β^{M} is negative). Since synergism in surface tension reduction effectiveness is the type of synergism that is most sought for practical applications, it is important to know how to maximize that difference.

1.3 Surfactant – Surfactant Interactions in the Mixed Monolayers at the Solid/Aqueous Solution Interface

Molecular interaction at the solid/liquid interface has been studied for some systems, which would provide more helpful information for understanding molecular interaction by regular solution theory. Interaction parameters at solid/liquid interface (β_{SL}^{σ}) are calculated by using the same equations (eqs. 5-6) as in calculating beta values at the air/aqueous solution interface, even though the determination of β_{SL}^{σ} is somewhat more complicated than that of β_{LA}^{σ} (the interaction at the air/aqueous solution interface), because interfacial tension at the solid/liquid interface is not so readily measured as the surface tension at the air/aqueous solution interface. The calculation of β_{SL}^{σ} involves investigation of the Gibbs equation as described below.

The interfacial pressure of a system, designated π, measures the difference between the interfacial tension of the pure solvent (e.g. H_2O), γ^0, and the interfacial tension of the surfactant solution, γ. Thus:

$$\pi = \gamma^0 - \gamma \qquad (9)$$

From equation 9, for any surfactant solution, the interfacial pressure at the solid/liquid interface is:

$$\pi_{SL} = \gamma^{0}_{SL} - \gamma_{SL} \qquad (10)$$

where γ_{SL} is the interfacial tension of a surfactant solution at the solid/liquid interface, γ^{0}_{SL} is the interfacial tension between the pure solvent (e.g., H_2O) and the solid at the solid/liquid interface.

According to the Gibbs adsorption equation, at the solid/liquid interface:

$$d\gamma_{SL} = - nRT\,\Gamma_{SL}\cdot d\ln C \qquad (11)$$

where γ_{SL} = the surface tension at the solid/liquid interface, in mN/m

Γ_{SL} = the adsorption at the solid/liquid interface, in mol/cm^2

C = concentration of surfactant in bulk solution below CMC in mol/L

T = temperature of the system, in K

n = the number of species whose interfacial concentration changes with the change of the surfactant bulk solution concentration, n = 1 for nonionic surfactants

R = 8.314 Joules·mol^{-1}·K^{-1}

If we integrate both sides of the equation 11, we get:

$$\int_{\gamma^{0}_{SL}}^{\gamma_{SL}} d\gamma_{SL} = \gamma_{SL} - \gamma^{0}_{SL} = -\pi_{SL} = -RT\int_{0}^{C}\Gamma_{SL}\cdot d\ln C \qquad (12)$$

Therefore, the interfacial pressure at solid/liquid interface can be calculated from:

$$\pi_{SL} = RT\int_{0}^{C}\Gamma_{SL}\cdot d\ln C \qquad (13)$$

Equation 13 can be used both for individual surfactant solutions (equation 14) and for two-component mixed surfactant systems, 1+2 (equation 15).

$$\pi_{SL}^{1} = RT \int_{0}^{C_A} \Gamma_{SL}^{A} \cdot d \ln C_A \qquad (14)$$

$$\pi_{SL}^{Mix} = RT \int_{0}^{C_{Total}} \Gamma_{SL}^{Total} \cdot d \ln C_{total} \qquad (15)$$

where, π_{SL}^{1} is the interfacial pressure at the solid/liquid interface caused by the solution of component 1; C_1, the concentration of the component 1 in the bulk solution by itself; Γ_{SL}^{1}, the adsorption of the component 1 at the solid/liquid interface. Similarly, π_{SL}^{Mix} is the interfacial pressure at the solid/liquid interface caused by the mixed solution of 1 and 2; C_{total}, the total concentration of the surfactant mixture in the bulk solution; Γ_{SL}^{Total}, the total adsorption of the surfactant mixture at the solid/liquid interface. The values of Γ_{SL} for use of equations 14 and 15 are obtained from adsorption isotherms of individual surfactants or mixtures of surfactants. A plot of Γ_{SL} vs lnC is integrated to obtain π_{SL} as a function of lnC. π_{SL} is then plotted as a function of lnC for the individual surfactant components and their mixture at a given value of α_1, the mole fraction of surfactant 1 (on a surfactant – only basis), as illustrated in Figure 7. Then interaction parameters at the solid/liquid interface, β_{SL}^{σ}, can be calculated from these plots, by applying equations 5 and 6, using values of C_1^0, C_2^0, and C_{12} required to produce the same value of π_{SL}.

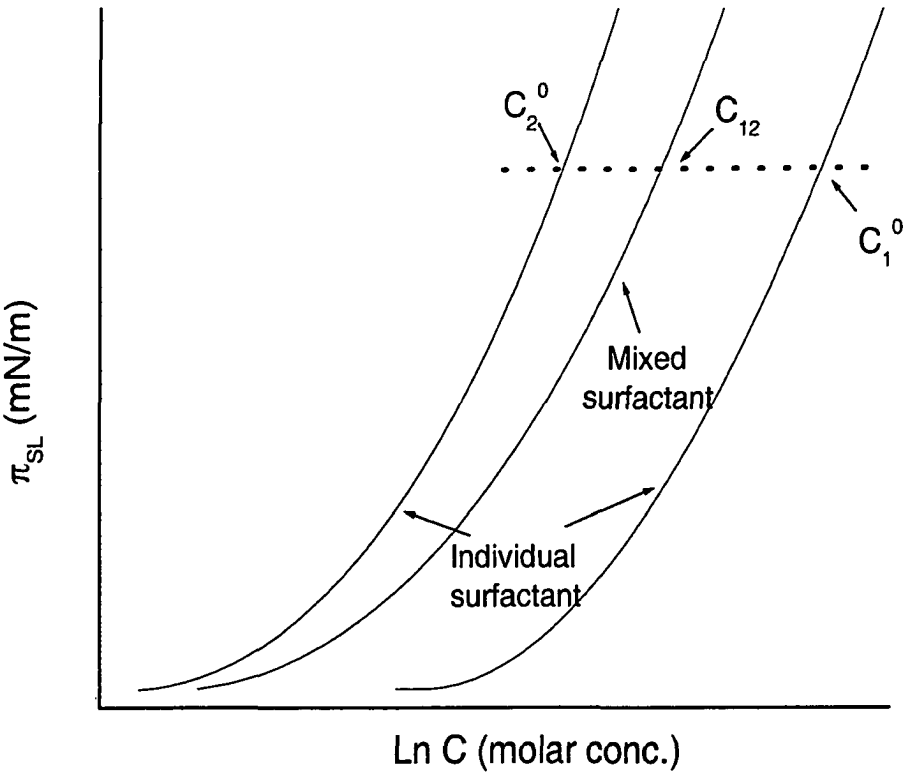

Figure 7. Plots of interfacial pressure, π_{SL}, vs ln C (bulk phase molar concentration) for both individual surfactants and their mixture, used for the calculation of β_{SL}^{σ}.

Chapter 2

Experimental Procedures

2.1 Materials. The structures of some of the studied branched-chain surfactants are shown below:

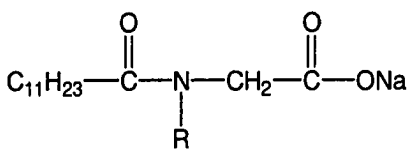

R: n-C_3H_7-, $C_{12}C_3G$
R: CH_3O-$(CH_2)_3$- $C_{12}MeOC_3G$

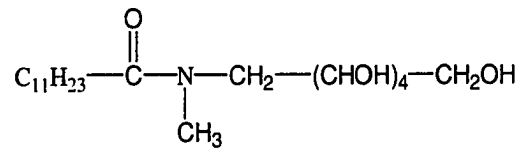

$C_{12}GA$

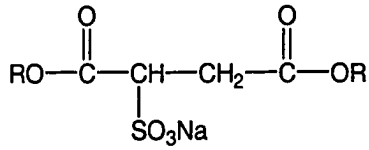

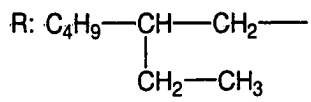

AOT

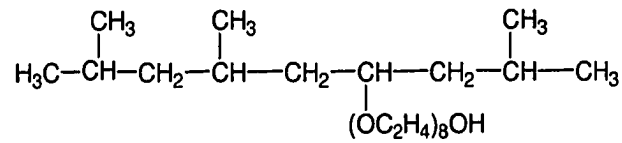

TMN6

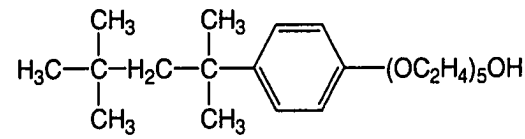

CA-520

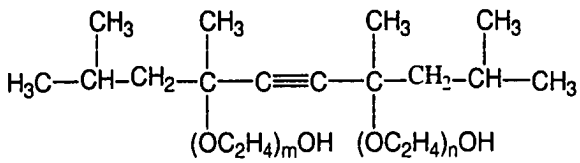

Su: 104, m+n=0
440, m+n=3.5
465, m+n=10

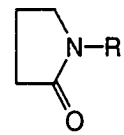

R: n-C_8H_{17}-, C8P
R: n-$C_{12}H_{25}$-, C12P

Nonionic surfactants (>98% purity): n-$C_{12}H_{25}(OC_2H_4)_4OH$ ($C_{12}EO_4$), n-$C_{12}H_{25}(OC_2H_4)_6OH$ ($C_{12}EO_6$), n-$C_{12}H_{25}(OC_2H_4)_7OH$ ($C_{12}EO_7$), n-$C_{14}H_{29}(OC_2H_4)_8OH$ ($C_{14}EO_8$), n-$C_{14}H_{29}(OC_2H_4)_4OH$ ($C_{14}EO_4$), supplied by the Procter & Gamble Company (Cincinnati, OH), courtesy of Dr. Stephen W. Morrall, were obtained by them from Nikko Chemical Co. (Tokyo, Japan). C_{12}–GA was supplied by the Procter & Gamble Company, courtesy of Dr. Phillip K. Vinson. TMN6, obtained from Union Carbide Chemicals and Plastics Company (Danbury, CT) now Dow Chemicals, was used as received. n-C_8H_{17}-N-pyrrolidone (C8P), n-$C_{12}H_{25}$-N-pyrrolidone (C12P) were supplied by ISP Technologies, Inc. (Wayne, NJ), Igepal CA-520 was supplied by Rhodia (Cranbury, NJ). All were used without further purification. Polyethylene powder was supplied by U.S.I. Chemicals, Co. (Cincinnati, OH), with a specific area of 0.36 m^2/g. n-$C_8H_{17}CHOHCH_2OH$ (1,2–C_{10}diol) was synthesized in a previous investigation.[106] n-$C_4H_9CHOHCHOHC_4H_9$ (5,6–C_{10}diol) and n-$C_3H_7CHOHCHOH$ C_5H_{11} (4,5–C_{10}diol) were synthesized using the Swern[107] method, by the reaction of the corresponding alkene with hydrogen peroxide, as shown in equation 11.

$$R_2\text{–}HC{=}CH\text{–}R_1 + H_2O_2 \xrightarrow[24h,\ 40^0C]{\text{Formic Acid}} \xrightarrow[2)\ \text{Hot } H_2O]{1)\ \text{KOH/EtOH}} R_2\text{—}\overset{OH}{\underset{|}{C}}{=}\overset{OH}{\underset{|}{C}}\text{—}R_1 \qquad (11)$$

AOT ($C_4H_9CH(C_2H_5)CH_2OOCCH(SO_3Na)CH_2COOCH_2CH(C_2H_5)C_4H_9$) was obtained from Cytec Industries Inc. (West Paterson, NJ), $C_{12}H_{25}SO_3^-Na^+$ ($C_{12}SO_3Na$) was purchased from Research Plus Inc. (Bayonne, NJ), and $C_{12}H_{25}(OC_2H_4)_2SO_4^-Na^+$ ($C_{12}E_2S$) was supplied by the Procter & Gamble

Company, courtesy of Dr. Stephen W. Morrall, and all were used as received. $C_{12}H_{25}N^{+}(CH_3)_3Cl^{-}$ (C_{12}TAC), $C_{12}C_3$PG and C_{12}MeOC_3PG were also supplied by the Procter & Gamble Company, but these three surfactants were purified by passage of a distilled water solution of the surfactant below its CMC at least four times through SEP-PAK C_{18} cartridges (high-density chromatographic columns of octadecylsilanized silica gel, Water Associates, Milford, MA) to remove any traces of impurities more surface-active than the corresponding parent surfactant.[108] The concentration of the surfactant solution from the column was determined by two-phase mixed indicator titration,[109] with a standardized solution of Hyamine 1622 (Gallard-Schlesinger Co., Carle Place, NY). n-C_4H_9O-$PhSO_3Na$ was synthesized previously in our laboratory.

Sodium chloride and potassium chloride used to increase the ionic strength and provide a constant counter-ion concentration in the aqueous surfactant solution were reagent-grade materials that had been baked for at least 5 h in a porcelain casserole at red heat to burn and remove traces of organic compounds. The surface tension of the aqueous solution of the baked salt was measured, to ensure the absence of traces of surface-active impurities. Ammonium chloride, lithium chloride and dihydrated calcium chloride, also used to increase the ionic strength and provide a constant counter-ion concentration in the aqueous surfactant solution, were reagent-grade materials and were used without any treatment.

2.2 Synthesis of Internal Diol. The reaction for the synthesis of 5,6–C_{10}diol or 4,5–C_{10}diol is shown in equation 11. In a 50mL round-bottom flask, 4.9g (0.035 mol) of trans-5-decene (99+%, Acros) or trans-4-decene (~99%, Fluka) was mixed with 20mL of formic acid (>88%, 4ml acid/g of alkene) and 7g (0.0618 mol) of H_2O_2 (~30%). The reaction was carried out at 40^0C, stirring for 24h. The intermediate was hydrolyzed in excess amount of alcoholic 3M KOH, boiling for 1h, followed by hot water washing to make the crude product alkali free. The crude product (slightly yellow) was recrystallized from hexane 3 times and then recrystallized from isopropanol-hexane mixed solvent 3 more times. Final products (diols) were white, fine crystals. The overall yield is 60% ~ 70%.

2.3 Surface Tension Measurements. Measurements were performed at 25°C with a torsion balance by the Wilhelmy vertical technique, using a sand-blasted platinum plate of ~ 5 cm perimeter. The solutions were immersed in a constant temperature bath at the desired temperature ±0.05°C. The instrument was calibrated against quartz-condensed, double-distilled water (the last distillation stage from alkaline permanganate through a 1-m-high Vigreaux column with quartz condenser and receiver), every day measurements were made. Sets of measurement were taken at certain intervals until the surface tension was constant for ~ 0.5h. The standard deviation for surface tension measurements was less than 0.2mN/m.

None of the individual surfactants investigated showed a minimum surface tension in the vicinity of its CMC. However, some ionic–nonionic surfactant

mixtures investigated showed a minimum surface tension in the CMC range, especially those systems in which the surface properties, such as the CMC and γ_{CMC} values of the two individual surfactants were far apart. In these cases, the CMC value was taken at the minimum point in the surface tension (γ) – concentration(C) curve.

2.4 Adsorption on Polyethylene Powder. Polyethylene powder was cleaned by washing at least 8 times with spectranalyzed methanol and then dried in a vacuum desiccator over anhydrous phosphorus pentaoxide (P_2O_5) for a few weeks. A series of surfactant solutions (25 to 40 mL) are mixed with the appropriate amount of purified polyethylene powder (0.5 to 1.0 gram). Vigorous overnight shaking at room temperature is carried out on the mixtures to ensure adsorption equilibrium. The mixture is centrifuged to separate the powder from the surfactant solution. For all the surfactant solutions studied, both the individual and mixed surfactant solutions, the equilibrium surfactant concentrations are measured by UV absorbance against corresponding calibration curves. Adsorption amount at corresponding equilibrium concentration was calculated from the surfactant concentration difference before and after adsorption.

2.5 Surfactant Concentration Measurement by UV Absorbance. The equilibrium concentrations of surfactants were determined by measuring their UV absorbance (UV/Vis Spectrophotometer, HITACHI, U-2001). For the individual pyrrolidinone surfactant solutions (C8P and C12P), even though they don't have a maximal wavelength in the UV-vis range, their UV absorbances still obey

Beer's Law, as shown in Figure 8. UV absorbance for C8P and C12P were measured at the wavelength λ=205 nm, and the corresponding decadic molar extinction coefficients (ε, $M^{-1}cm^{-1}$) are: C8P: 6.05×10^3; C12P: 5.77×10^3. When λ > 225 nm, ε is less than 500 for both C8P and C12P. The measured decadic molar extinction coefficients (ε, $M^{-1}cm^{-1}$) for CA-520 at its maximal wavelength, λ_{max}=223 nm, is 1.05×10^4, the measured molar extinction coefficients (ε, $M^{-1}cm^{-1}$) for n-C_4H_9O-$PhSO_3Na$ at its maximal wavelength, λ_{max}=233 nm, is 1.57×10^4.

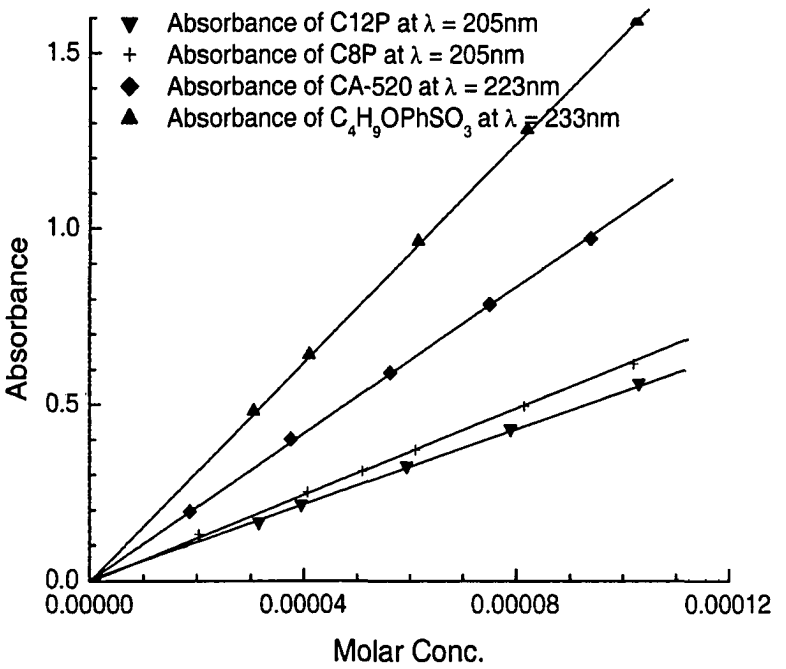

Figure 8. Absorbance calibration curves for the studied surfactants at different wavelengths.

According to Beer's Law, the total absorbance for a binary system is given by[110]: $A_{total} = A_1 + A_2 = \varepsilon_1 bC_1 + \varepsilon_2 bC_2$. So, in a binary mixture solution, for example mixture of C8P/CA-520, when the concentration of pyrrolidinone is

determined by UV absorbance, the contribution from CA-520 to the UV absorbance must be deducted. The measured molar extinction coefficients (ε) for CA-520 and n-C_4H_9O-$PhSO_3Na$ at the wavelength λ=205 nm are 8.75×10^3 and 9.25×10^3 respectively. The concentration of n-C_4H_9O-$PhSO_3Na$ or of CA-520 for use in the above equation was that determined from its UV absorbance at 223nm or 233nm respectively.

2.6 Equilibrium Contact Angle Measurements on Polyethylene Film. Advancing contact angles were measured with a Contact Angle Image Analysis System (Model 100-00, Ramé-hart, Inc.). Several drops of solution, each about 10μL, were applied to the solid surface, which was placed in a thermostatic environmental chamber (Model 100-07, Ramé-hart, Inc.) saturated with solvent vapor to retard droplet evaporation. Angles were measured on both sides of the drops for at least 1 hour at 25 °C. Equilibrium contact angle values were assumed to be obtained when no changes were observed for 30 min. The equilibrium contact angle values were reproducible within ±1.0°. The polyethylene film was made by melting the polyethylene powder (after it had been cleaned by washing at least 8 times with spectranalyzed methanol and then dried in a vacuum desiccator) on a piece of clean, dry glass, then removing the polyethylene film from the glass. In order to remove the polyethylene film from the glass safely and get a whole big piece of the film, the removal process has to be performed in boiling distilled water. For measuring advancing contact angles,

the polyethylene film should be used only on the side that had contacted the glass (because it is much smoother than the other side).

2.7 Dynamic Contact Angle Measurements on Polyethylene Film. Dynamic advancing contact angles were measured with a Contact Angle Image Analysis System (Model 100-00, Ramé-hart, Inc.). One drop of surfactant solution, around 10μL, was applied to the polyethylene film (prepared as described above), which was placed in a thermostatic environmental chamber (Model 100-07, Ramé-hart, Inc.) saturated with solvent vapor to retard droplet evaporation. Angles were measured on both sides of the drop at 25 °C. The measurement of dynamic contact angles is started as soon as possible, usually less than 10 seconds after the solution drop has been placed on the solid substrate, and is continued for the first 180 seconds.

2.8 Spreading Factor Measurements. Polyethylene film was made by melting purified polyethylene powder on a 10cm×10cm clean glass square and removing it (as described above) when it had cooled down. The side of the polyethylene film that had contacted the glass was used for measuring the spreading factor. Four pieces of glass (about 1 cm^2) were placed at the corners of the polyethylene film, which is mounted horizontally (using a small spirit level) on an optically flat glass plate (10cm×10cm) resting upon the horizontal mouth of a glass bottle. Using a microsyringe, which had previously been rinsed with the solution being tested, a 20 μL drop of the solution is placed on the polyethylene film. The stop watch is started and another 10cm×10cm glass square is

immediately placed over the four pieces of glass so that it is parallel to the polyethylene film. After three minutes (when the solution has stopped spreading), an outline of the spread solution is traced onto the top glass. This area is then retraced onto standard white paper from which it is cut and weighed. The exact spreading area is then calculated from the mass of a piece of the same paper of known area, with the assumption that the paper has a constant mass per unit area.

After each measurement, the polyethylene substrate is thoroughly rinsed with methanol, tap water and distilled water, and is then put into boiling distilled water for at least 30 minutes in order to remove any adsorbed surfactant. The solutions, all at 1.0g/L total surfactant concentration, are far above the CMC of the mixture. Each spreading measurement was done three to five times until reproducibility was satisfactory, to ensure minimal relative error. The spreading area is the average of the areas obtained in each set of measurements. The spreading factor (SF) is the ratio: spreading area of the surfactant solution to spreading area of the same volume of solvent in the same time (three minutes).

2.9 NMR Measurements. The ^1H NMR spectra were measured using a Bruker 250 Fourier-transform spectrometer (250 MHz for the proton resonance) at room temperature. The resonance was 0.001 ppm. The surfactant was dissolved in D_2O (>99.9%, Aldrich) and the solution was then transferred to a 5 mm diameter NMR cell. HDO residual in D_2O was used as an internal reference peak.

Chapter 3.

Surfactant – Surfactant Interactions in Mixed Monolayer at Air/Aqueous Solution Interface and in Mixed Micelle Formation

3.1 β^{σ}–β^{M} values. Figure 9 shows the equilibrium surface tension (γ) versus log bulk surfactant molar concentration (C) plots for a $C_{12}SO_3Na$ – $C_{12}EO_7$ binary system. Plots such as these were used to calculate β^{σ} and β^{M} values, by use of equations 5-8. Values for some surfactant mixtures in 0.1M NaCl at 25 °C are shown in Table 1. The 0.1M NaCl provides an aqueous medium of constant ionic strength and constant counter-ion concentration, a requirement for accurate calculation of β values, for systems containing an ionic surfactant component.

The data show that all the mixtures have β^{σ}-β^{M} values that are negative, except for mixtures of anionic surfactants with polyoxyethylenated (POE) nonionic surfactants, where the β^{σ}-β^{M} values are positive. As mentioned before, one of the most important types of synergy shown by surfactant mixtures is synergism in surface tension reduction effectiveness. The conditions for this type of synergy to occur, which requires β^{σ} values more negative than β^{M} values, are shown in Section 1.2 of the Introduction. From the above discussion, these anionic – POE nonionic mixtures, which are of the type that is commonly used in

consumer and industrial applications, can therefore never show synergism in surface tension reduction effectiveness (i.e., they can never have surface tension values that are lower than those of the individual surfactants by themselves), although they may show other types of synergism (i.e., synergism in surface tension reduction efficiency, or in mixed micelle formation). The data also show the following:

1. *Polyoxyethylenated (POE) nonionics are the only type of nonionic* surfactant studied, which, when mixed with anionic surfactants, yield β^{σ}-β^{M} values that are positive. The other types of nonionics tested (diol, glucamides, glucosides, maltosides) yield β^{σ}-β^{M} values that are negative, when mixed with the same anionic surfactants. The positive value for the POE – containing mixtures appears to be due to larger negative β^{M} values for this type of mixture than for mixtures with the other nonionic types.

2. The cationic surfactant, C_{12}TMAC, when mixed with similar POE nonionics, yields β^{σ}-β^{M} values that are negative. This has been confirmed in our laboratory using other cationics.[97]

3.2 Effect of pH value change on β^{σ}–β^{M} values. The difference between the β^{σ}-β^{M} values for anionic – POE nonionic and cationic – POE nonionic mixtures suggested that there might be a charge effect that enhances the interaction in the mixed micelles of anionic – POE nonionic mixtures, making β^{M} more negative than that in cationic – POE nonionic mixtures. In previous investigations on mixtures of anionic and weakly basic surfactants (betaines or

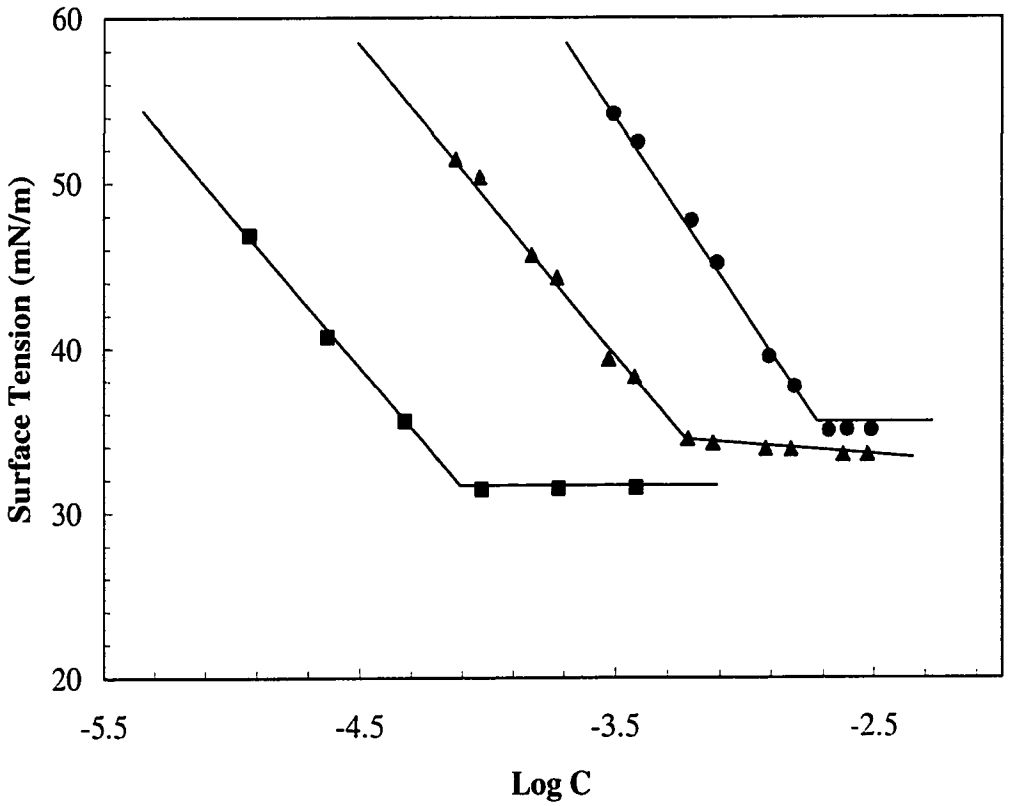

Figure 9. Surface tension vs. log C plots of $C_{12}SO_3Na$, $C_{12}EO_7$ and their mixture (α_{non} = 0.0381) in 0.1M NaCl at 25°C. ●: $C_{12}SO_3Na$; ■: $C_{12}EO_7$; ▲: mixture.

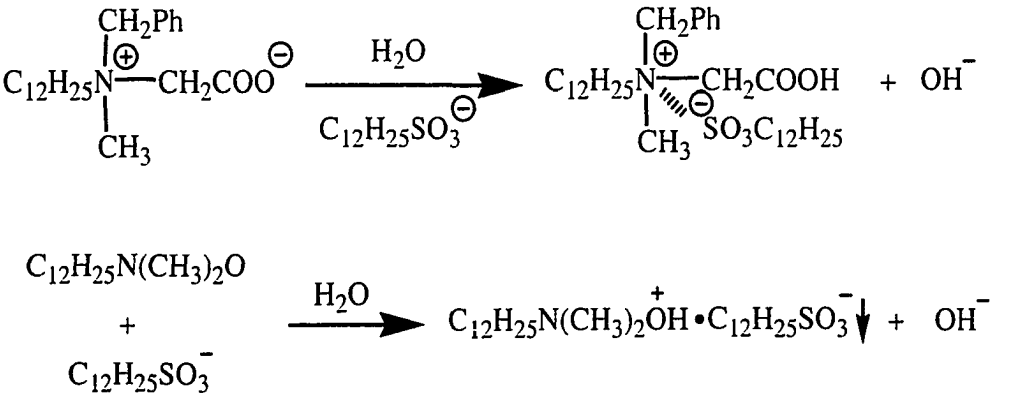

Figure 10. Betaines and amine oxides can pick up a proton from water, acquire a positive charge, and interact fairly strongly with anionic surfactants.

Table 1: β^{σ} and β^{M} Values in 0.1M NaCl for some surfactant mixtures

Surfactant Mixture	α_{non}	X^{σ}	X^{M}	β^{σ}	β^{M}	$\beta^{\sigma} - \beta^{M}$
$C_{12}SO_3Na$ – 1,2–C_{12}diol [97]	0.033	0.51	0.77	–3.03	–1.45	–1.58
$C_{12}SO_3Na$ – 1,2–C_{10}diol	0.614	0.60	0.54	–2.75	–1.34	–1.41
$C_{12}SO_3Na$ – $C_{12}GA$	0.213	0.56	0.52	–2.73	–1.77	–0.96
$C_{12}E_2S$ – $C_{12}GA$	0.490	0.51	0.44	-1.76	-1.2	–0.56
$C_{12}ES$ – C_{10} Glucoside [113]	0.90	0.65	0.60	–1.82	–1.42	–0.40
$C_{12}ES$ – C_{10} Maltoside [113]	0.82	0.47	0.50	–1.5	–1.2	–0.30
$C_{12}SO_3Na$ – $C_{12}EO_7$	0.0381	0.56	0.50	–1.73	–2.38	+0.65
$C_{12}SO_3Na$ – $C_{14}EO_8$	0.007	0.56	0.54	–1.43	–2.0	+0.57
$C_{12}E_2S$ – $C_{12}EO_6$	0.2	0.58	0.50	–1.50	–1.95	+0.45
$C_{12}TAC$ – $C_{14}EO_8$	0.00256	0.71	0.63	–1.04	–0.53	–0.51
$C_{12}TAC$ – $C_{12}EO_7$	0.0119	0.67	0.53	–1.76	–1.23	–0.53

amine oxides),[111,112] it was observed that, in the presence of the anionic surfactant, even at neutral pH, the weakly basic surfactant picked up a proton (from water), acquired a positive charge, and interacted fairly strongly with the anionic surfactant, as shown in Figure 10. This suggested that the weakly basic POE group of the nonionic surfactant, in the presence of the anionic surfactant in their mixed micelles, might acquire a proton from the water and enhance the interaction of the two surfactants. Therefore, it was expected that a lower pH would produce a higher absolute value of β^M; a higher pH, a lower value. Table 2 shows the results. No effect of pH change, in the range of 2.7 – 9.1, on the negative value of β^σ was observed, and only a slight increase, considered insignificant, was observed on that of β^M.

Table 2: Effect of pH on β^σ and β^M Values for $C_{12}SO_3Na - C_{12}EO_7$ in 0.1M NaCl

pH	α_{non}	X^σ	X^M	β^σ	β^M	$\beta^\sigma - \beta^M$
2.7	0.0378	0.56	0.49	−1.73	−2.16	+0.43
5.9	0.0381	0.56	0.50	−1.73	−2.38	+0.65
9.1	0.0376	0.55	0.50	−1.73	−2.32	+0.59

The effect of addition of $C_{12}SO_3Na$ solution on the pH value of a $C_{12}EO_6$ solution at an initial pH of 5.11 was measured, with the expectation that a significant increase in pH value would be observed when oxygen atoms in polyoxyethylene chain of the nonionic surfactant acquire a proton from water and enhance the interaction of the two surfactants in the presence of the anionic surfactant in their mixed micelles. Table 3 shows the pH value and $[H^+]$ change

of the $C_{12}EO_6$ solution upon the addition of $C_{12}SO_3Na$ solution. Table 4 shows the pH value and $[H^+]$ change of the $C_{12}EO_6$ solution upon the addition of $C_{12}TAC$ solution. The pH value and $[H^+]$ change of the $C_{12}EO_6$ solutions, with the addition of either $C_{12}SO_3Na$ or $C_{12}TAC$, does not show any obvious sign of acquisition by $C_{12}EO_6$ of a proton from water, otherwise, a significant pH change would have been observed. This is also confirmed by the fact that pH change produces no obvious effect on the negative value of β.

Table 3. $[H^+]$ change of 50.0 mL $C_{12}EO_6$ solution ($C=1.77\times10^{-4}$ M, pH=5.11) with the addition of $C_{12}SO_3Na$ solution (C=0.02M, pH=5.60) in H_2O.

Addition of $C_{12}SO_3Na$	α_{non}	pH of the solutions	Measured $[H^+]$	Calculated $[H^+]$*
0	1.0	5.11	7.76E-06	7.76E-06
2.00mL	0.181	5.52	3.02E-06	3.47E-06
6.00mL	0.0686	5.46	3.47E-06	2.88E-06
10.00mL	0.0423	5.46	3.47E-06	2.74E-06
15.00mL	0.0286	5.45	3.55E-06	2.67E-06
20.00mL	0.0216	5.46	3.47E-06	2.63E-06
30.00mL	0.0145	5.49	3.24E-06	2.59E-06
40.00mL**	0.0109	5.50	3.16E-06	2.57E-06

*: Calculated $[H^+] = \alpha_{non} \times [H^+]$ of $C_{12}EO_6 + (1-\alpha_{non}) \times [H^+]$ of $C_{12}SO_3Na$

**: with further addition, $C_{12}SO_3Na$ precipitates due to solubility limit.

Table 4. $[H^+]$ change of 50.0 mL $C_{12}EO_6$ solution (C=8.85 $\times 10^{-5}$ M, pH=5.30) with the addition of $C_{12}TAC$ solution (C=0.031M, pH=5.60) in H_2O.

Addition of $C_{12}SO_3Na$	α_{non}	pH of the solutions	Measured $[H^+]$	Calculated $[H^+]$*
0	1.0	5.30	5.01E-06	5.01E-06
2.00mL	0.0666	5.15	7.08E-06	2.68E-06
6.00mL	0.0232	5.31	4.90E-06	2.57E-06
11.00mL	0.0128	5.37	4.27E-06	2.55E-06
16.00mL	0.00884	5.44	3.63E-06	2.54E-06
21.00mL	0.00671	5.51	3.09E-06	2.53E-06
31.00mL	0.00458	5.53	2.95E-06	2.53E-06
41.00mL	0.00347	5.58	2.63E-06	2.52E-06
51.00mL	0.00279	5.61	2.46E-06	2.52E-06

*: Calculated $[H^+] = \alpha_{non} \times [H^+]$ of $C_{12}EO_6 + (1-\alpha_{non}) \times [H^+]$ of $C_{12}TAC$

3.3 Effect of ionic strength on β^{σ}–β^{M} values. Since the POE group was apparently not acquiring a positive charge by picking up a proton, our next hypothesis was that the POE nonionic surfactant might acquire a positive charge by adding a Na^{+} from the solution phase. It is well known that the POE group, if it contains sufficient oxyethylene units, can form an open "crown ether" with Na^{+} or K^{+}. We therefore added NaCl and, in one case, KCl to the mixtures. Results are shown in Table 5. Here, there was only a slight increase in the absolute value of both β^{σ} and β^{M} with addition of NaCl up to 0.1 molar for anionic – POE nonionic mixtures, followed by a leveling off in the case of β^{σ} and possibly a small decrease in β^{M} with increase of the NaCl concentration to 0.2M.

However, this was very different from the effect on β^{σ} and β^{M} of the addition of NaCl in this range to cationic – POE nonionic mixtures. In the case of the cationic – POE nonionic mixtures, the absolute values of both β^{σ} and β^{M} decrease considerably with addition of NaCl to 0.5M concentration. This is the expected decrease in the electrostatic interaction between the two surfactants as a result of the compression of the electrical double layer around the ionic head group with increase in ionic strength of the solution. The observation that the anionic – POE nonionic mixture does not show this behavior suggests that the addition of NaCl in this case produces two simultaneous effects: (1) a decrease in the absolute values of β^{σ} and β^{M} due to compression of the electrical double layer surrounding the anionic SO_3^- group, and (2) an increase in the absolute values of β^{σ} and β^{M} as a result of increased interaction of the anionic and POE

Table 5: Effect of Electrolyte Concentration on β^{σ} and β^{M} Values

Surfactant Mixture	Medium	α_{non}	X^{σ}	X^{M}	β^{σ}	β^{M}	$\beta^{\sigma} - \beta^{M}$
$C_{12}SO_3Na - C_{12}EO_7$	H_2O	0.0104	0.67	0.52	–1.05	–2.02	+0.97
$C_{12}SO_3Na - C_{12}EO_7$	0.05M NaCl	0.0368	0.63	0.54	–1.50	–2.24	+0.74
$C_{12}SO_3Na - C_{12}EO_7$	0.1M NaCl	0.0381	0.56	0.50	–1.73	–2.38	+0.65
$C_{12}SO_3K - C_{12}EO_7$	0.1M KCl	0.0413	0.54	0.49	–1.72	–2.23	+0.51
$C_{12}SO_3Na - C_{12}EO_7$	0.2M NaCl	0.0599	0.55	0.52	–1.73	–2.16	+0.43
$C_{12}TAC - C_{12}EO_7$	0.05M NaCl	0.00965	0.65		–2.24		
$C_{12}TAC - C_{12}EO_7$	0.1M NaCl	0.0119	0.67	0.53	–1.76	–1.23	–0.53
$C_{12}TAC - C_{12}EO_7$	0.5M NaCl	0.0259	0.69	0.51	–1.20	–0.38	–0.82
C_{12} PyrCl – $C_{12}EO_8$ [97]	H_2O	0.0011	0.49	0.31	–2.82	–2.67	–0.15
C_{12} PyrCl – $C_{12}EO_8$ [97]	0.1M NaCl	0.0051	0.48	0.30	–1.98	–1.46	–0.52
C_{12} PyrCl – $C_{12}EO_8$ [97]	0.5M NaCl	0.0139	0.50	0.36	–1.75	–1.01	–0.74

nonionic surfactants. This second effect is apparently larger than the first effect up to 0.1M NaCl concentration, producing the observed net increase in the absolute values of β^{σ} and β^{M}.

This increase in the negative value of β^{σ} upon addition of NaCl to anionic – POE nonionic surfactant mixtures had been observed previously and was attributed to complexing of the Na^{+} with the polyoxyethylene chain in the form of an open crown ether.[97] The resulting positive charge on the POE nonionic would produce stronger electrostatic interaction with the anionic $C_{12}H_{25}SO_3^-$. Here, the addition of electrolyte in all systems investigated (Table 5), both for anionic – POE nonionic mixtures and for cationic – POE nonionic systems, results in the values of β^{σ}-β^{M} becoming less positive or more negative. This suggested that the decreased bulkiness of the combined hydrophilic head groups of the ionic – nonionic surfactant mixture, as a result of the compression of the electrical double layer surrounding the ionic surfactant, might be a factor determining the value of β^{σ}-β^{M}. This was supported by the data for the mixtures that contained the smallest head groups: the $C_{12}SO_3Na$ – 1,2-diol mixtures (Table 1). They have the largest negative β^{σ} values and fairly small negative β^{M} values. This results in their having considerably more negative β^{σ}-β^{M} values than any of the other mixtures investigated.

3.4 Effect of bulky group from surfactant on β^{σ}–β^{M} values. To test the hypothesis regarding the effect of bulkiness in the surfactant molecules on the value of β^{σ}-β^{M}, mixtures containing surfactants with branched hydrophobic

groups were investigated. Data are shown in Table 6. The data show that the replacement of a straight –chain hydrophobic group of a surfactant in an anionic – POE nonionic mixture whose β^{σ}-β^{M} value is positive by a branched- chain hydrophobic group causes the β^{σ}-β^{M} value to become less positive, or even negative. This is regardless of whether the straight – chain hydrophobic group that is replaced is in the anionic surfactant (AOT versus $C_{12}SO_3Na$) or in the POE nonionic surfactant (TMN6 versus $C_{12}EO_6$) of the original mixture. The effect of the branched hydrophobic group appears to be mainly in reducing the negative value of β^{M}, the interaction between the two surfactants in the mixed micelle. This is in agreement with the known greater steric effect on micellization than on adsorption at the aqueous–air interface.[51g]

Table 6: Effect of Branching in the Hydrophobic Group (0.1M NaCl)

Surfactant Mixture	α_{non}	X^{σ}	X^{M}	β^{σ}	β^{M}	$\beta^{\sigma} - \beta^{M}$
$C_{12}SO_3Na - C_{12}EO_7$	0.0381	0.56	0.50	–1.73	–2.38	+0.65
$C_{12}SO_3Na$ – TMN6	0.201	0.67	0.50	–1.74	–2.07	+0.33
$C_{12}SO_3Na - C_{14}EO_8$	0.007	0.56	0.54	–1.43	–2.0	+0.57
AOT – $C_{14}EO_8$	0.0248	0.30	0.51	–1.98	+0.07	–2.05
$C_{12}E_2S - C_{12}EO_6$	0.2	0.58	0.50	–1.50	–1.95	+0.45
$C_{12}E_2S$ – TMN6	0.6	0.67	0.50	–1.64	–0.89	–0.75
AOT – $C_{12}EO_6$	0.162	0.38	0.50	–1.64	–1.47	–0.17

The effect of bulkiness in the hydrophobic group of the molecule on the value of β^{M} is confirmed by some data on anionic gemini surfactant – POE nonionic mixtures, obtained several years ago in our laboratory.[114] Data are

shown in Table 7. Here, there is a marked reduction in the negative value of β^M when $C_{12}SO_3Na$ is replaced by various anionic gemini surfactants, whose structure are shown in Figure 11. Note the larger reduction in the negative value of β^M for a gemini surfactant with three hydrophobic groups, compared to one with two similar hydrophobic groups.

Table 7: β^σ and β^M Values of Gemini Surfactants in 0.1M NaCl, at 25°C[114]

Surfactant Mixture	β^σ	β^M	$\beta^\sigma - \beta^M$
$C_{12}SO_3Na - C_{12}EO_7$	–1.73	–2.38	+0.65
$C_{10}DADS - C_{12}EO_7$[114]	–5.9	–0.8	–5.1
$C_8C_1C_8 - C_{12}EO_7$[114]	–1.5	–0.2	–1.3
$C_8C_8C_8 - C_{12}EO_7$[114]	–3.2	+0.7	–3.9
$C_{10}OC_{10} - C_{12}EO_8$[114]	–1.5	–0.6	–0.9
$C_{12}SO_3Na - C_{12}EO_8$[97]	–2.6	–3.1	+0.5

The introducing of branching close to the hydrophilic group of the anionic surfactant was then studied. The results are shown in Table 8. The data show that branching close to the hydrophilic group of the anionic surfactant (in $C_{12}C_3G$ and in $C_{12}MeOC_3G$) also makes the values of β^σ-β^M become less positive or more negative. Unlike the effect of branching in the hydrophobic group, branching close to the hydrophilic group of the anionic in the mixture reduces the absolute values of both β^σ and β^M. However, it reduces the negative value of β^M more dramatically than β^σ, making the β^σ-β^M value less positive or more negative. It is noteworthy that adding two oxyethylene groups adjacent to the hydrophilic

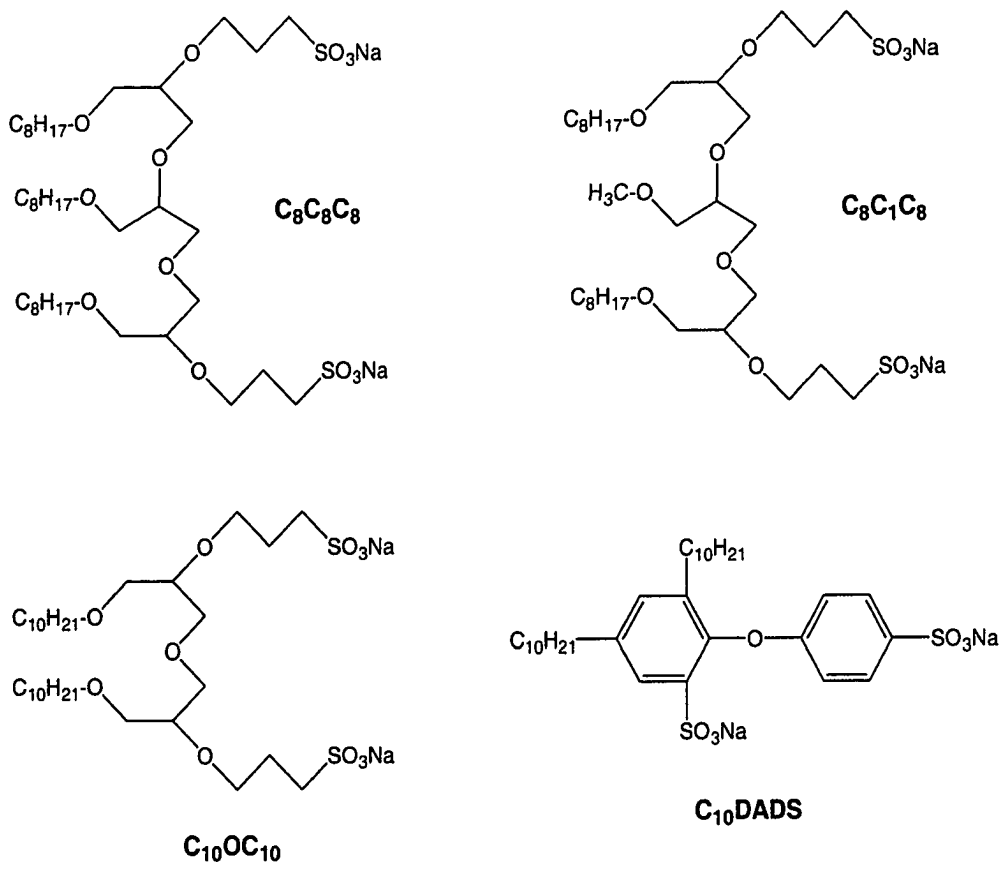

Figure 11: Structures of Gemini surfactants investigated[114]

sulfate group, in $C_{12}E_2S$ – $C_{12}GA$ versus $C_{12}SO_3Na$ – $C_{12}GA$ (Table 1), also results in a decrease in both the absolute values of β^{σ} and β^{M}, although in this case the absolute value of β^{σ} is decreased more than that of β^{M}. When both surfactants contain highly branched hydrophobic groups and one of them also contains branching close to the hydrophilic group (AOT–TMN6, Table 8), interaction between them in both the mixed monolayer and mixed micelle is very weak.

Table 8: Effect of Branching Close to the Hydrophilic Group of Anionics (0.1M NaCl)

Surfactant Mixture	α_{non}	X^{σ}	X^{M}	β^{σ}	β^{M}	$\beta^{\sigma} - \beta^{M}$
$C_{12}SO_3Na$ – $C_{12}EO_7$	0.0381	0.56	0.50	–1.73	–2.38	+0.65
$C_{12}C_3G$ – $C_{12}EO_6$	0.11	0.69	0.57	–0.69	–1.23	+0.54
$C_{12}MeOC_3G$ – $C_{12}EO_6$	0.0481	0.70	0.51	–0.69	–0.83	+0.14
$C_{12}SO_3Na$ – TMN6	0.201	0.67	0.50	–1.74	–2.07	+0.33
$C_{12}C_3G$ – TMN6	0.299	0.68	0.50	–1.35	–1.19	–0.16
$C_{12}MeOC_3G$ – TMN6	0.208	0.78	0.50	–0.78	0.0	–0.78
AOT – TMN6	0.523	0.49	0.50	–0.47	–0.49	+0.02

3.5 Effect of oxyethylene units on β^{σ}–β^{M} values. As mentioned above, the only cases that produce positive β^{σ}-β^{M} values are mixtures of anionic and POE nonionic surfactants. The investigation was therefore extended to study the effect of the number of oxyethylene units in the POE nonionic surfactants on β^{σ} and β^{M}. The results are shown in Table 9. The data show that, even for anionic – POE nonionic mixtures, the value of β^{σ}-β^{M} can be negative, if the number of

oxyethylene units in the POE nonionic surfactant is small. However, when the polyoxyethylene chain contains sufficient units to complex Na^+ in an open chain crown ether structure, the absolute value of β^M increases sharply, due to the increased interaction at the micelle/aqueous solution interface, and the β^σ-β^M values change from negative to positive. Since the β^σ value stays almost the same, it appears that the convex micelle/aqueous solution interface is better able to accommodate the bulky open crown ether structures than the planar air/aqueous solution interface.

Table 9: Effect of Oxyethylene Units on β^σ and β^M Values in 0.1M NaCl

Surfactant Mixture	α_{non}	X^σ	X^M	β^σ	β^M	$\beta^\sigma - \beta^M$
$C_{12}SO_3Na$ – $C_{14}EO_4$	0.00632	0.68	0.63	–1.08	–0.48	–0.60
$C_{12}SO_3Na$ – $C_{14}EO_8$	0.007	0.56	0.54	–1.43	–2.0	+0.57
$C_{12}SO_3Na$ – Su 104[a]	0.751	0.59		–2.75		
$C_{12}SO_3Na$ – Su 440	0.772	0.65	0.50	–2.70	–2.1	–0.60
$C_{12}SO_3Na$ – Su 465	0.812	0.64	0.50	–2.37	–2.9	+0.53
$C_{12}E_2S$ – Su 440	0.950	0.67	0.49	–1.9	–1.7	–0.20
$C_{12}E_2S$ – Su 465	0.959	0.64	0.49	–1.93	–2.47	+0.54

a: due to solubility limitation, CMC for Su 104 is not available.

From the above, for synergism in surface tension reduction effectiveness to be possible in anionic – POE nonionic mixtures, the number of oxyethylene groups in the latter surfactant must be small.

3.6 Conclusions

1. The pH value of the mixture has no significant effect on β^{σ} or β^{M} values for anionic – POE nonionic surfactant mixtures.
2. The ionic strength of the mixture seems to have only a small effect on the absolute values of both β^{σ} and β^{M} for POE nonionic – anionic surfactant mixtures, although the value of β^{σ}-β^{M} becomes more negative or less positive with increase in ionic strength of the solution. This is in marked contrast to its effect on POE nonionic – cationic surfactant mixtures, where increase in the ionic strength of the mixture results in sharp decreases in the negative values of both β^{σ} and β^{M}.
3. Interaction in the mixed micelle is reduced by branching in the hydrophobic group in either surfactant of the mixture.
4. Interaction in both the mixed micelle and the mixed monolayer is decreased by branching close to the hydrophilic group of one of the surfactants in the mixture.
5. Interaction in the anionic – POE nonionic mixed micelle (larger negative β^{M} value) is enhanced by a POE group in the nonionic surfactant with sufficient oxyethylene content to complex the Na^{+} of the anionic surfactant.
6. Synergism in surface tension reduction effectiveness is possible for POE nonionic – anionic mixtures, if the number of oxyethylene groups in the former surfactant is small.

Chapter 4.

The Regular Solution Approach to Surfactant – Surfactant Molecular Interaction

4.1 Regular Solution Theory

Beta parameters measure the interaction between two different surfactants, relative to the self-interaction of the two surfactants under the same conditions before mixing. This latter half of the above sentence is usually ignored or neglected by investigators because of the difficulty of measuring it quantitatively. This often leads to misunderstanding of the meaning of the measured values of the beta parameters and of the difficulty in explaining them.

Thus, negative beta values are commonly described as indicating attractive interaction between the two surfactants, while what is actually observed is an interaction more attractive or less repulsive than the self-interaction of the two surfactants before mixing. The "regular solution" equation relates the value of the β parameter to molecular interaction energies before and after mixing:[102]

$$\beta = [W_{AB} - (W_{AA} + W_{BB})/2]/RT \qquad (12)$$

where W_{AB} is the molar interaction energy between the mixed surfactants, W_{AA} is the molar self interaction energy of the first surfactant and W_{BB} the molar self interaction energy of the second surfactant, R = the molar gas constant and T the absolute temperature. This is a convenient method of handling this problem,

even when the values of W_{AB}, W_{AA} and W_{BB} are only known non-quantitatively. Interaction energies are negative when attractive, positive when repulsive.

The types of molecular interaction encountered in surfactant systems include: 1) electrostatic interaction between ionic hydrophilic groups, 2) ion-dipole interaction between ionic and nonionic hydrophilic groups, 3) steric interactions between bulky hydrophilic or hydrophobic groups, 4) van der Waals interactions between hydrophobic groups, and 5) hydrogen bonding between hydrogen acceptor and donor groups in the two surfactant molecules.

Thus, it can be assumed that the head groups of ionic surfactants will cause electrostatic self-repulsion before mixing and that bulky groups in the hydrophobic and/or hydrophilic portions of the surfactant will produce steric self-repulsion before mixing. Moreover, it can be assumed that electrostatic self-repulsion will decrease with increase in the ionic strength of the aqueous medium and that steric repulsion will increase with increased bulkiness of the group. Furthermore, it has been shown that reduction of electrostatic interaction by increase in the ionic strength of the aqueous medium has greater effect at the planar air/aqueous interface than at the convex micellar surface in aqueous medium and that bulkiness in the hydrophobic group has a greater steric effect in the convex mixed micellar interior than in the mixed monolayer at the planar air/aqueous solution interface.[51g] Ion-dipole interactions will be significant in ionic – nonionic systems only after mixing of the two components. van der Waals

interactions are always attractive and depend upon the length, degree of branching, and closeness of packing of the hydrophobic groups.

These principles permit interpretation of the values of the beta parameters observed in many binary mixtures, both in mixed monolayers and in mixed micelles in aqueous medium. In order to ensure the validity of both the β^{σ} and β^{M} values for the nonionic – ionic mixtures to be discussed, they were all measured in 0.1M NaCl. Thus, all interactions, both before and after mixing, were in media of the same ionic strength.

4.2 Dilution Effect After Mixing

In Table 10, the beta values are typical of what has been observed in numerous mixtures of this type. The values of both β^{σ} and β^{M} are negative. This indicates that the interactions between the two different surfactants after mixing (W_{AB}) are more attractive or less repulsive than before mixing. Before mixing, the ionic surfactant, A, has a strong electrostatic self-repulsion (W_{AA}); the nonionic, B, a steric self-repulsion (W_{BB}), whose magnitude depends upon the size of the head group. Upon mixing, both of these interactions are weakened by a dilution effect (Figure 12). Thus, even when the average A_{min} value for the ionic surfactant before mixing is the same as the average A_{min} value for the mixture after mixing (e.g., the $C_{12}SO_3Na$ – $C_{12}GA$ system in Table 1), as shown in Figure 12, the distance between the self-repelling ionic surfactant molecules will be much larger after mixing, making the repulsion interaction, W_{AB}, less than the average self-repulsion before mixing, $\frac{1}{2}(W_{AA} + W_{BB})$, and, in some cases, replaced by

Table 10. Some Ionic – Ionic and Ionic – Nonionic mixtures in 25 ºC and 0.1M NaCl Medium

System (A – B mixture)	α_{non}	X_{non}^{σ}	X_{non}^{M}	β^{σ}	β^{M}	Individual A_{min}(Å^2) A	B	Mixture (Å^2) A_{expt} [c]	A_{ideal}	A_{expt} - A_{ideal}
C_8SO_4Na – C_8TAB [a, 115]				-14.2	-10.2	70	61	32		
$C_{12}SO_4Na$ – $C_{12}TAB$ [a, 116]				-27.8	-25.5	53	57	30.5		
$C_{12}SO_4Na$ – $C_{12}N^+H_2(CH_2)_2COO^-$ [a, 117]				-15.7	-14.1	53				
$C_{12}SO_3Na$ – $C_{12}\phi SO_3Na$ [b, 118]				-0.3	-0.3	37	46			
$C_{14}EO_8$ – $C_{12}EO_4$	0.164	0.39	0.52	-0.33	0.0	52	41.4	45.0	45.5	-0.5
$C_{12}SO_3Na$ – 1,2–C_{12} diol [97]				-3.03	-1.45	37	26	26		
$C_{12}SO_3Na$ –1,2–C_{10} diol	0.256	0.44	0.30	-2.66	-1.16	37	24	28.9	31.3	-2.4
	0.614	0.60	0.54	-2.75	-1.34	37	24	28	29.2	-1.2
	0.805	0.70	0.67	-2.70	-1.38	37	24	26.9	27.9	-1.0
$C_{12}SO_3Na$ – C_{12}-GA	0.0533	0.40	0.31	-2.76	-1.74	37	42.6	37.0	39.2	-2.2
	0.213	0.56	0.52	-2.73	-1.8	37	42.6	37.5	40.1	-2.6
	0.567	0.72	0.72	-2.81	-1.85	37	42.6	38.0	41.0	-3.0
$C_{12}SO_3Na$ – $C_{12}EO_4$	0.0100	0.45	0.34	-1.62	-0.88	37	41.4	40.5	39.0	1.5
	0.0254	0.59	0.50	-1.57	-0.84	37	41.4	42.0	39.6	2.4
	0.0603	0.71	0.66	-1.53	-0.80	37	41.4	42.1	40.1	2.0
$C_{12}TAC$ – $C_{12}EO_4$	0.00402	0.59	0.41	-1.79	-0.38	56	41.4	47.1	47.4	-0.3
	0.00793	0.67	0.55	-1.86	-0.34	56	41.4	47.1	46.2	0.9
	0.0198	0.78	0.74	-1.82	-0.33	56	41.4	44.9	44.6	0.3

α_{non}: molar fraction of nonionic surfactant in the bulk solution.
$C_{12}\phi SO_3Na$: commercial material
a: in H_2O medium
b: 30 ºC
c: mixture A_{min} is the area per hydrophobic group

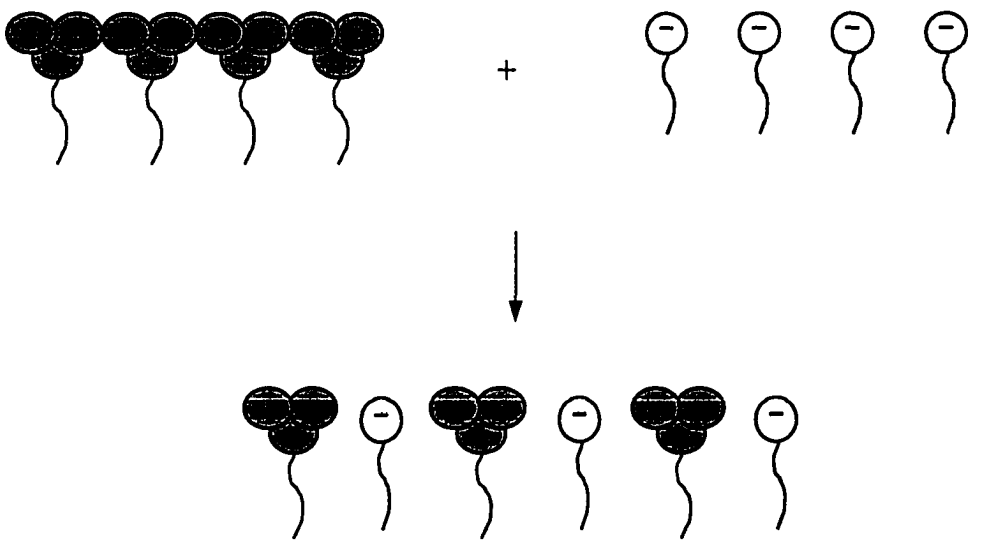

Figure 12. Decrease in electrostatic self-repulsion and steric repulsion after mixing, with equal area/molecule at air / aqueous solution interface before and after mixing.

electrostatic or ion-dipole attractions, yielding negative values for β. In those cases where steric interactions are weak (i.e., nonionic head groups are relatively small and hydrophobic groups are linear), the value of β^{σ} is more negative than β^{M}, since reduction of the electrostatic repulsion of the ionic group has a greater effect at the planar air/aqueous solution interface than at the convex micelle surface.[51g] Also, two hydrophobic groups can more easily be accommodated at the planar air/aqueous solution interface than in the interior of a spherical or cylindrical micelle.

For the C_8SO_4Na – C_8TAB system, there are strong electrostatic self-repulsions of the individual components before mixing and strong attractive

interactions between them after mixing, yielding large β^{σ} and β^{M} values. The even larger values of β^{σ} and β^{M} for the $C_{12}SO_4Na$ – $C_{12}TAB$ system can be ascribed to the larger electrostatic self-repulsion before mixing, as indicated by their smaller area/molecule before mixing, and larger van der Waals attraction between the longer hydrophobic groups of this system after mixing, compared to the C_8SO_4Na – C_8TAB system.

The much smaller negative values of both β^{σ} and β^{M}, for $C_{12}SO_4Na$ – $C_{12}N^{+}H_2(CH_2)_2COO^{-}$ system, compared to $C_{12}SO_4Na$ – $C_{12}TAB$ system, is probably due to the much weaker self-repulsion of the zwitterionic, $C_{12}N^{+}H_2(CH_2)_2COO^{-}$, before mixing and its weaker electrostatic attraction for the anionic, $C_{12}SO_4Na$, after mixing.

When the two ionic surfactants have electrical charges of the same sign (the $C_{12}SO_3Na$ – $C_{12}\phi SO_3Na$ mixture), it can be expected that the magnitude of their self-repulsion before mixing and mutual repulsion after mixing will be similar, yielding β values close to zero.

For the anionic – nonionic systems, $C_{12}SO_3Na$ –1,2–C_{10} diol and $C_{12}SO_3Na$ –1,2–C_{12} diol, we can assume that whereas there will be significant electrostatic self-repulsion for the anionic, $C_{12}SO_3Na$, before mixing, there will be only weak steric self-repulsion for the nonionic1,2–C_{10} diol, before mixing. After mixing, the electrostatic self-repulsion of the ionic will be replaced by ion-dipole attraction between the two different hydrophilic groups. The cross sectional area A_{min} values of the two surfactants, $C_{12}SO_3Na$ and 1,2–C_{10} diol, at the air/aqueous

solution interface before mixing, are 37 $Å^2$ and 24 $Å^2$, respectively. The ideal mixing values, A_{ideal}, calculated from the equation: $A_{ideal} = X_1A_1 + (1-X_1)A_2$, where X_1 refers to molar fraction of component 1 in mixed monolayer, A_1 and A_2 designate the ionic and nonionic surfactant respectively, are all slightly larger than the corresponding experimental values, A_{expt}. This reduction upon mixing is presumably due to ion-dipole attractive interaction and possibly, hydrogen bonding between the two surfactants in the mixed monolayer. The reduction of the electrostatic self-repulsion of the anionic surfactant and its replacement by ion-dipole attractive interaction after mixing of the two surfactants results in negative β values. The very small area/molecule after mixing also implies strong van der Waals attraction between the hydrophobic groups after mixing. Similar considerations apply to the $C_{12}SO_3Na$ –1,2–C_{12} diol system, where the reduction of the area/molecule at the air/aqueous solution interface is even larger after mixing, and the β^{σ} value more negative than for the $C_{12}SO_3Na$ –1,2–C_{10} diol system.

These interactions may also occur in the $C_{12}SO_3Na$ – $C_{12}GA$ system, in which the nonionic surfactant contains multiple hydroxyl groups capable of hydrogen bonding. Again, A_{expt} is smaller than A_{ideal}, indicating contraction upon mixing, producing a negative β^{σ} value close to that of the $C_{12}SO_3Na$ – 1,2–C_{10} diol system.

It is known that a polyoxyethylene chain containing several oxyethylene units in the presence of a large anion or an anionic surfactant acquires a weak

positive charge.[97,119,120] The expansion upon mixing ($A_{expt} > A_{ideal}$) seen in the $C_{12}SO_3Na - C_{12}EO_4$ system, may be due to the acquisition of this positive charge by the polyoxyethylene chain in the presence of the anionic surfactant, $C_{12}SO_3Na$, resulting in an increase in the area per molecule of the nonionic at the air/aqueous solution interface. Since the A_{min} value of the nonionic used in calculating A_{ideal} is the head group size of the nonionic in the absence of a positive charge on it, this may make A_{ideal} too small, also resulting in $A_{expt} > A_{ideal}$. This expansion is not seen when $C_{12}SO_3Na$ is mixed with other non-polyoxyethylenated nonionics, C_{12}–GA, 1,2–C_{10} diol or 1,2–C_{12} diol. Since $C_{12}SO_3Na$ has a relatively small A_{min} value (37 $Å^2$), it is possible that there is some van der Waals self-attraction between the hydrophobic portions of the molecule before mixing, which is reduced upon mixing with the polyoxyethylenated nonionic, also contributing to the expansion observed. This expansion of cross-sectional area after mixing in the adsorbed film at the air/aqueous solution interface, for the system of C_8EO_4 and sodium dodecyl sulfate, despite the attractive interaction between them, has also been observed by Matsubara et al.[121]

The hydrophilic head group of the nonionic surfactant in the system, $C_{12}SO_3Na - C_{12}EO_4$, is also more bulky than that in the $C_{12}SO_3Na$ – 1,2–C_{10} diol system. This should result in weaker ion-dipole interaction after mixing, which may account for the less negative β values compared to those of the $C_{12}SO_3Na$ – 1,2–C_{10} diol system. The β^{σ} value is more negative than β^{M} value because of the

greater difficulty to incorporating two hydrophobic groups in the interior of the convex micelle.

In the case of the $C_{12}TAC - C_{12}EO_4$ mixture, there is negligible expansion upon mixing of the two surfactants, and this is expected, since the polyoxyethylene group would not acquire a positive charge when mixed with a cationic surfactant. The negative β^{σ} value, consequently, is presumably due to the decrease in self-repulsion of the cationic and the decrease in steric self-repulsion of the nonionic upon mixing, due to the dilution effect mentioned previously. Again, the β^{M} value is less negative than β^{σ}, due to the greater difficulty of incorporating the hydrophobic group in the convex micelle than at the planar air/aqueous solution interface.

Table 11. Effect of Increase in the Length of the Polyoxyethylene Group of the Nonionic Surfactant

System	β^{σ}	β^{M}	Ionic	Nonionic	Mixture ($Å^2$)		A_{expt} -
			$A_{min}(Å^2)$	$A_{min}(Å^2)$	A_{expt}	A_{ideal}	A_{ideal}
$C_{12}SO_3Na - C_{12}EO_4$	-1.57	-0.84	37	41.4	42.0	39.6	+2.4
$C_{12}SO_3Na - C_{12}EO_7$	-1.73	-2.38	37	50	46	44.3	+1.7
$C_{12}SO_3Na - C_{14}EO_4$	-1.08	-0.48	37	33.6	40	34.7	+5.3
$C_{12}SO_3Na - C_{14}EO_8$	-1.43	-2.0	37	52	50	45.4	+4.6
$C_{12}E_2S - C_{12}EO_4$	-1.43	-0.89	47	41.4	40.7	43.7	-3.0
$C_{12}E_2S - C_{12}EO_6$	-1.50	-1.95	47	51	45.6	49.3	-3.7
$C_{12}TAC - C_{12}EO_4$	-1.82	-0.33	56	41.4	44.9	44.6	+0.3
$C_{12}TAC - C_{12}EO_7$	-1.76	-1.23	56	50	51.5	52	-0.5

4.3 Effect of Increase in the Size of the Hydrophilic Group

When the length of the polyoxyethylene group of the nonionic becomes even larger (Table 11), its steric effect becomes larger. A bulky hydrophilic group is more readily accommodated at the surface of a convex micelle in aqueous solution than at the planar air/aqueous solution interface.[122] Consequently, there is greater reduction of the steric self-repulsion, after mixing of the nonionic, at the former location than at the latter. The negative value of β^M is consequently increased relative to the β^σ value.

There is also the acquisition of a positive charge by the polyoxyethylene group, which should be greater when the length of the polyoxyethylene group is increased. This would cause attractive interaction with the anionic surfactant in both the mixed monolayer and mixed micelle. The effect of the greater positive charge on the longer polyoxyethylene chain is seen in the anionic – nonionic systems in Table 11, causing less expansion or greater contraction upon mixing, resulting in more negative β^σ values, compared to analogous systems with shorter chain polyoxyethylene nonionic surfactants. The greater ease in accommodating a bulky polyoxyethylene group at the convex micellar surface relative to the planar air/aqueous solution interface, and the electrostatic interaction between the anionic surfactant and the positively charged polyoxyethylene group, results in β^M values more negative than β^σ values in anionic – nonionic mixtures with larger polyoxyethylene chains. Matsubara et al also reported the relatively stronger interaction in the mixed micelle than in the

adsorbed film at the air/aqueous solution interface for a mixture of sodium dodecyl sulfate and a polyoxyethylenated nonionic,[121] and ascribed it to the more favorable conformation for the attractive interaction in the mixed micelle. Anionic – polyoxyethylenated nonionic mixtures are the only systems observed to date where β^M is more negative than β^σ.[122] As before, in the systems where $C_{12}SO_3Na$ is part of the mixture, the van der Waals self-attraction of the anionic before mixing, and its reduction upon mixing it with a bulky nonionic, may be a contributor to the expansion observed after mixing. Note that this expansion does not occur with the anionic, $C_{12}E_2S$, which has a considerably larger cross-sectional area at the air/aqueous solution interface before mixing, and consequently should show less van der Waals self-attraction before mixing.

No expansion upon mixing is seen when $C_{12}EO_7$ is mixed with the cationic surfactant, $C_{12}TAC$, since the polyoxyethylene chain of the nonionic surfactant would not be expected to acquire a positive charge when mixed with a cationic surfactant. The β^σ value is also about the same as for the $C_{12}TAC$ – $C_{12}EO_4$ system, indicating no increase in attractive interaction with increase in the length of the polyoxyethylene chain, in contrast to that observed with the anionic – polyoxyethylene nonionic systems. Again, the β^M values are less negative than β^σ values.

The $C_{12}SO_3Na$ – $C_{14}EO_4$ and the $C_{12}SO_3Na$ – $C_{14}EO_8$ mixtures, with alkyl chains of different length, when compared to the $C_{12}SO_3Na$ – $C_{12}EO_4$ and $C_{12}SO_3Na$ – $C_{12}EO_7$ system, respectively, and the $C_{12}SO_3Na$ – 1,2–C_{10} diol

mixture, when compared to the $C_{12}SO_3Na$ – 1,2–C_{12} diol system (Table 10), illustrate the effect of van der Waals attraction between the hydrophobic groups after mixing, which is greater when the lengths of the two groups are equal, resulting in larger negative values for both β^{σ} and β^{M}. This effect has been observed previously.[97]

Table 12: Effect of Increase in the Size of the Hydrophilic Group of Anionic Surfactant in Anionic – Nonionic Mixtures in 0.1M NaCl Medium

System	β^{σ}	β^{M}	Ionic $A_{min}(Å^2)$	Nonionic $A_{min}(Å^2)$	Mixture ($Å^2$) A_{expt}	A_{ideal}	A_{expt} - A_{ideal}
$C_{12}SO_3Na$ – C_{12}-GA	-2.76	-1.74	37	42.6	37.0	39.2	-2.2
$C_{12}E_2S$ – C_{12}-GA	-1.76	-1.2	47	42.6	42	44.8	-2.8
$C_{12}SO_3Na$ – $C_{12}EO_7$	-1.73	-2.38	37	50	46	44.3	+1.7
$C_{12}E_2S$ – $C_{12}EO_7$	-1.15	-1.53	47	50	45.1	48.8	-3.7
$C_{12}SO_3Na$ –1,2–C_{10} diol	-2.70	-1.38	37	24	26.9	27.9	-1.0
$C_{12}E_2S$ – 1,2–C_{10} diol	-1.39	≈ 0	47	24	31	33.7	-2.7
$C_{12}SO_3Na$ – $C_{12}EO_7$	-1.73	-2.38	37	50	46	44.3	+1.7
$C_{12}C_3G$ – $C_{12}EO_6$	-0.69	-1.23	55	51	54	52.2	+1.8
$C_{12}MeOC_3G$ – $C_{12}EO_6$	-0.69	-0.83	57	51	54	52.8	+1.2
$C_{12}SO_3Na$ – TMN6	-1.74	-2.07	37	54	43	48.4	-5.4
$C_{12}C_3G$ – TMN6	-1.35	-1.19	55	54	54	54.3	-0.3
$C_{12}MeOC_3G$ – TMN6	-0.78	0.0	57	54	54	54.7	-0.7

When the size of the hydrophilic group of the ionic surfactant at the air/aqueous solution interface is increased, then we can expect that its

electrostatic self-repulsion before mixing will decrease and that there will also be a decrease in ion-dipole attraction between the hydrophilic groups of the two surfactants after mixing. This will result in a decrease in the negative value of β^{σ}, and possibly also of β^{M}, and this can be seen (Table 12) in the $C_{12}E_2S$ – containing, $C_{12}C_3G$ – containing and $C_{12}MeOC_3G$ – containing anionic – nonionic systems, when compared to the $C_{12}SO_3Na$ – containing anionic – nonionic systems.

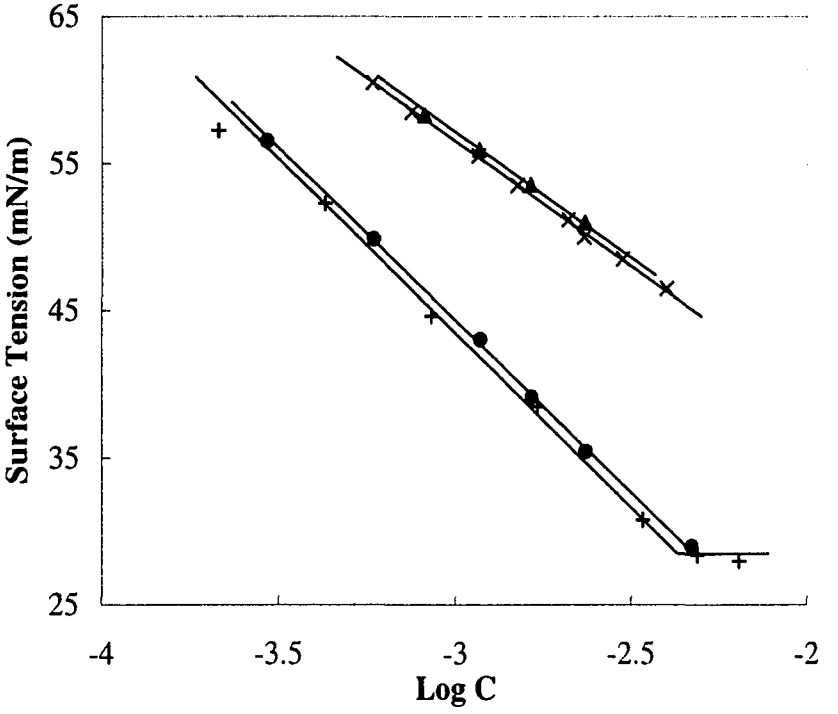

Figure 13. Surface tension vs. log C plots of 5,6 – C_{10}diol, 4,5 – C_{10}diol and their mixtures with ionic surfactants in 0.1M NaCl at 25°C. ▲: 5,6 – C_{10}diol; x: 4,5 – C_{10}diol; •: 5,6 – C_{10}diol / $C_{12}SO_3Na$ (α_{non} = 0.638); +: 4,5 – C_{10}diol/$C_{12}SO_3Na$ (α_{non} = 0.655). α_{non}: the molar fraction of nonionic surfactant in the bulk solution.

As stated above, for the mixed systems of ionic surfactant and nonionic surfactant, both β^{σ} and β^{M} values will be negative in most cases, since the ionic surfactant molecules will be further apart from each other upon mixing with the nonionic surfactant molecules. We can assume that the further apart the ionic surfactant molecules are after mixing, the greater the decrease in electrostatic self-repulsion. Table 13 shows mixtures of the same ionic surfactants with nonionic surfactants having the same hydrophilic and hydrophobic groups, but with the hydrophilic group at different positions in the hydrophobic group. Replacement of the terminal 1,2–diol by an internal 5,6–diol or 4,5–diol, which has a relatively much larger cross sectional area (data from Figure 13), should produce much weaker self-repulsion after mixing, and consequently, more negative β^{σ} values. In addition, in the 1,2–diol, with its very small area/molecule (24 $Å^2$) at the air/aqueous solution interface, there is much stronger van der Waals attractive interaction before mixing that must be overcome upon mixing, than in the internal diols, where the area/molecule (56 $Å^2$) is much larger.

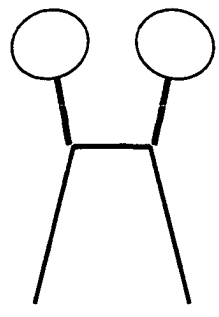

Figure 14: Gemini-like structures of internal 4,5–C_{10} and 5,6–C_{10} diols.

Table 13. Effect of Position of the Hydrophilic group in the Molecule

System	medium	X_{non}^{σ}	β^{σ}	Nonionic A_{min} (Å^2)	Mixture (Å^2) A_{expt}	A_{ideal}	A_{expt} - A_{ideal}
$C_{12}SO_3Na$ – 1,2–C_{10} diol	0.1M NaCl	0.60	-2.70	24	26.9	27.9	-1.0
$C_{12}SO_3Na$ – 4,5–C_{10} diol*	0.1M NaCl	0.34	-3.23	56	39.6	43.5	-3.9
$C_{12}SO_3Na$ – 5,6–C_{10} diol*	0.1M NaCl	0.33	-3.38	56	39.6	43.4	-3.8

*: Data from figure 11.

Finally, the 4,5–C_{10} and 5,6–C_{10} diols have the structure at the air/aqueous solution interface shown in Figure 14. The presence of the hydrophilic groups between the two hydrophobic chains makes it possible that there exists van der Waals attractive interaction between these hydrophobic groups and the hydrophobic chains of neighboring anionic molecules. This combination of stronger van der Waals attractive interaction in the terminal diol before mixing, and weaker self-repulsion and stronger van der Waals attraction in the internal diols after mixing, make the values of β^{σ} more negative when the diol is internal, rather than terminal.

4.4 Effect of Branching of the Hydrophobic Group

Branching of the hydrophobic group in the ionic surfactant should decrease self-repulsion before mixing with a second surfactant, if this branching results in an increase in the area per molecule of the surfactant at the interface. It may also decrease ion-dipole attractive interaction with the second surfactant after mixing at the planar air/aqueous solution interface. On the other hand, after mixing with a second surfactant in a micelle, there should be greater difficulty in incorporating

the branched hydrophobic chain, compared to a linear hydrophobic group, into the interior of the micelle.

In the AOT – 1,2–C_{10} diol system (Table 14), the bulky anionic, which has a 72 $Å^2$ area/molecule, should show little electrostatic self-repulsion before mixing with the nonionic, but some steric self-repulsion. The 1,2–C_{10} diol, on the other hand, with its small area/ molecule should show strong van der Waals self-attraction before mixing. After mixing, the AOT should show reduction of the steric self-repulsion of the hydrophobic groups because of the mixing with the linear hydrophobic group of diol. On the other hand, the strong van der Waals self-attraction in 1,2–C_{10} diol will be considerably reduced by mixing with the bulky hydrophobic groups of AOT. In addition, there will be little ion-dipole interaction (or even hydrogen bonding) in the AOT – 1,2–C_{10} diol system, because of the large area/molecule of the AOT. The result is a net expansion of the average area/molecule upon mixing, with A_{expt} of 53 $Å^2$ significantly larger than the A_{ideal} value of 48 $Å^2$. These may account for the much smaller negative β^{σ} value (-1.27) of the AOT – 1,2–C_{10} diol system, compared to the $C_{12}SO_3Na$ – 1,2–C_{10} diol system (-2.70). In the AOT – $C_{12}EO_6$ system, on the other hand, the A_{expt} value is smaller than the A_{ideal} value, indicating a small net attractive interaction between the two surfactants after mixing. This may be due to the positive charge on the long polyoxyethylene chain of the nonionic surfactant and the weakened repulsion between the anionic head groups after mixing because of the bulkiness of that chain. Therefore, as compared to the $C_{12}SO_3Na$ – $C_{12}EO_7$

Table 14. Effect of Branched or Multiple Hydrophobic Groups in Ionic – Nonionic Mixtures

System	β^{σ}	β^{M}	Ionic $A_{min}(Å^2)$	Nonionic $A_{min}(Å^2)$	Mixture ($Å^2$) A_{expt}	A_{ideal}	A_{expt} - A_{ideal}
$C_{12}SO_3Na$ –1,2–C_{10} diol	-2.75	-1.34	37	24	28	29.2	-1.2
AOT –1,2–C_{10} diol	-1.27	-1.22	72	24	52.6	48	+4.6
$C_{12}SO_3Na$ – $C_{12}EO_7$	-1.73	-2.38	37	50	46	44.3	+1.7
AOT – $C_{12}EO_6$	-1.64	-1.47	72	51	63	64	-1.0
$C_{12}SO_3Na$ – $C_{14}EO_8$	-1.43	-2.0	37	52	50	45.4	+4.6
AOT – $C_{14}EO_8$	-2.05	-0.23	72	52	65.3	66	-0.7
$C_{12}SO_3Na$ – $C_{12}EO_7$	-1.73	-2.38	37	50	46	44.3	+1.7
$C_{12}SO_3Na$ – TMN6	-1.74	-2.07	37	54	43	48.4	-5.4
$C_{12}E_2S$ – $C_{12}EO_6$	-1.50	-1.95	47	51	51	49.3	+1.7
$C_{12}E_2S$ – TMN6	-1.64	-0.89	47	54	51	51.7	-0.7
$C_{12}MeOC_3G$ – $C_{12}EO_6$	-0.69	-0.83	57	51	54	52.8	+1.2
$C_{12}MeOC_3G$ – TMN6	-0.78	0.0	57	54	54	54.7	-0.7
$C_{12}C_3G$ – $C_{12}EO_6$	-0.69	-1.23	55	51	54	52.2	+1.8
$C_{12}C_3G$ – TMN6	-1.35	-1.19	55	54	54	54.3	-0.3
AOT – TMN6	-0.47	-0.49	72	54	66	63.2	+2.8

system, there is only a small reduction in the negative value of β^{σ} because of the branching, but a considerable decrease in the negative value of β^{M}, because of the difficulty of incorporating a bulky hydrophilic group in the micelle.

In the AOT – $C_{14}EO_8$ system, the AOT, as mentioned above, because of its large area/molecule at the air/aqueous solution interface, should show relatively less electrostatic self-repulsion and some steric self-repulsion of the hydrophobic group before mixing. The $C_{14}EO_8$, on the other hand, should show steric repulsion of the bulky hydrophilic groups before mixing. Upon mixing, each of these steric repulsions should be reduced at the planar air/aqueous solution interface. The bulky hydrophobic groups of the AOT will be mixed with the linear hydrophobic groups of the $C_{14}EO_8$, while the bulky hydrophilic groups of the $C_{14}EO_8$ will be mixed with the small hydrophilic groups of the AOT. This results in a small contraction in the average area/molecule at the planar air/aqueous solution interface, A_{expt} 65.3 $Å^2$ and A_{ideal} 66 $Å^2$, compared to the expansion shown by the $C_{12}SO_3Na$ – $C_{14}EO_8$ system, and a larger negative β^{σ} value than that system. On the other hand, it is still difficult to accommodate the two-branched hydrophobic groups of AOT in the interior of the convex micelle and β^{M} is close to zero.

Branching in the hydrophobic group of the nonionic surfactant produces effects in the ionic – nonionic mixtures that are attributable mainly to steric effects. Four systems were investigated in which the anionic surfactant has a linear hydrophobic group and the nonionic surfactant (TMN6) has a highly

branched, bulky hydrophobic group: $C_{12}SO_3Na$ – TMN6, $C_{12}E_2S$ – TMN6, $C_{12}C_3G$ – TMN6, $C_{12}MeOC_3G$ – TMN6. In contrast to the analogous systems that contain the nonionic surfactant, $C_{12}EO_6$ (Table 14), which has a linear hydrophobic group, and which showed expansion at the air/aqueous solution interface upon mixing, the TMN6 – containing systems showed contraction after mixing. At first, this appears contrary to what would be expected. However, the cross-sectional area of a nonionic surfactant molecule with a highly branched, bulky hydrophobic group, when its polyoxyethylene group acquires a positive charge in the presence of an anionic surfactant, will possibly not increase. This lack of increase in the cross-sectional area of the molecule will make its ion-dipole attractive interaction after mixing with the latter stronger than when the hydrophobic group is linear. In addition, the bulky hydrophobic group of the TMN6 should produce greater steric repulsion in the molecule before mixing than the linear hydrophobic group of $C_{12}EO_6$. And there will also be greater reduction of electrostatic self-repulsion of the anionic upon mixing with the bulky nonionic. This larger decrease of the original steric repulsion and the greater reduction of the original electrostatic repulsion upon mixing of the TMN6 with the anionic surfactant, by the dilution effect described above, could account for its lack of expansion and the somewhat more negative β^{σ} value of the TMN6 – containing systems, compared to the corresponding $C_{12}EO_6$ – containing ones. The less negative β^{M} values of TMN6 – containing mixtures, compared to the analogous $C_{12}EO_6$ – containing mixtures, are again due to the greater difficulty of

incorporating a branched hydrophobic group, compared to linear one, into the interior of a spherical or cylindrical micelle.

In the AOT – TMN6 system, in contrast to the other TMN6 – containing systems in Table 12, there is expansion upon mixing. Since, with bulky hydrophobic groups in both surfactants determining the area per molecule at the interface, both before and after mixing, there should be only a small dilution effect after mixing (Figure 15). The result is that both β^{σ} and β^{M} values are very small.

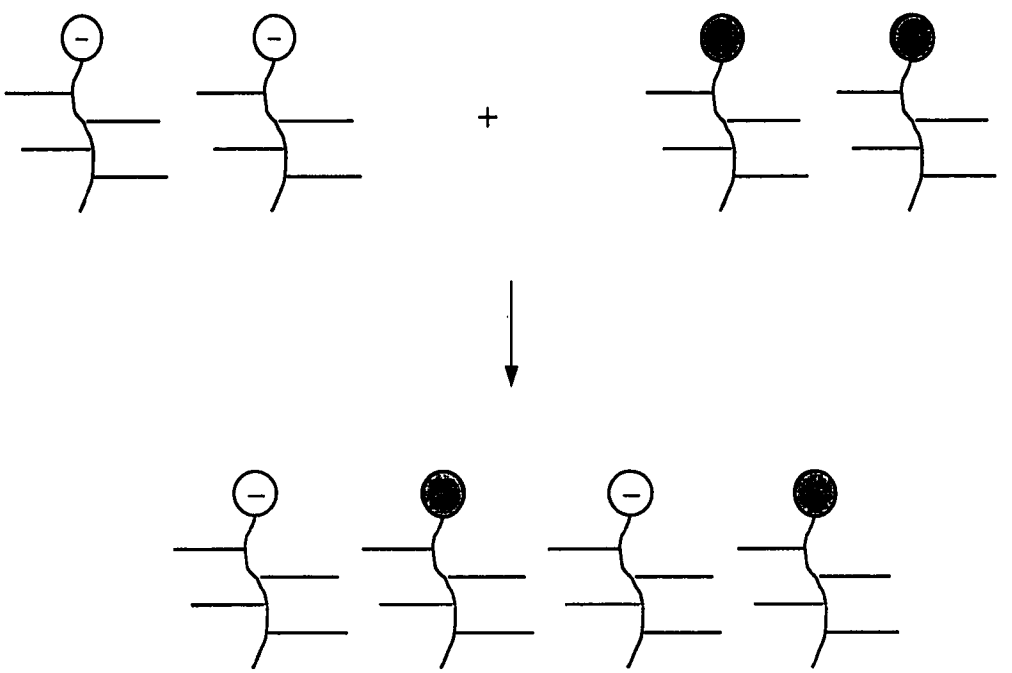

Figure 15. Surfactants, both with bulky hydrophobic groups, showing only a small dilution effect after mixing.

4.5 Effect of Counter-Cations

The effect of different counter-cations, e.g., Li^+, NH_4^+ and K^+, on beta parameters of anionic – POE nonionic surfactant mixtures was investigated, as compared to the Na^+ medium. Figure 16 shows the surface tension curves of $C_{12}SO_3Na$ in 0.1M LiCl, 0.1M NaCl, 0.1M KCl and 0.1M NH_4Cl mediums, respectively. It is clear that the surface activity of $C_{12}SO_3^-$ in those univalent counter-cation mediums is in the order of $NH_4^+ \approx K^+ > Na^+ > Li^+$. The corresponding surface properties of $C_{12}SO_3Na$ in those media are listed in Table 15. Figure 17 shows the change of the surface properties of $C_{12}SO_3$ with the change of the radius of hydrated counter-cations.

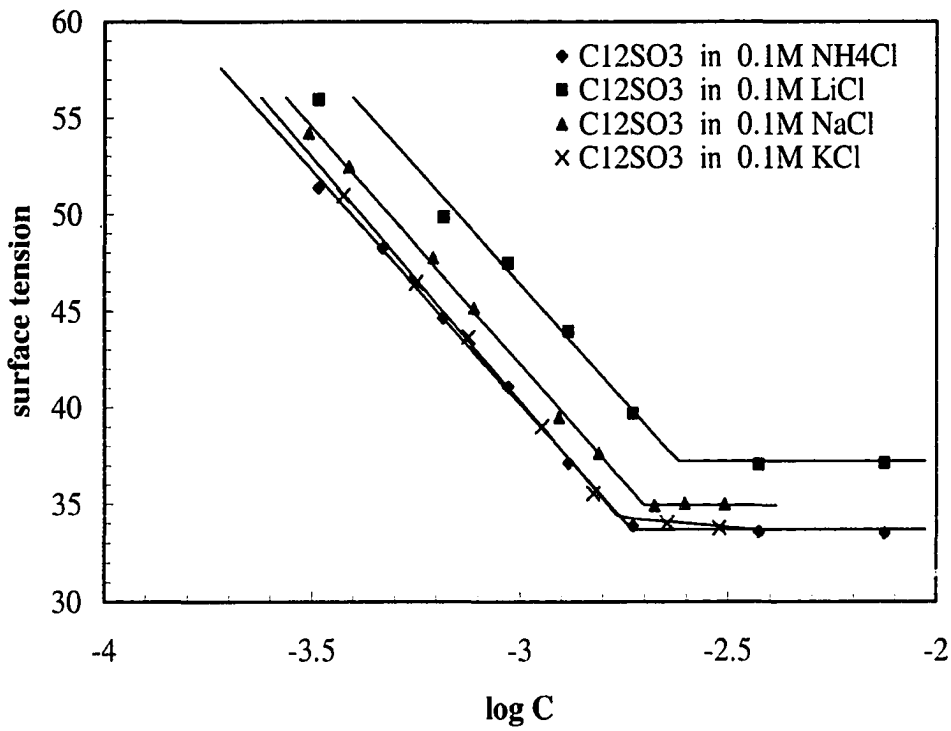

Figure 16. Plots of surface tension curves of $C_{12}SO_3Na$ in 0.1M LiCl, 0.1M NaCl, 0.1M KCl and 0.1M NH_4Cl medium.

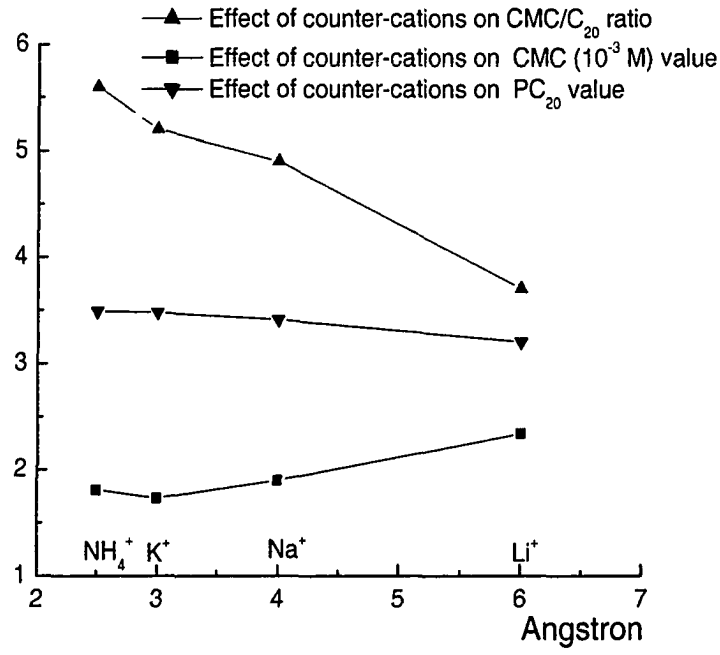

Figure 17. Plots of the surface properties of $C_{12}SO_3$ vs. radius of hydrated counter-cations.

Table 15. Surface Properties of Anionic Surfactant in Different Counter-Ion Media, at 25°C Without any pH Adjustment

compound	medium	CMC (M)	γ_{CMC} mN/m	PC_{20}	$\Gamma \times 10^{10}$ mol/cm^2	A_{min} Å^2	CMC/C_{20}
$C_{12}SO_3Na$	0.1M KCl	1.73E-3	34.0	3.48	4.56	36	5.2
$C_{12}SO_3Na$	0.1M LiCl	2.34E-3	37.1	3.20	4.63	36	3.7
$C_{12}SO_3Na$	0.1MNH_4Cl	1.81E-3	33.6	3.49	4.28	39	5.6
$C_{12}SO_3Na$	0.1M NaCl	1.90E-3	35.0	3.41	4.49	37	4.9
$C_{12}E_2S$	0.1M NaCl	3.13E-4	35.2	4.37	3.5	47	7.3
$C_{12}E_2S$	0.05M $CaCl_2$	1.47E-4	31.4	4.76	3.96	41.9	8.5
$C_{12}E_2S$	0.033M $CaCl_2$	1.58E-4	31.7	4.70	4.01	41.4	7.9

For anionic surfactant $C_{12}SO_3^-$, its surface-active performance depends on the properties of the counter-cation present, when the rest of the conditions (ionic strength, temperature, solvent etc) are the same. Increased binding of the

counter-ion, in aqueous solution, causes a decrease in the CMC of the ionic surfactant. Table 15 shows the CMC of $C_{12}SO_3^-$ in the order of $Li^+ > Na^+ > NH_4^+ > K^+$. The CMC/C_{20} ratio, measuring the relative effects of some structural or micro-environmental factor on micellization and on adsorption, is increased greatly by the use of a more tightly bound counter-ion, because reduction in the electrical charge of the surfactant produces a larger decrease in C_{20} than in CMC. From Table 15, CMC/C_{20} ratio of $C_{12}SO_3^-$ is in the order of $NH_4^+ > K^+ > Na^+ > Li^+$. The efficiency of adsorption of a surfactant at the air/aqueous solution interface, as measured by the pC_{20} value, is increased by use of a more tightly bound (less hydrated) counter-ion. pC_{20} values of $C_{12}SO_3^-$ show the same order as the CMC/C_{20} ratio. So, from the view of pC_{20} and CMC/C_{20} ratio, NH_4^+ is the most tightly bound counter-ion, and from the view of CMC, NH_4^+ is only less tightly bound than K^+. On the other hand, the slightly higher A_{min} value of $C_{12}SO_3^-$ in 0.1M NH_4Cl medium than in the other studied mediums indicates that NH_4^+ is possibly the least tightly bound counter-cation among them. The strength of the binding (electrostatic) between anionic surfactant head group SO_3^- and its counter-cation affects both the interfacial and micellar properties of the surfactant. So, even when mixed with the same POE nonionic surfactant, $C_{12}SO_3^-$ should experience different molecular interaction in the strength, as measured by the beta parameters. Also different effects in the mixed micelle and mixed monolayer should be produced, due to the greater reduction of electrostatic interaction at the planar air/aqueous interface than at the convex micellar surface in aqueous medium.

Surface and micellar properties of the mixed system of $C_{12}SO_3Na$ and POE nonionic surfactants in different ionic media have been examined, for the experimental calculation of beta parameters in both the mixed micelle and the mixed monolayer. Table 16 shows the results. As typical for anionic – POE nonionic surfactant mixtures, all the measured beta parameters are negative, indicating that upon mixing, there exists an interaction more attractive or less repulsive than the self-interaction of the two surfactants before mixing. The absolute values of the beta parameters indicate the strength of the interaction between the two surfactants upon mixing and also the extent of the deviation of the mixture solution from the ideal behavior.

In all cases of both β^{σ} and β^{M}, except for β^{M} in the $C_{12}SO_3Na$ – $C_{12}EO_7$ system, the order of increasing negative β parameter is: $Li^+ > Na^+ > Ca^{2+}$. That is, the weaker the binding of the counter-ion to the anionic surfactant, the more negative the value of β^{σ} or β^{M}. Since the polyoxyethylene chain of the nonionic is basic, rather than acidic, i. e. the oxygen groups are electron rich, it is difficult to see why a more negative anionic surfactant (whose counter-ion is more loosely bound) would interact more strongly with the nonionic after mixing with it. On the other hand, if the self-repulsion of the anionic surfactant before mixing is considered, the self-repulsion of the anionic surfactant with a more loosely bound counter-ion would be greater than one with a more tightly bound counter-ion, and that could account for the increase in negative value of the β parameter as the degree of binding of the counter-ion becomes looser.

Table 16. Effect of Different Counter-Ions on Beta Parameters of Anionic – POE Nonionic Surfactant Mixtures

system	medium	α_{non}	X_1^{σ}	X_1^{M}	β^{σ}	β^{M}
$C_{12}SO_3Na$ / $C_{12}EO_7$	0.1M LiCl	0.0311	0.60	0.50	-2.05	-1.88
$C_{12}SO_3Na$ / $C_{12}EO_7$	0.1M NH_4Cl	0.0378	0.55	0.50	-1.83	-2.01
$C_{12}SO_3Na$ / $C_{12}EO_7$	0.1M NaCl	0.0381	0.56	0.50	-1.73	-2.38
$C_{12}SO_3Na$ / $C_{12}EO_4$	0.1M LiCl	0.0232	0.61	0.52	-2.09	-1.02
$C_{12}SO_3Na$ / $C_{12}EO_4$	0.1M NH_4Cl	0.0255	0.56	0.50	-1.94	-0.75
$C_{12}SO_3Na$ / $C_{12}EO_4$	0.1M NaCl	0.0254	0.59	0.50	-1.57	-0.84
$C_{12}SO_3Na$ / $C_{14}EO_8$	0.1M LiCl	0.00598	0.59	0.55	-2.10	-2.33
$C_{12}SO_3Na$ / $C_{14}EO_8$	0.1M NH_4Cl	0.00598	0.52	0.55	-1.83	-0.97
$C_{12}SO_3Na$ / $C_{14}EO_8$	0.1M NH_4Cl	0.00795	0.56	0.58	-1.93	-1.03
$C_{12}SO_3Na$ / $C_{14}EO_8$	0.1M NaCl	0.007	0.56	0.54	-1.43	-2.0
$C_{12}SO_3Na$ / $C_{14}EO_4$	0.1M LiCl	0.00404	0.68	0.59	-1.37	-1.07
$C_{12}SO_3Na$ / $C_{14}EO_4$	0.1M NH_4Cl	0.00499	0.63	0.59	-1.59	-1.45
$C_{12}SO_3Na$ / $C_{14}EO_4$	0.1M NH_4Cl	0.00792	0.70	0.66	-1.41	-1.30
$C_{12}SO_3Na$ / $C_{14}EO_4$	0.1M NaCl	0.00632	0.68	0.632	-1.08	-0.48
$C_{12}E_2S$ / $C_{12}EO_7$	0.1M NaCl	0.198	0.59	0.48	-1.15	-1.53
$C_{12}E_2S$ / $C_{12}EO_7$	0.05M $CaCl_2$	0.358	0.54	0.50	-1.18	-1.14
$C_{12}E_2S$ / $C_{12}EO_7$	0.033M $CaCl_2$	0.343	0.55	0.50	-1.02	-0.91
$C_{12}E_2S$ / $C_{12}EO_4$	0.05M $CaCl_2$	0.250	0.54	0.50	-1.0	-0.24
$C_{12}E_2S$ / $C_{12}EO_4$	0.033M $CaCl_2$	0.246	0.55	0.51	-1.03	-0.17
$C_{12}E_2S$ / $C_{12}EO_4$	0.1M NaCl	0.149	0.59	0.50	-1.43	-0.89

The effect of the NH_4^+ counter-ion is difficult to explain. This may be because it has two effects: 1) its degree of binding, which is stronger than that of Na^+, and this should make its β parameters less negative than that with Na^+, and 2) its acidity, which could protonate the basic oxygen atoms in polyoxyethylene group of the nonionic after mixing with the anionic; this should make the interaction of the latter stronger after mixing, with a consequent more negative β parameter. Thus, in some cases (the β^M values for the $C_{12}SO_3Na$ – $C_{12}EO_4$, $C_{12}SO_3Na$ – $C_{12}EO_7$ and $C_{12}SO_3Na$ – $C_{14}EO_8$ systems) the β value is less negative than that of Na^+ (the effect of the tighter binding) and in other cases (the β^σ values for the $C_{12}SO_3Na$ – $C_{12}EO_4$, $C_{12}EO_7$, $C_{14}EO_8$, $C_{14}EO_4$ systems and the β^M values for the $C_{12}SO_3Na$ – $C_{14}EO_4$ system) the β value is more negative than that for Na^+ (possibly the effect of acidity from NH_4^+).

4.6 Conclusion

Dilution upon mixing is believed to be a major cause of the negative beta parameters observed for ionic – nonionic surfactant mixtures, mainly by decreasing the electrostatic self-repulsion of the ionic surfactant after mixing. In anionic – POE nonionic surfactants mixture systems, more tightly bound counter-cations present in the bulk phase solution produce less negative β^σ and β^M values, presumably because the resulted decrease in electrical double layer of anionic surfactant head groups and the corresponding decrease in the strength of its electrostatic self-repulsion before mixing generate less reduction on electrostatic self-repulsion of the ionic surfactant upon mixing.

Larger attractive van der Waals interaction between neighboring hydrophobic chains after mixing two longer straight-chain surfactants produces stronger surfactant molecular interaction, resulting in more negative beta parameters, compared to two shorter chain surfactants.

Increase in the size of the hydrophilic group of ionic surfactant in anionic – nonionic surfactant mixtures decreases electrostatic self-repulsion of the ionic surfactant before mixing, and produces less interaction energy reduction after mixing, resulting in less negative beta values. When increase in the size of the hydrophilic group of the nonionic surfactant is caused by increased length of the polyoxyethylene chain, there is an increased interaction energy reduction after mixing, presumably because of the positive charge on the polyoxyethylene chain of the nonionic surfactant upon mixing with the anionic surfactant, resulting in more negative beta values.

The greater difficulty of incorporating a branched hydrophobic chain into the interior of the micelle, compared to the corresponding linear hydrophobic chains, produces less negative β^M values. Branching in the hydrophobic group of the ionic surfactant (AOT) decreases electrostatic self-repulsion before mixing with a nonionic surfactant. Branching in the hydrophobic group of the nonionic surfactant (TMN6) produces greater interaction energy reduction upon mixing with a linear chain anionic surfactant, due to the greater steric repulsion in the bulky molecule of TMN6 before mixing, resulting in slightly more negative β^σ values than with the corresponding linear hydrophobic chain nonionic surfactant.

Chapter 5.

Surfactant-Surfactant Molecular Interactions in Mixed Monolayers at a Highly Hydrophobic Solid/Aqueous Solution Interface and Their Relationship to Enhanced Spreading on the Solid Substrate

5.1 Spreading on Purified Polyethylene Film

Previous work in our laboratory[123] has shown that the spreading enhancement of aqueous solutions on a highly hydrophobic substrate by surfactant mixtures of L77 and N-alkyl pyrrolidones corresponds to stronger molecular interaction at the solid/aqueous solution interface than molecular interaction at the air/aqueous or air/solid interfaces, as indicated by their β_{SL}^{σ} and β_{LA}^{σ} values, and the enhancement of adsorption of the surfactant mixture onto the solid substrate. When a liquid spreads on a solid surface, a precursor film (leading film) is formed surrounding the drop due to the Marangoni effect.[124] The surface tension gradient at the edge of the solution drop is thought to be the driving force for the spreading. A simple scheme of surfactant solution spreading on purified polyethylene film is shown in Figure 18. As the spreading front stretches, concentration of the solution in the precursor film decreases because of the adsorption of surfactant at the solid/aqueous solution interface.

Consequently, the surface tension increases at the front relative to the top of the droplet, thereby establishing a surface tension gradient. The greater and faster the adsorption at the solid/aqueous solution interface, the sharper the gradient, and the faster the spreading.

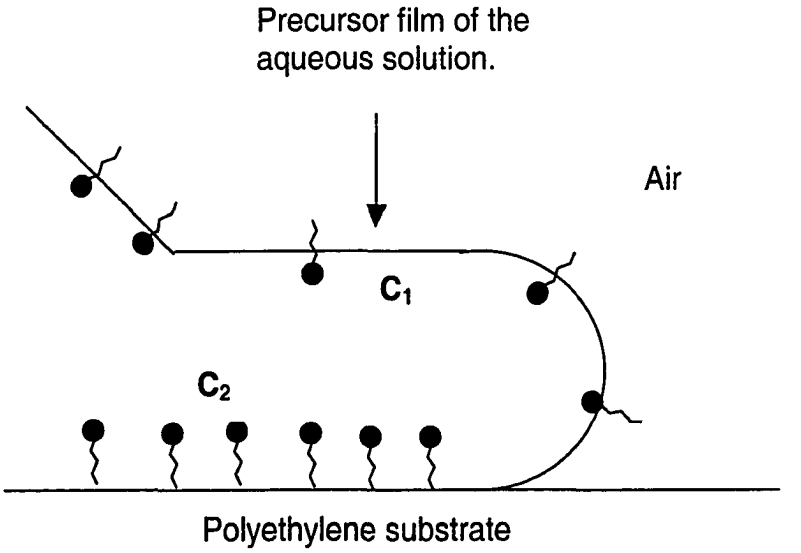

Figure 18. Precursor film of aqueous surfactant solution on polyethylene substrate, with surfactant concentration gradient $C_1 < C_2$, due to the greater adsorption of the surfactant at the solid/liquid than that at air/liquid interface.

The spreading coefficient at the solid/liquid interface ($S_{L/S}$) is quantitatively defined as: $S_{L/S} = \gamma_{SA} - (\gamma_{SL} + \gamma_{LA})$, where γ_{SA} is the interfacial tension of the solid substrate with liquid-saturated air above it, γ_{SL} is the interfacial tension at the solid substrate/liquid interface, and γ_{LA} is the surface tension of the liquid. The quantity $\gamma_{SA} - (\gamma_{SL} + \gamma_{LA})$ is a measure of the driving force behind the spreading

process. When $S_{L/S}$ is positive, the spreading process can occur spontaneously. When $S_{L/S}$ is negative, the liquid will not spread spontaneously over the substrate. Furthermore, it is expected that the more positive the spreading coefficient, the greater the spreading area made by the liquid over the substrate. Since spreading is a dynamic process, it is possible that the value of the spreading coefficient, $S_{L/S}$, will not be a constant during the process of spreading of the solution.

Figure 19 shows the spreading results of some aqueous solutions of surfactants on purified polyethylene film, for both individual and mixed surfactant solutions. The mixed solutions of surfactant CA-520 and C8P show better spreading on purified polyethylene film than either individual component in both H_2O and 0.1M NaCl media. The maximal spreading enhancement occurs when there is *ca.* 60% (wt%) replacement by C8P in the mixed surfactant solution, with larger enhancement from the mixed surfactant solution in 0.1M NaCl medium. On the other hand, no spreading enhancement is observed for either of the mixed solutions C8P / C_4H_9O-$PhSO_3Na$ or C8P / $C_{12}EO_4$. Figure 20 shows the effect of C12P replacement on spreading enhancement from the mixed solution of C12P / C_4H_9O-$PhSO_3Na$. The maximal spreading enhancement in this system also occurs when there is *ca.* 60% (wt%) replacement by C12P in the mixture solution, with somewhat larger enhancement from the mixed solution in 0.1M NaCl medium.

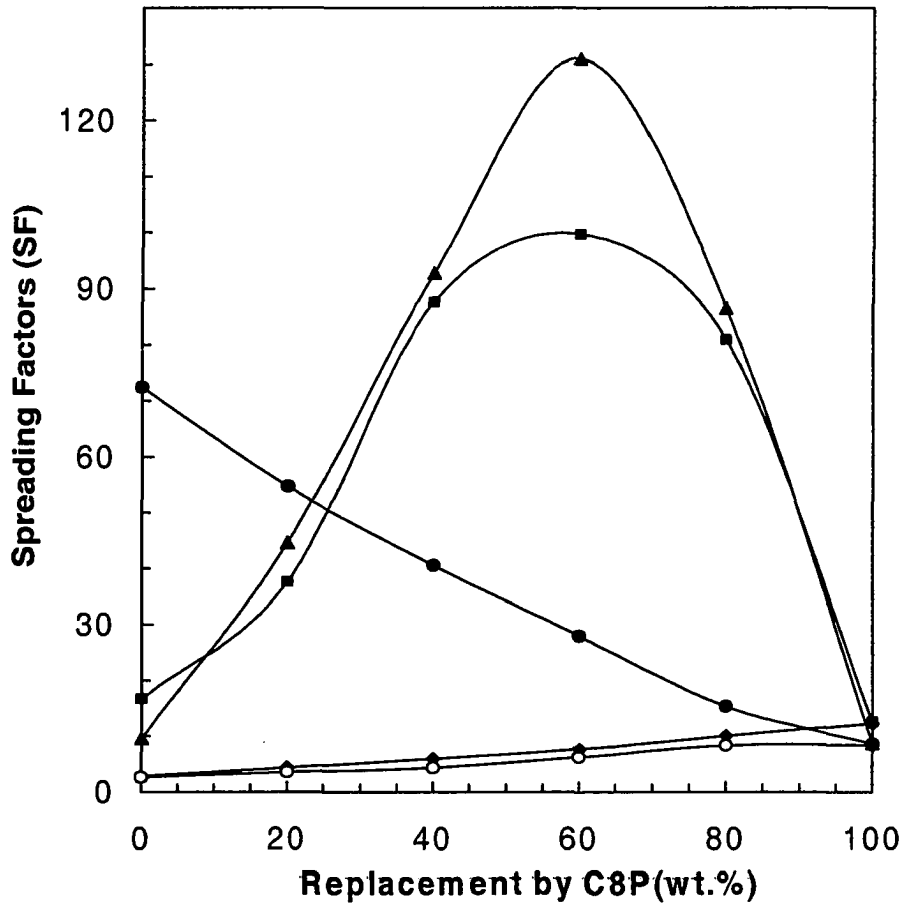

Figure 19. Effect of C8P replacement on spreading factors of some surfactant mixture systems on purified polyethylene film, total concentration for the mixture is 1.0g/L. ▲: CA-520 / C8P system in 0.1M NaCl medium, ■: CA-520 / C8P system in H_2O, ◆: $C_4H_9OPhSO_3Na$ / C8P system in H_2O, ○: $C_4H_9OPhSO_3Na$ / C8P system in 0.1M NaCl, ●: $C_{12}EO_4$ / C8P system in 0.1M NaCl.

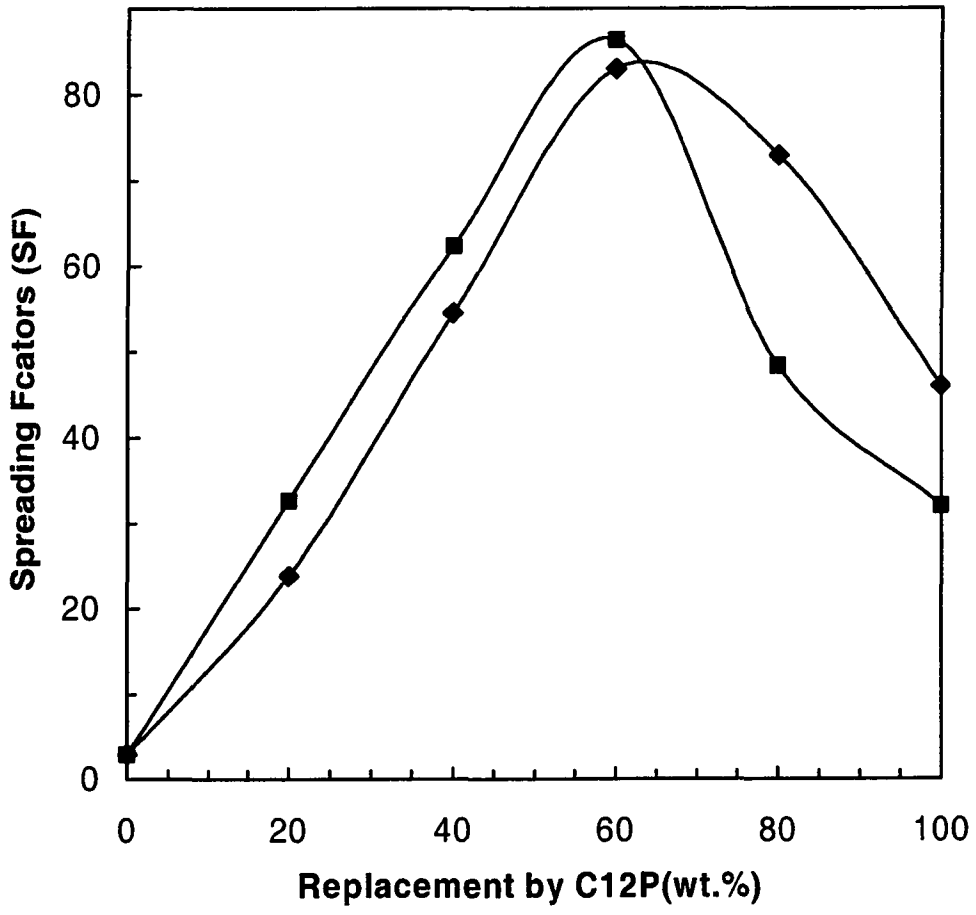

Figure 20. Effect of C12P replacement on spreading factors of some surfactant mixture systems on purified polyethylene film, total concentration for the mixture is 1.0g/L. ■: $C_4H_9OPhSO_3Na$ / C12P system in 0.1M NaCl medium, ◆: $C_4H_9OPhSO_3Na$ / C12P system in H_2O.

In our current investigation, we are studying the relationship between spreading enhancement, adsorption, molecular interaction and dynamic contact angles. For convenience of comparison, in all the surfactant mixtures studied, the molar fractions of the components in the mixed solutions, used for the study of adsorption isotherms, molecular interactions and dynamic contact angles, have been picked according to the condition that produces maximal spreading enhancement with the mixed surfactant solutions.

5.2 Adsorption Enhancement from Mixed Solutions

Figures 21 and 22 show the difference between adsorption of the individual surfactants from their pure solutions and from their mixed surfactant solutions for the CA-520 / C8P system in 0.1M NaCl medium, with fixed initial α values (all α values shown in subsequent figures are fixed initial values). Clearly, C8P has greater adsorption from the pure C8P surfactant solution than from the mixed surfactant solution. But CA-520 in the mixture shows a substantial increase in adsorption compared to that from a pure CA-520 surfactant solution. Since CA-520 contributes much more than C8P to the total adsorption from the CA-520 / C8P mixture solution under the conditions of this study, the resulting observed adsorption from the CA-520 / C8P mixture is higher than its calculated ideal adsorption, as shown in Figure 23. Here, the ideal adsorption of the mixture is the sum of the individual adsorptions of the two components obtained from their individual adsorption isotherms at the same individual bulk phase concentrations of the two components as in the mixture at that same initial α value.

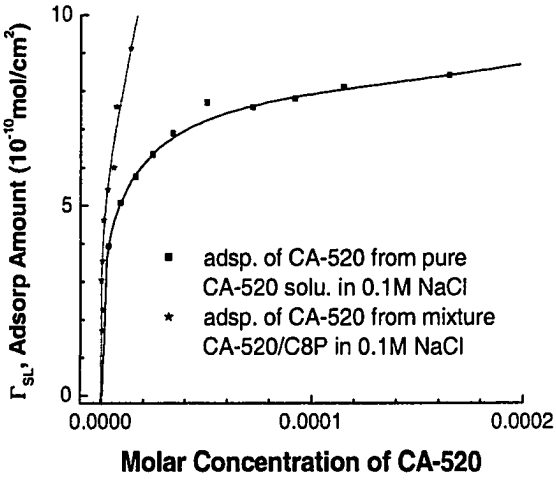

Figure 21. Increased adsorption of CA-520 from the C8P/CA-520 mixture relative to a pure CA-520 solution in 0.1M NaCl medium.

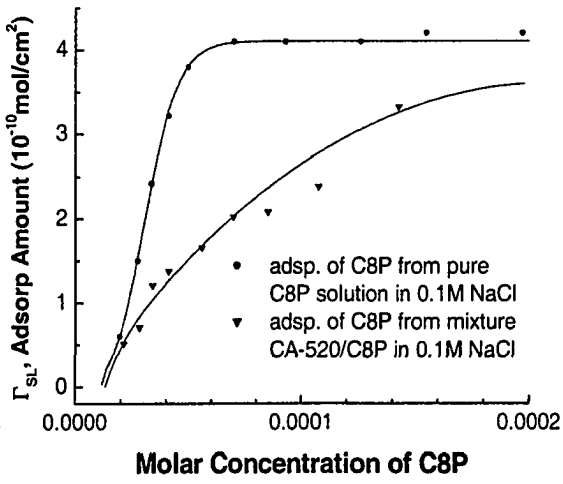

Figure 22. Decreased adsorption of C8P from the C8P / CA-520 mixture relative to a pure C8P solution in 0.1M NaCl medium

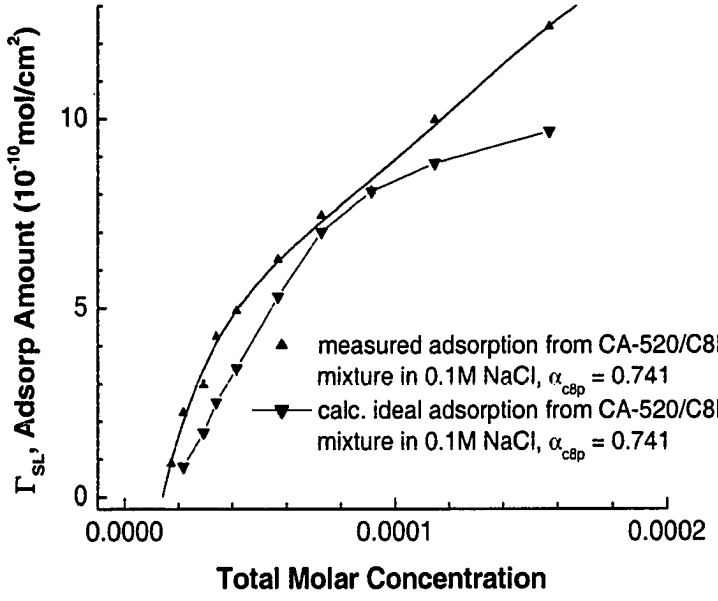

Figure 23. Increased adsorption from the C8P/CA-520 mixture, compared to its calculated ideal adsorption, in 0.1M NaCl medium.

The adsorption difference between the CA-520/C8P mixed solution and its individual components in H_2O is almost the same as in 0.1M NaCl medium. Again, there is stronger adsorption of C8P from pure C8P solution than from the mixture, but stronger adsorption of CA-520 from the mixture than from the pure CA-520 solution. And since CA-520 contributes more than C8P to the total adsorption from the CA-520 / C8P mixture under the conditions of the study, the resulting total adsorption from the CA-520 / C8P mixture in H_2O is higher than its calculated ideal adsorption, as shown in Figures 24 –26. The observed increase in the adsorption after mixing CA-520 and C8P surfactants does not change with the medium change from 0.1M NaCl to H_2O, only more adsorption amount has been observed in the latter medium.

Compared to the adsorption of C8P in H_2O, C8P shows a substantial decrease in adsorption amount onto purified polyethylene powder in 0.1M NaCl medium. Calculated A_{min} (area per molecule) values indicate that there is monolayer adsorption formation on hydrophobic polyethylene powder in 0.1M NaCl medium, but multilayer adsorption formation on polyethylene powder in H_2O. The decreased adsorption and monolayer formation on polyethylene powder have also been observed in phosphate buffer medium[125]. The decrease of the adsorption in high ionic strength medium may be ascribed to the stabilization of the ionic resonance structure of C8P by the NaCl in the solution, as shown in Figure 27. Since ionic surfactants usually show monolayer adsorption onto nonpolar hydrophobic surfaces, ionic-like C8P surfactant in high ionic strength medium presumably results in the monolayer adsorption.

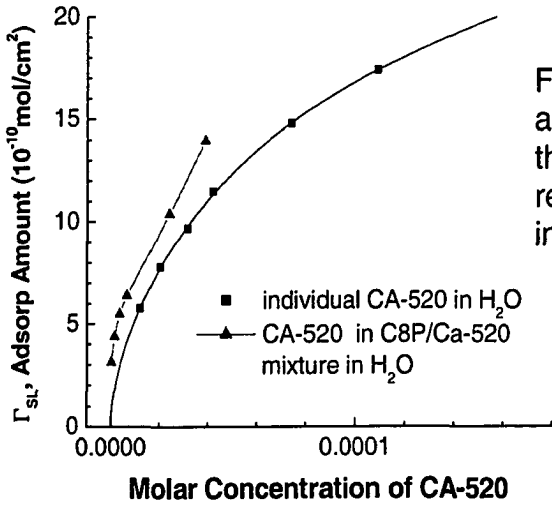

Figure 24. Increased adsorption of CA-520 from the C8P/CA-520 mixture relative to a pure solution in H_2O.

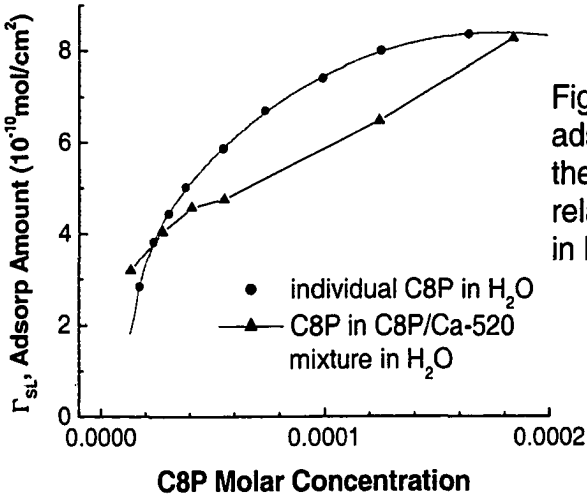

Figure 25. Decreased adsorption of C8P from the C8P/CA-520 mixture relative to a pure solution in H_2O.

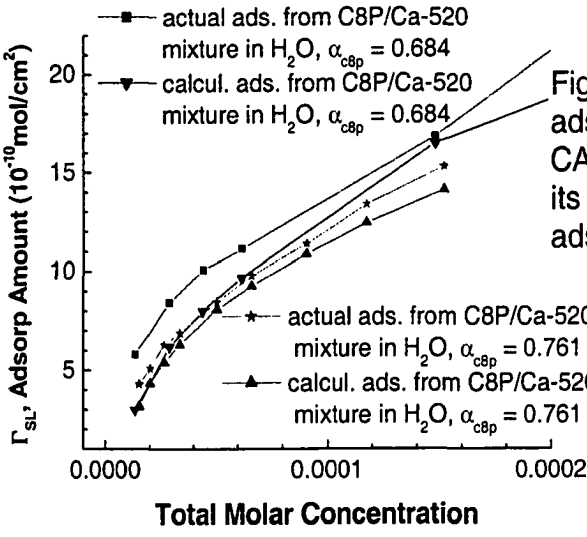

Figure 26. Increased adsorption from the C8P / CA-520 mixture compared to its calculated ideal adsorption, in H_2O.

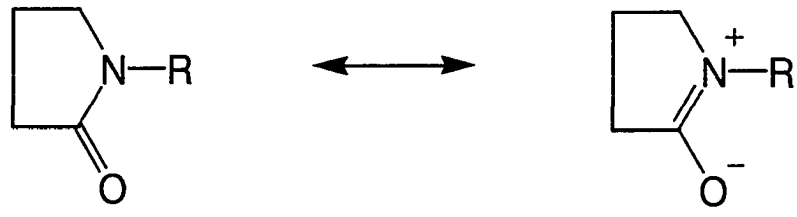

nonionic structure zwitterionic structure

Figure 27. Stabilization of the ionic-like structure of pyrrolidone in high ionic strength medium.

For the mixed system, C8P / C_4H_9O-$PhSO_3Na$, both C_4H_9O-$PhSO_3Na$ and C8P show higher adsorption from their pure solutions than from their mixed solutions in both 0.1M NaCl and H_2O media, as shown in Figures 28 – 33. Consequently, the measured total adsorption of C8P + C_4H_9O-$PhSO_3Na$ from the mixed solutions is lower than that calculated for ideal adsorption, and these systems show no synergistic enhancement of the spreading factors.

Compared to C8P, the individual C12P solution has a much higher adsorption (Figure 34), because of the longer hydrophobic alkyl chain and its limited solubility in aqueous solution. Even in the C12P / C_4H_9O-$PhSO_3Na$ mixture solution, where C12P can be completely dissolved, it still shows very high adsorption ability. Because of this extraordinarily strong adsorption ability, there is no apparent difference between the adsorption of C12P from a pure solution and from the C12P / C_4H_9O-$PhSO_3Na$ mixed solution. On the other

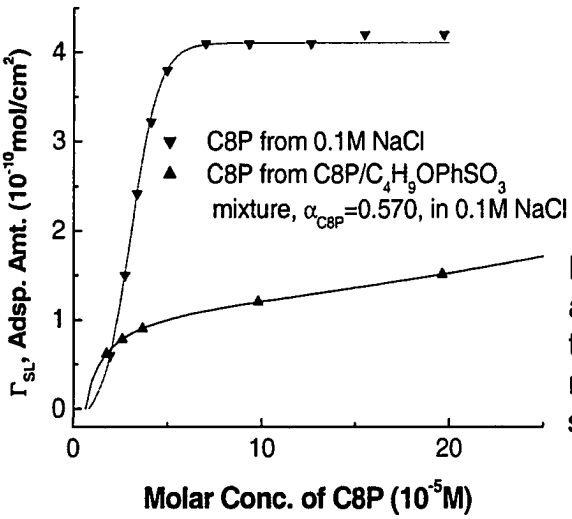

Figure 28. Decreased adsorption of C8P from the $C8P/C_4H_9OPhSO_3$ mixture relative to a pure solution in 0.1M NaCl.

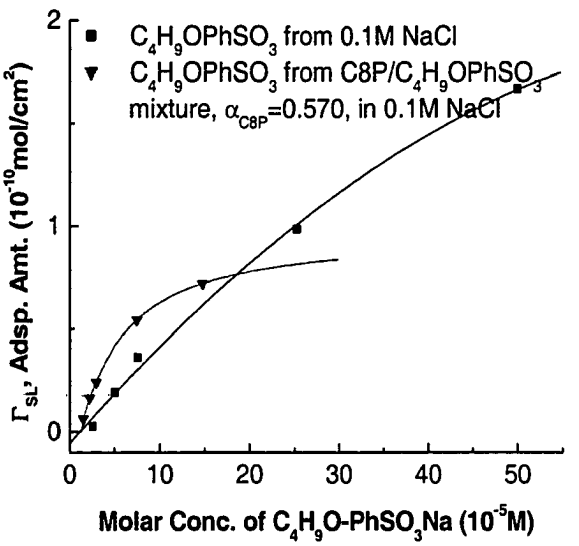

Figure 29. Decreased adsorption of C_4H_9Oph-SO_3 from the C8P / $C_4H_9OPhSO_3$ mixture relative to a pure solution in 0.1M NaCl.

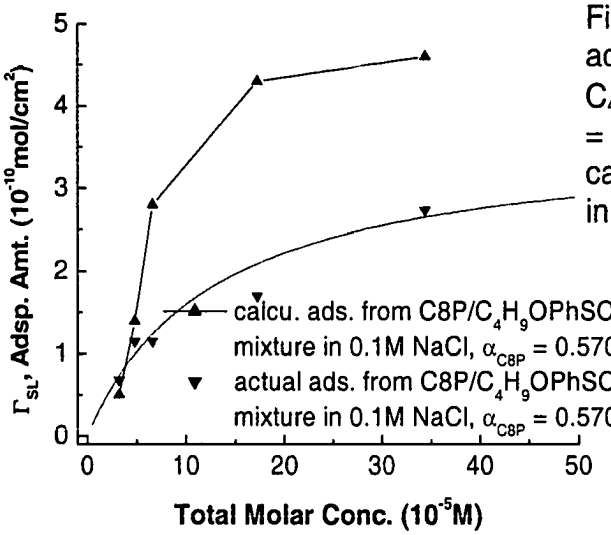

Figure 30. Decreased adsorption from the C8P / $C_4H_9OPhSO_3$ mixture, α_{C8P} = 0.570, compared to its calculated ideal adsorption, in 0.1M NaCl.

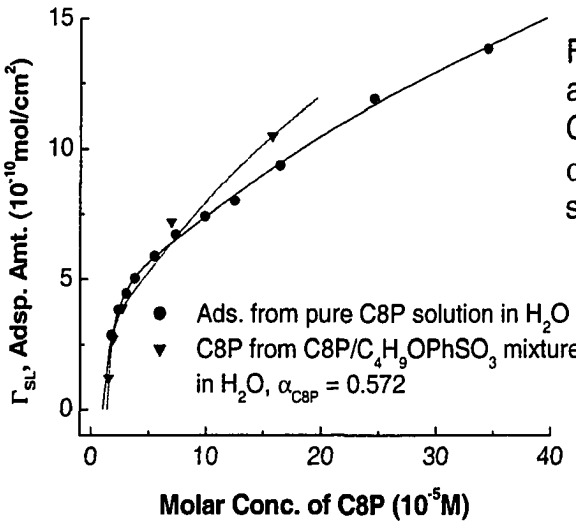

Figure 31. Almost the same adsorption of C8P from the $C_4H_9OPhSO_3$ / C8P mixture, α_{C8P}=0.572, as from a C8P solution in H_2O.

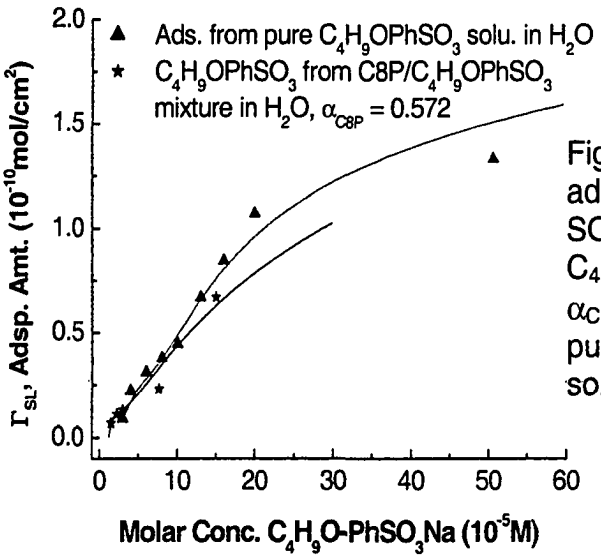

Figure 32. Decreased adsorption of C_4H_9OPh-SO_3 from the C8P / $C_4H_9OPhSO_3$ mixture, α_{C8P}=0.572, relative to a pure $C_4H_9OPhSO_3$ solution in H_2O.

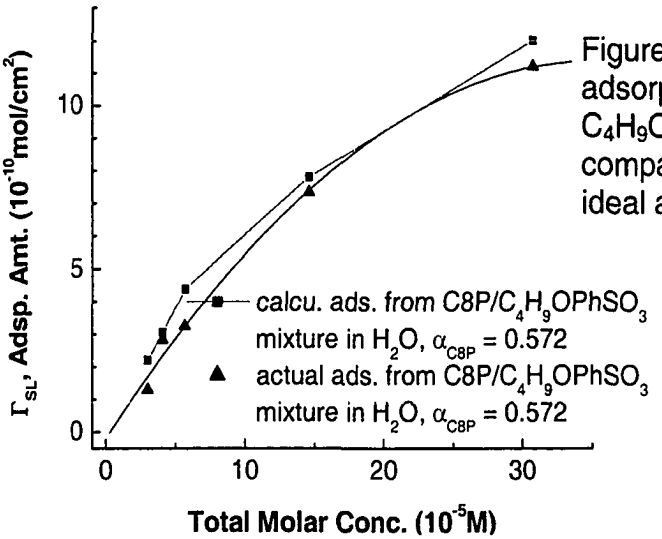

Figure 33. Decreased adsorption from the C8P / $C_4H_9OPhSO_3$ mixture, compared to its calculated ideal adsorption in H_2O.

hand, in the presence of C12P, C_4H_9O-$PhSO_3Na$ in the mixture shows much higher adsorption than from a pure C_4H_9O-$PhSO_3Na$ solution in both H_2O and 0.1M NaCl media (Figures 35 and 36). Also the resulting observed total adsorptions from the C12P / C_4H_9O-$PhSO_3Na$ solutions are higher than the correspondingly calculated ideal adsorptions from the mixture, as shown in Figures 37 and 38.

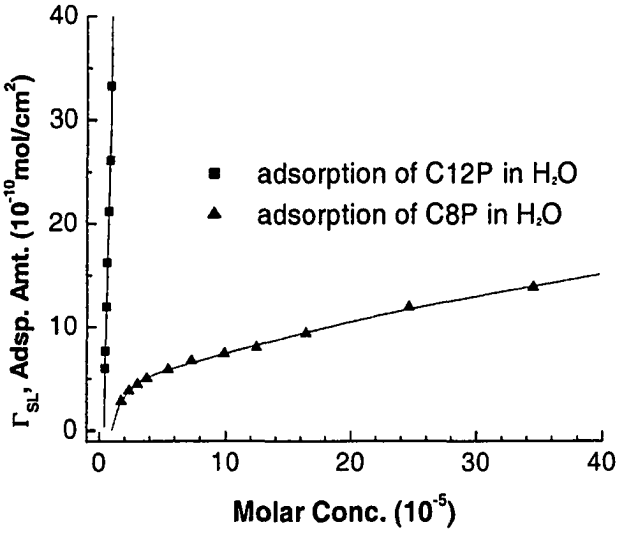

Figure 34. Comparison of the adsorptions of C8P and C12P in H_2O.

5.3 Dynamic Contact Angles

Contact angles of aqueous solutions on a solid substrate measure the hydrophobic/hydrophilic property of the solid. A high contact angle against water means a highly hydrophobic surface of the solid. The hydrophobic surface of a solid can be modified to be more hydrophilic by adsorbing surfactant molecules with their hydrophilic head groups oriented towards the aqueous phase, and then lower contact angles towards the aqueous solution result. Therefore, the

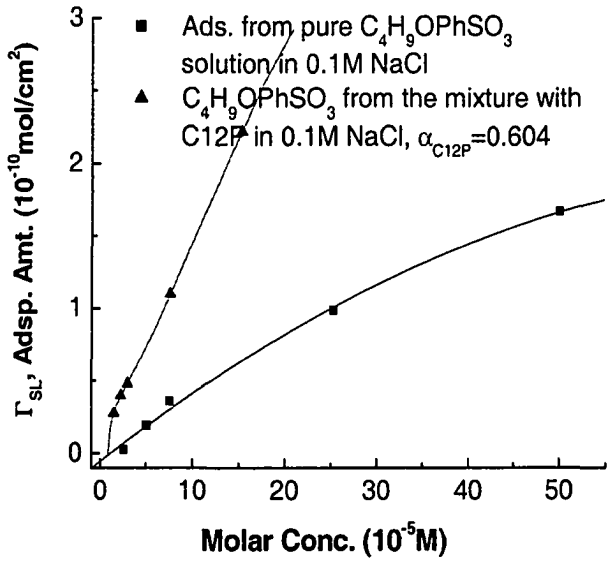

Figure 35. Increased adsorption of $C_4H_9OPhSO_3Na$ from the C12P/$C_4H_9OPhSO_3Na$ mixture, relative to a pure solution in 0.1M NaCl medium.

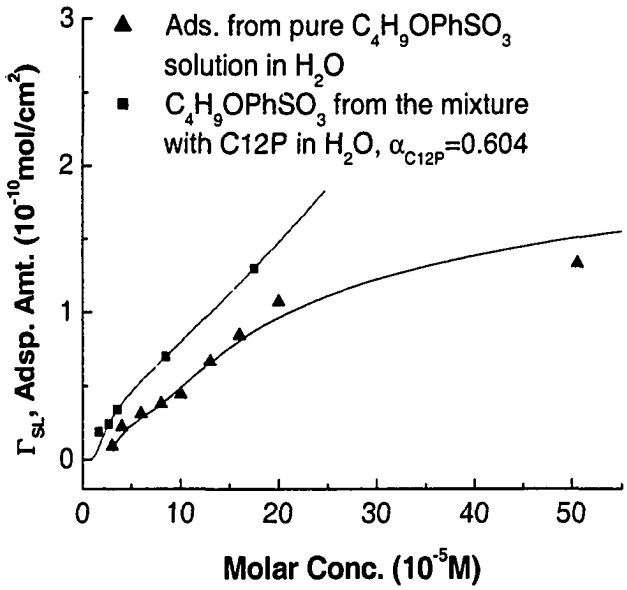

Figure 36. Increased adsorption of $C_4H_9OPhSO_3Na$ from the C12P/$C_4H_9OPhSO_3Na$ mixture, relative to a pure $C_4H_9OPhSO_3Na$ solution in H_2O.

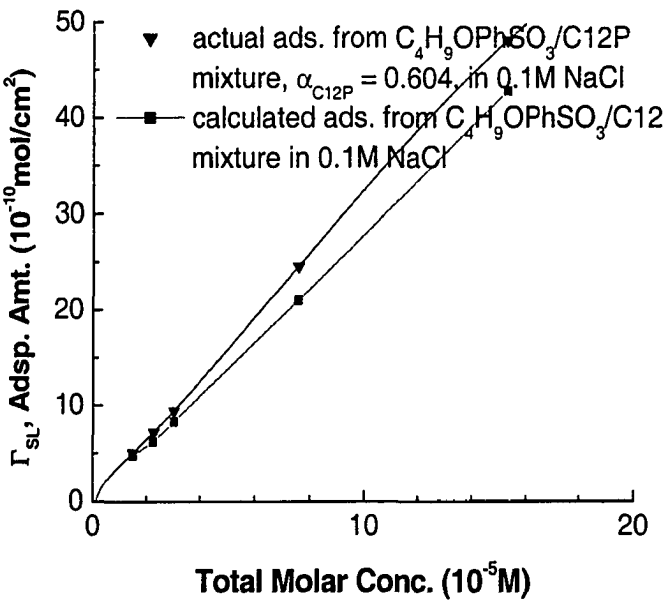

Figure 37. Increased adsorption from the $C_4H_9OPhSO_3Na$ / C12P mixture, α_{C12P}=0.604, compared to its calculated ideal adsorption in 0.1M NaCl medium.

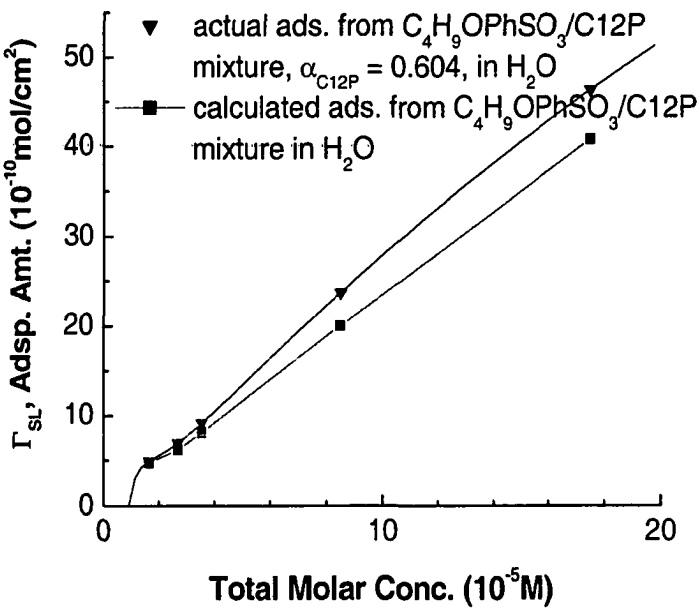

Figure 38. Increased adsorption from the $C_4H_9OPhSO_3Na$ / C12P mixture, α_{C12P}=0.604, compared to its calculated ideal adsorption in H_2O.

resulting contact angle indicates the adsorption ability of the surfactant onto the hydrophobic surface of the solid substrate.

Figure 39 shows the observed dynamic contact angle measurements of the surfactant solutions C8P, CA-520 and their mixture in H_2O, with the surfactant component concentration in the mixture the same as its concentration in its pure solution. The measurement was taken every 15 seconds for the first 3 minutes after the solution drop had just settled on the purified polyethylene film. Lower dynamic contact angles were observed for the C8P/CA-520 mixture solution than for the solutions of either of the individual components. The lower the dynamic contact angle as a function of time, the faster adsorption is occurring at the interfaces, and probably the sharper the surfactant concentration and surface tension gradients in the precursor film of the solution droplet. For hydrocarbon chain surfactants, adsorption at the solid/air interface is considered a constant with change of surfactant concentration on highly hydrophobic solid substrates, and this adsorption has been shown to be at least one order of magnitude smaller than those at the solid/aqueous solution and air/aqueous solution interfaces[125]. We have also shown that adsorption of C8P onto purified polyethylene powder at the solid / aqueous solution interface, is much greater than its adsorption at the air / aqueous solution interface. The observed lower contact angles for the C8P/CA-520 mixture are consistent with the observed adsorption enhancement in C8P/CA-520 mixture at the solid / aqueous solution interface (Figure 26), and the dynamic contact angles indicate faster adsorption, which should generate a larger concentration difference between solutions in the

precursor film and bulk solutions in the droplet, than either of the component surfactant. Consequently, the spreading coefficient at the solid/liquid interface ($S_{L/S}$) for the C8P/CA-520 mixture, defined as: $S_{L/S} = \gamma_{SA} - (\gamma_{SL} + \gamma_{LA})$, will increase, compared to its individual components C8P and CA-520, because of the major decrease in γ_{SL}, which results from the enhanced adsorption from the mixture at the solid / aqueous solution interface. Therefore, the observed lower dynamic contact angles from the C8P/CA-520 mixture result in spreading enhancement on polyethylene film, as shown in Figure 19.

The same results have been observed for the C8P/CA-520 mixture in 0.1M NaCl and the C12P/C_4H_9O-$PhSO_3Na$ mixtures in both H_2O and 0.1M NaCl. As shown in Figures 40 – 42, C8P/CA-520 and C12P/C_4H_9O-$PhSO_3Na$ mixtures show lower dynamic contact angles than either of the components in the mixture, and at the same time, both adsorption enhancement and spreading enhancement have been observed in these mixtures. Once again, enhanced spreading after mixing of the two surfactants results from the major decrease in γ_{LS}, due to the observed adsorption enhancement at the solid/aqueous solution interface and the faster adsorption (as shown by the contact angles) after mixing. Larger spreading coefficients at the solid/liquid interface ($S_{L/S}$) and sharper surfactant concentration and surface tension gradients in the precursor film of the solution droplet have been produced.

Contrary to the C8P/CA-520 and C12P/C_4H_9O-$PhSO_3Na$ mixtures, the C8P / C_4H_9O-$PhSO_3Na$ mixture shows no spreading enhancement (Figure 19). From

Figures 43 and 44, the dynamic contact angles of the C8P/C_4H_9O-$PhSO_3Na$ mixtures lie between those of the two components, in both H_2O and 0.1M NaCl media. No enhancement in contact angle reduction is observed after mixing, and no adsorption enhancement has been observed in either H_2O or 0.1M NaCl medium. Those properties are just the average of the two components. As a result, the spreading wetting ability of the C_4H_9O-$PhSO_3Na$ / C8P mixture is the average of the two individual components.

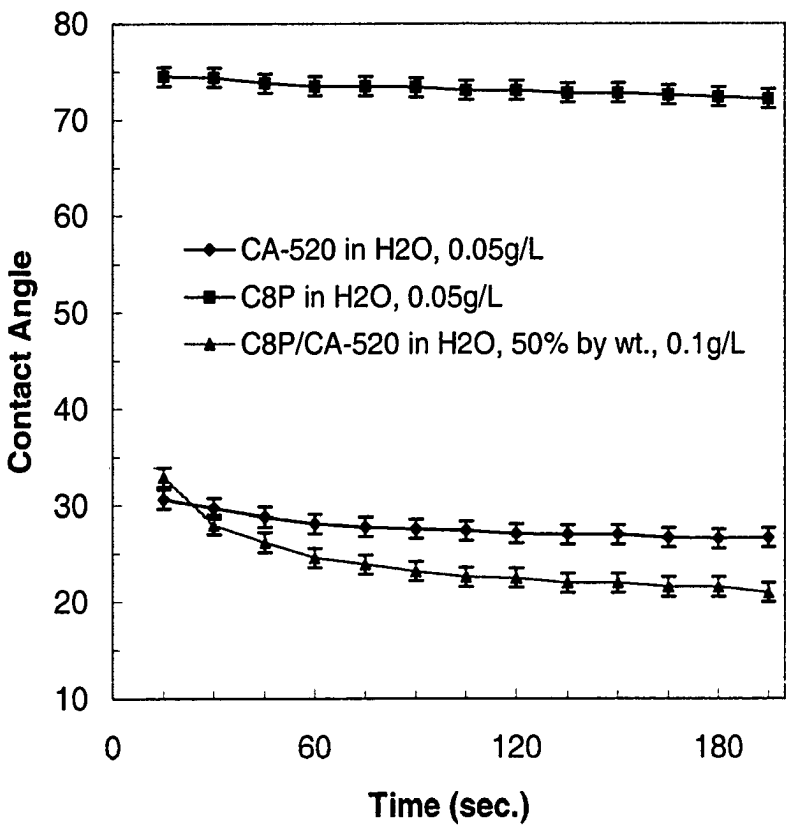

Figure 39. Dynamic contact angles of the surfactant solutions C8P, CA-520 and their mixture in H_2O.

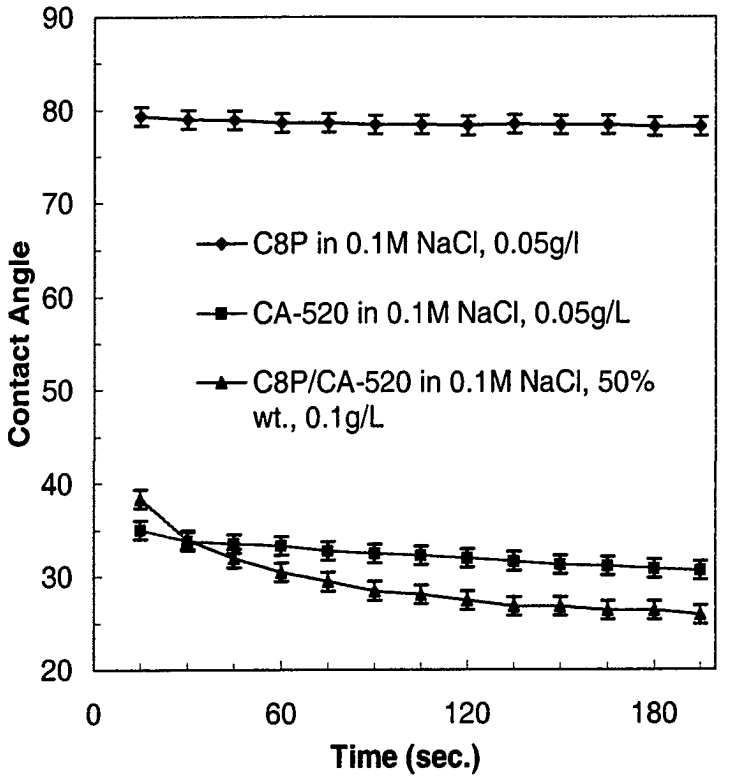

Figure 40. Dynamic contact angles of the surfactant solutions C8P, CA-520 and their mixture in 0.1M NaCl.

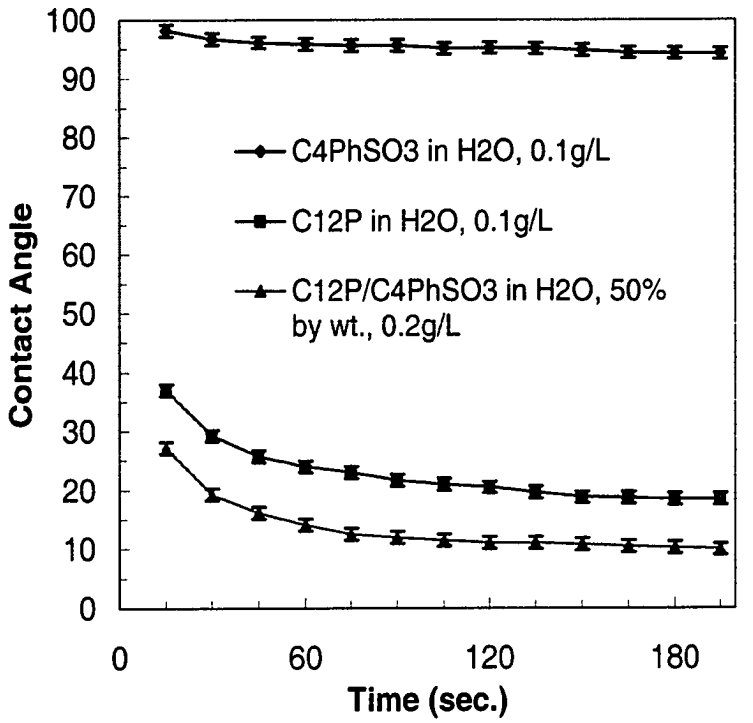

Figure 41. Dynamic contact angles of the surfactant solutions C12P, $C_4H_9OPhSO_3Na$ and their mixture in H_2O.

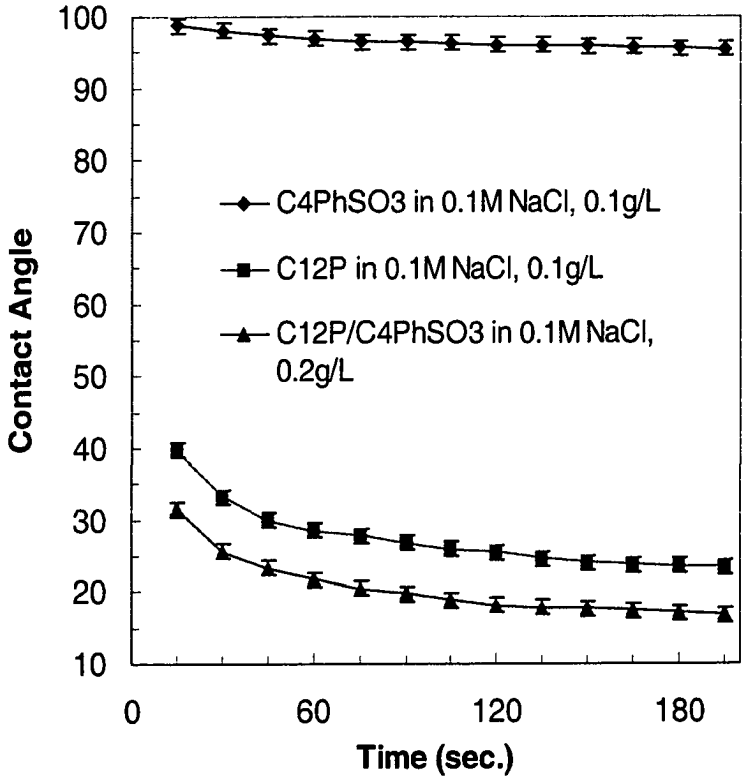

Figure 42. Dynamic contact angles of the surfactant solutions C12P, $C_4H_9OPhSO_3Na$ and their mixture in 0.1M NaCl.

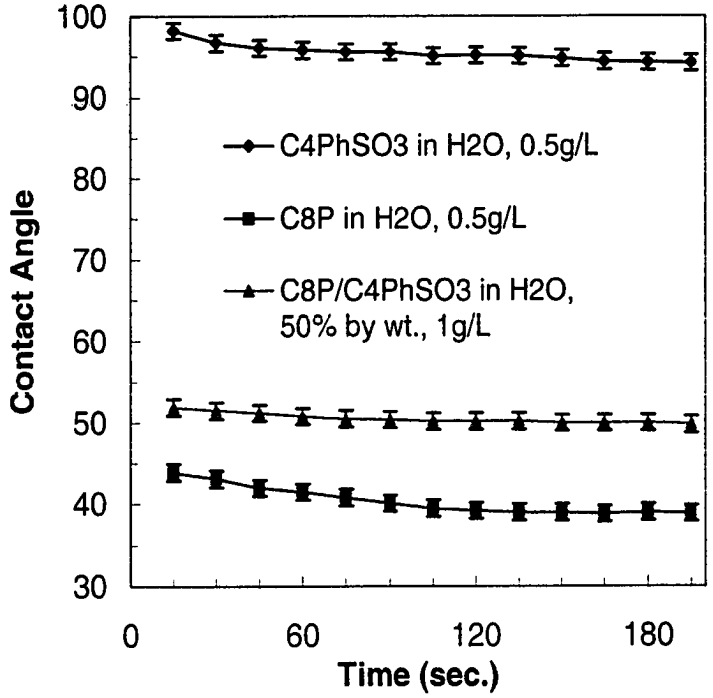

Figure 43. Dynamic contact angles of the surfactant solutions C8P, $C_4H_9OPhSO_3Na$ and their mixture in H_2O.

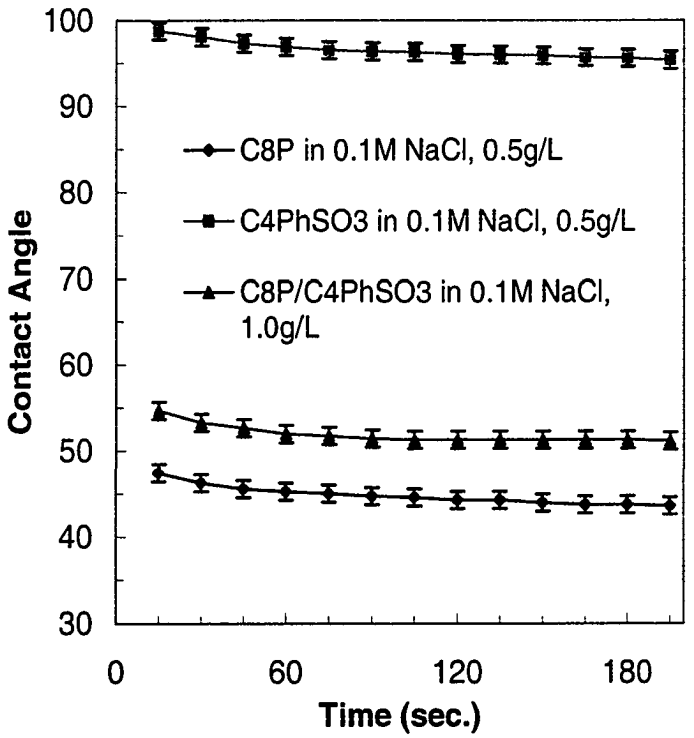

Figure 44. Dynamic contact angles of the surfactant solutions C8P, $C_4H_9OPhSO_3Na$ and their mixture in 0.1M NaCl.

5.4 Molecular Interactions at the Solid/Aqueous Solution Interface

Surfactant molecular interactions at the purified polyethylene powder / aqueous solution interface have been studied. The calculation of interaction parameters at this solid/aqueous solution interface involves surfactant adsorption isotherms instead of interfacial tension. Figure 45 shows the adsorption isotherms of both the individual nonionic surfactants CA-520, C8P and their mixtures in H_2O. From their adsorption isotherms, Γ_{SL}^{Total} and Γ_{SL}^{C8P} can be plotted as a function of LnC_{total} and LnC_{C8P}, respectively (as shown in Figure 46). From these, π_{SL}^{Mix} and π_{SL}^{C8P} can be calculated from the integration of plots of Γ_{SL}^{Total} vs. LnC_{total} and Γ_{SL}^{C8P} vs. LnC_{C8P} (equations 15 and 14, respectively). The definite integrals in equations 14 and 15 are just the areas under the plots of Γ vs. LnC

from C equal 0 to C. (Area integrals are calculated from the fitting equations obtained by use of Origin 6.0.) Figure 47 shows the plots of the calculated interfacial pressure, π_{SL}, at the purified polyethylene powder/aqueous solution interface vs. LnC for both individual surfactants and their mixtures. These plots are used for the calculation of beta parameters.

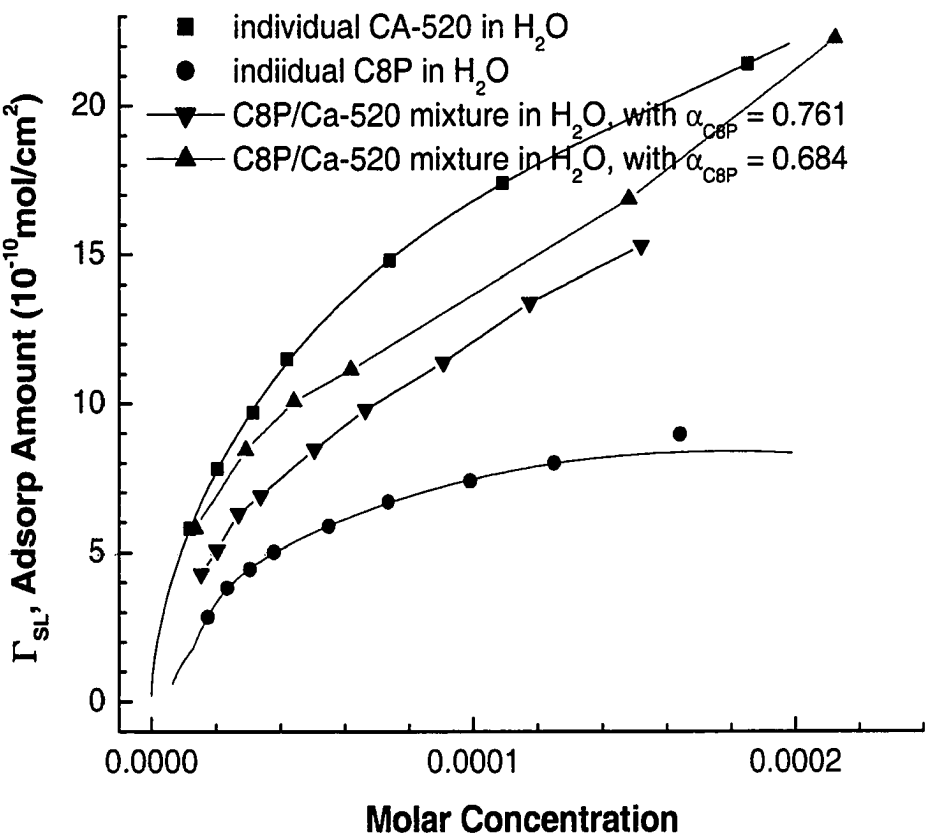

Figure 45. Adsorption isotherms of C8P, Igepal CA-520 and their mixtures onto purified polyethylene powder in quartz-condensed water.

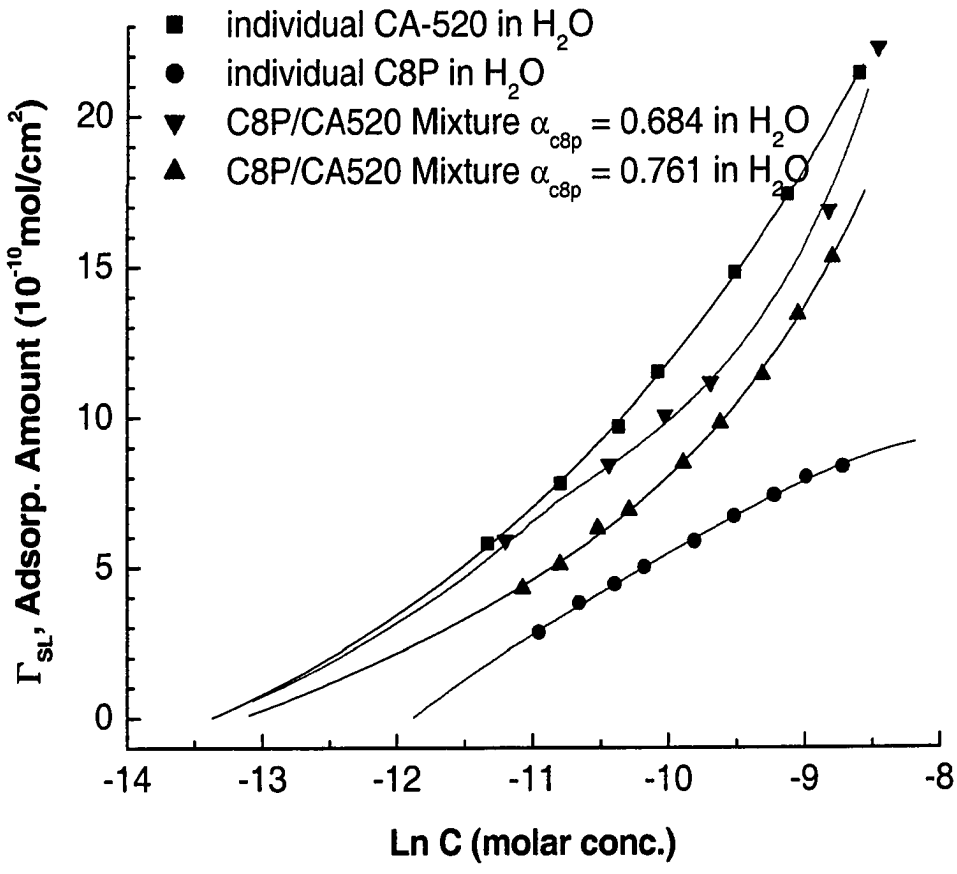

Figure 46. Plots of adsorption amount, Γ_{SL}, vs. LnC of C8P, CA-520 and their mixtures in quartz-condensed water. Concentration, C, is in mol/L.

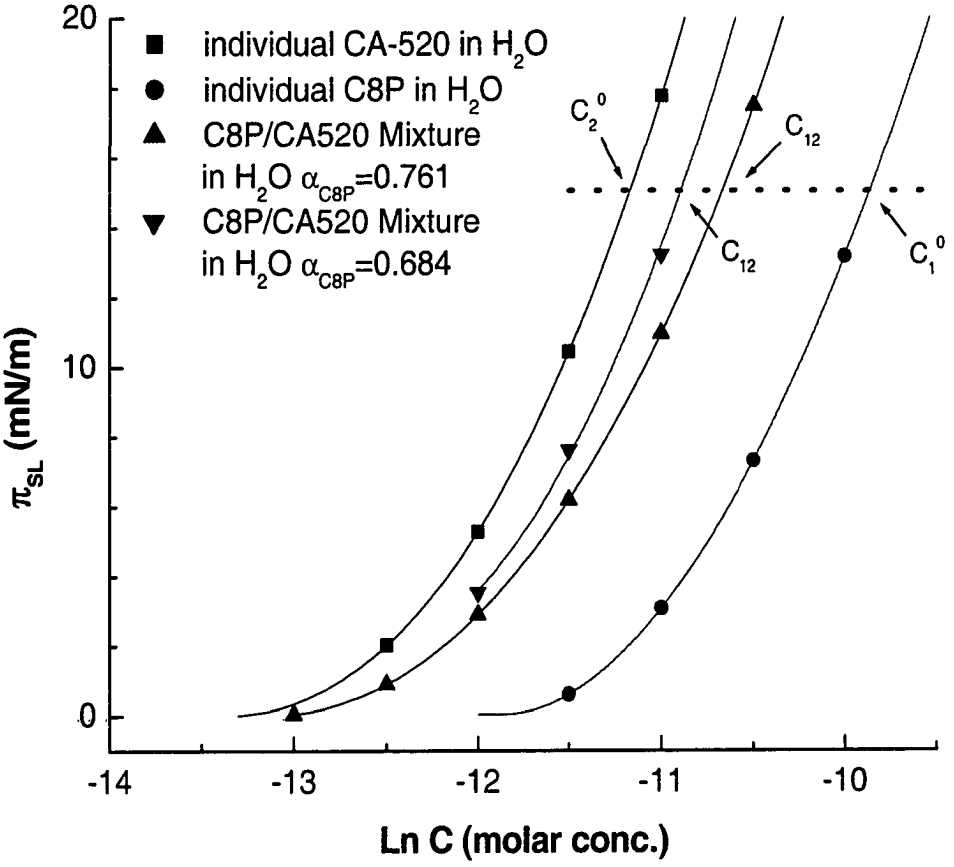

Figure 47. Plots of interfacial pressure, π_{SL}, at purified polyethylene powder / aqueous solution interface vs. LnC for C8P, CA-520 and their mixtures in quartz-condensed water. Concentration, C, is in mol/L.

Interaction parameters at the polyethylene powder / aqueous solution interface (β_{SL}^{σ}) are calculated by using the same equations (equations 5 and 6) as for calculating beta values at the air/aqueous solution interface. The values of C_1^0, C_2^0 and C_{12} in the equations are taken from the interfacial pressure (π_{SL}) plots instead of their surface tension curves for aqueous solutions. Like the calculation of β^{σ} at the air/aqueous solution interface, where the concentration values, C_1^0, C_2^0, and C_{12}, correspond to the lowest possible common surface tension in both individual and mixed solutions, concentration values for the β_{SL}^{σ} calculation correspond to the highest common value of π_{SL} below the monolayer value, as shown in Figure 47. The value of α_{C8P}, the molar fraction of C8P in the bulk solution phase at adsorption equilibrium, is generally not equal to the initial value, due to the different adsorption ability of the two individual surfactants onto purified polyethylene powder. The experimental equilibrium values of α_{C8P} are calculated by finding the bulk concentrations of both components in the mixed solution, which is achieved by UV-Vis spectroscopy. Then experimental equilibrium values of X_{C8P}, the molar fraction of C8P at solid/aqueous solution interface at adsorption equilibrium, are calculated from the concentration difference before and after surfactant adsorption. The variations of calculated α_{C8P} and X_{C8P} values with equilibrium concentration change of the surfactant mixture solution are shown in Figure 48. Since CA-520 is more strongly adsorbed onto polyethylene powder than C8P (Figure 45), substantial increases in the values of α_{C8P} are observed after surfactant adsorption from the mixed solutions.

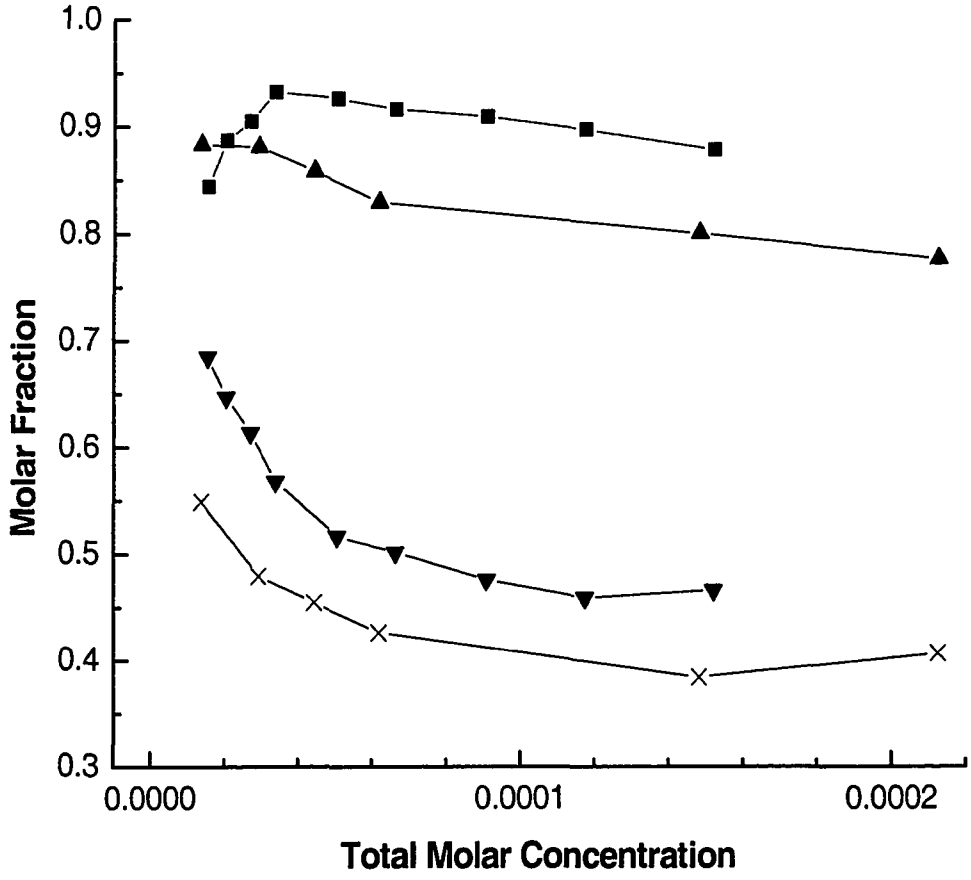

Figure 48. Plots of the molar fraction of C8P (α_{C8P}) in the bulk solution phase and the molar fraction of C8P (X_{C8P}) at the solid / aqueous solution interface at adsorption equilibrium vs. total mixture concentration at different fixed initial molar fractions of C8P in the bulk solution of C8P/CA-520 mixtures in H_2O. ■: α_{C8P} with initial fixed α_{C8P} = 0.761, ▲: α_{C8P} with initial fixed α_{C8P} = 0.684, ▼: X_{C8P} with initial fixed α_{C8P} = 0.761, ✕: X_{C8P} with initial fixed α_{C8P} = 0.684.

Tables 17 and 18 list the calculated β_{SL}^{σ} values for the two C8P/CA-520 mixtures studied in H_2O. All the beta parameters calculated under the studied interfacial pressures are negative, indicating a net attractive interaction at the polyethylene powder / aqueous solution interface after mixing of the two surfactants. Interaction parameters at the air/aqueous solution interface (β_{LA}^{σ}) for the C8P/CA-520 mixture in H_2O have also been calculated. The corresponding surface tension plots for the individual surfactants and their mixtures were shown in Figure 49, and the calculated beta parameters at the air/aqueous solution interface are listed in Table 19. From Table 19, only small negative β_{LA}^{σ} values resulted after mixing of the two surfactants, C8P and CA-520, in H_2O, which indicate an almost ideal mixing behavior at the air/aqueous solution interface.

Table 17. Interaction Parameters at the Purified Polyethylene Powder / Aqueous Solution Interface for the C8P/CA-520 Mixture in H_2O, with Initial α_{C8P} = 0.684

π (mN/m)	10	15
β_{SL}^{σ}	-3.10	-3.15
equili. α_{C8P}	0.89	0.88
calc. X_{C8P}	0.58	0.57
exp. X_{C8P}	0.56	0.54
A_{min} of CA-520	32	27
A_{min} of mixture	29	23
A_{min} of C8P	35	29

A_{min} : area/molecule at the concentration used for beta calculation, in units of $Å^2$.

Table 18. Interaction Parameters at the Purified Polyethylene Powder / Aqueous Solution Interface for the C8P/CA-520 Mixture in H_2O, with Initial α_{C8P} = 0.761

π (mN/m)	10	15
β_{SL}^{σ}	-2.21	-2.38
equili. α_{C8P}	0.86	0.89
calc. X_{C8P}	0.56	0.59
exp. X_{C8P}	0.64	0.63
A_{min} of CA-520	32	27
A_{min} of mixture	31	27
A_{min} of C8P	35	29

A_{min} : area/molecule at the concentration used for beta calculation, in unit of $Å^2$.

Table 19. Interaction Parameters at the Air / Aqueous Solution Interface for the C8P/CA-520 Mixture in H_2O

α_{C8P}	0.900	0.763
β_{LA}^{σ}	-0.25	-0.24
X_{C8P}	0.20	0.09
A_{min} of CA-520	43.5	43.5
A_{min} of mixture	42	43
A_{min} of C8P	38.5	38.5

A_{min} : area/molecule at the concentration used for beta calculation, in unit of $Å^2$.

Comparing the values of β_{SL}^{σ} and β_{LA}^{σ}, it is clear that more negative beta parameters were obtained at the polyethylene powder/aqueous solution interface than at the air/aqueous solution interface and strong net attractive interaction after mixing only occurred at the solid/aqueous solution interface. As can be seen

from Figure 19, the net "attractive" interaction at the polyethylene powder / aqueous solution interface after mixing, rather than the weak molecular interaction occurring at the air/aqueous solution interface, results in spreading enhancement with the C8P/CA-520 mixtures. The strength of the surfactant molecular interaction at the polyethylene powder/aqueous solution interface, as indicated by the absolute value of β_{SL}^{σ}, is related to the adsorption performance of the surfactant mixture at the solid / aqueous solution interface. The more enhancement of adsorption of the surfactant mixture at the solid / aqueous solution interface, the more negative the β_{SL}^{σ} value, and the more deviation from the ideal mixing behavior on adsorption of the solutions. As discussed above in Section 5.2, adsorption from the C8P/CA-520 mixture onto purified polyethylene powder was stronger than the calculated ideal adsorption from the same mixture.

The same study has been performed for C8P/CA-520 system in 0.1M NaCl medium. The corresponding adsorption isotherms and interfacial pressure plots are shown in Figures 50 – 52. In 0.1M NaCl medium, the C8P/CA-520 mixture solution also shows stronger adsorption than either of the individual component surfactants onto purified polyethylene powder, and fairly negative β_{SL}^{σ} values has been observed at the polyethylene powder/aqueous solution interface (as listed in Table 20). The net "attractive" interaction at the solid/aqueous solution interface after mixing, rather than the weak molecular interaction occurring at the air/aqueous solution interface, indicated by the small negative β_{LA}^{σ} value (Table 20), accounts for the spreading enhancement with the C8P/CA-520 mixtures.

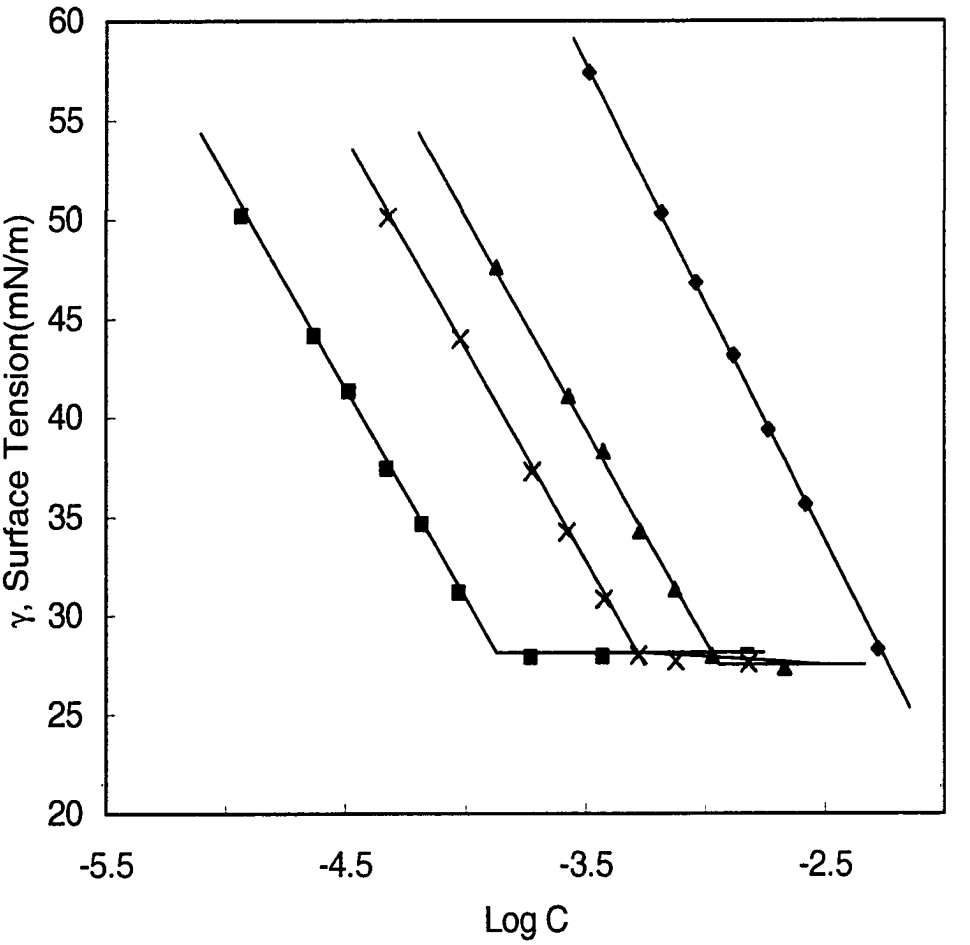

Figure 49. Plots of the surface tension, γ, vs. Log C (bulk phase concentration) for of C8P, CA-520 and their mixtures in H_2O. ■: CA-520, ✕: C8P/CA-520 mixture with initial α_{C8P} = 0.763, ▲: C8P/CA-520 mixture with initial α_{C8P} = 0.900, ◆: C8P.

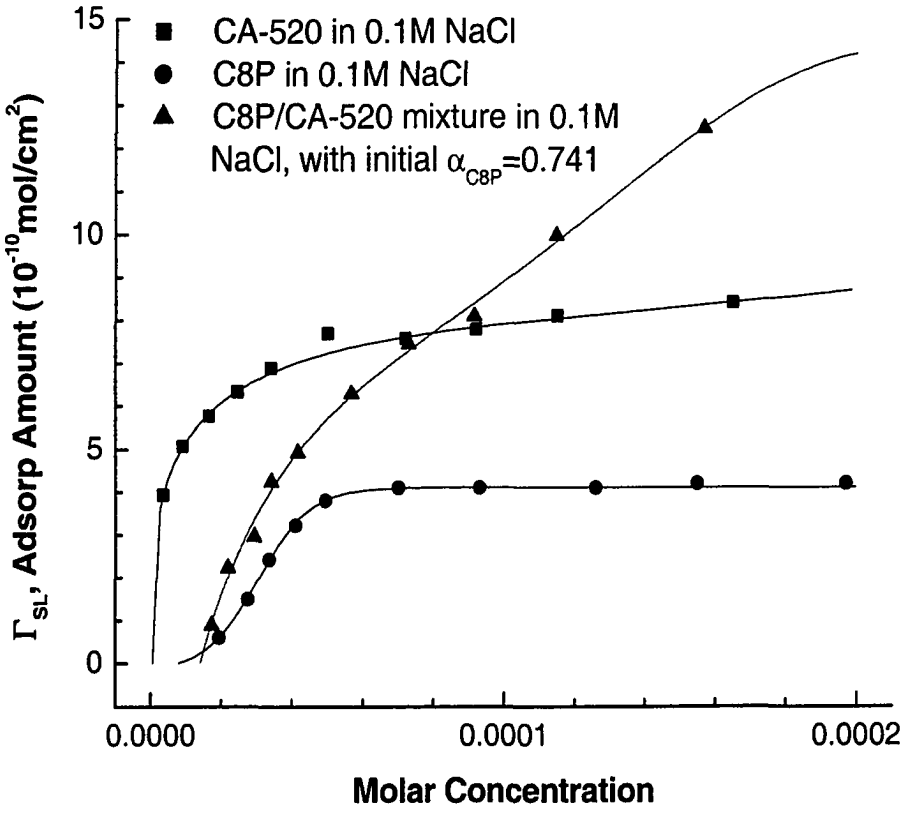

Figure 50. Adsorption isotherms of C8P, Igepal CA-520 and their mixture onto purified polyethylene powder in 0.1M NaCl medium.

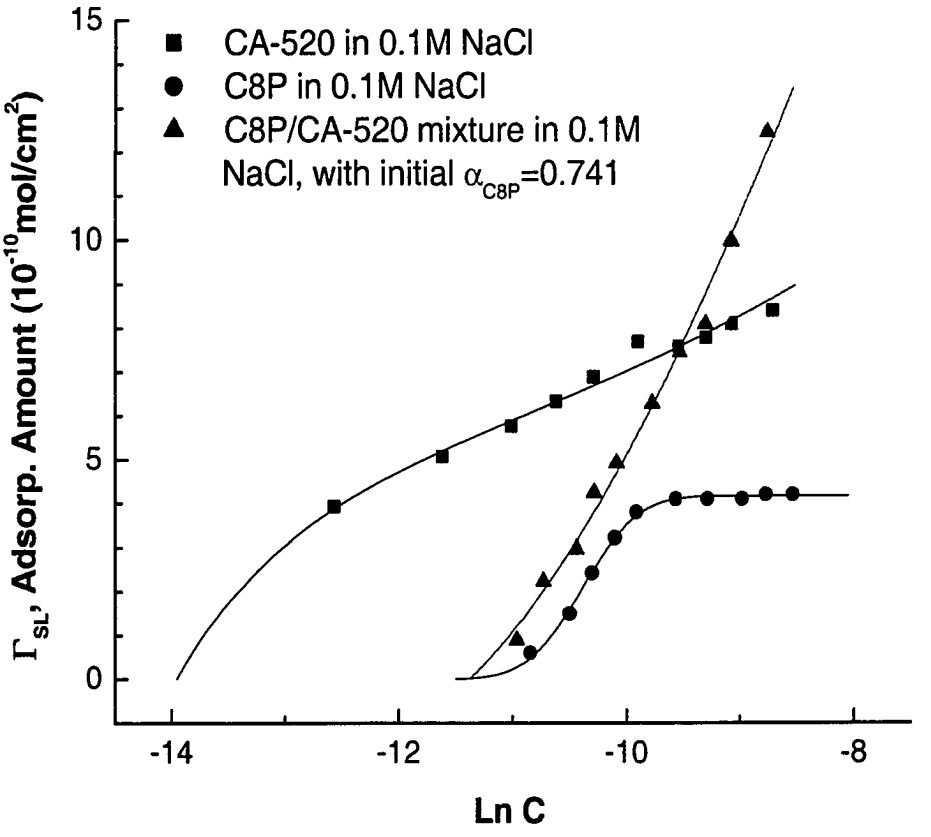

Figure 51. Plots of adsorption amount, Γ_{SL}, vs. LnC of C8P, Igepal CA-520 and their mixture in 0.1M NaCl medium. Concentration, C, is in mol/L.

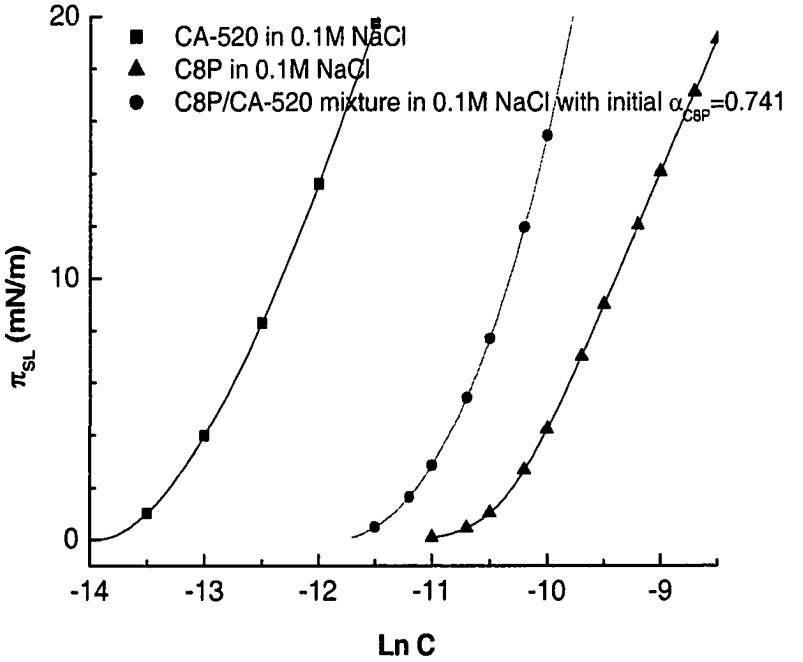

Figure 52. Plots of interfacial pressure, π_{SL}, at purified polyethylene powder/aqueous solution interface vs. LnC for C8P, CA-520 and their mixture in 0.1M NaCl medium.

Table 20. Interaction Parameters at the Purified Polyethylene Powder / Aqueous Solution Interface for the C8P/CA-520 Mixture in 0.1M NaCl Medium, with Initial α_{C8P} = 0.741

π (mN/m)	10	15
β_{SL}^{σ}	-1.51	-1.64
equili. α_{C8P}	0.982	0.976
calc. X_{C8P}	0.37	0.34
exp. X_{C8P}	0.29	0.27
A_{min} of CA520	40	36
A_{min} of mixture	40	32
A_{min} of C_8P	40	40
β_{LA}^{σ}	-0.35±0.05	

A_{min} : area/molecule at the concentration used for beta calculation, in unit of $Å^2$.

The calculation of the interaction parameters at the purified polyethylene powder/aqueous solution interface (β_{SL}^{σ}) was also performed for some other systems. Adsorption isotherms of the surfactants C8P, n-$C_4H_9OphSO_3Na$ and their mixtures in both 0.1M NaCl and H_2O media have been measured, and the corresponding plots of adsorption vs. LnC and interfacial pressure (π_{SL}) vs. LnC for both individual and mixtures, which is used for the calculation of β_{SL}^{σ}, have been determined. As can be seen from the adsorption isotherms in Figures 53 – 58, C8P/n-$C_4H_9OphSO_3Na$ mixtures show no observed adsorption enhancement, compared to the calculated ideal adsorption in both 0.1M NaCl and H_2O media. This results in positive interaction parameters at the polyethylene powder / aqueous solution interface (β_{SL}^{σ}), as shown in Table 21, and no spreading enhancement has been observed for either mixture. Also, small negative beta parameters (β_{LA}^{σ}) and weak molecular interactions at the air/aqueous solution interface were observed.

Table 21. Interaction Parameters at Purified Polyethylene Powder / Aqueous Solution Interface for C8P/n-$C_4H_9OphSO_3Na$ Mixture, with Fixed Initial α_{C8P}

initial α_{C8P}	medium	π (mN/m)	equilibium α_{C8P}	equilibium X_{C8P}	β_{SL}^{σ}	β_{LA}^{σ}
0.572	H_2O	5	0.47	0.96	>1	-0.20
0.570	0.1M NaCl	5	0.56	0.69	>1	-0.32

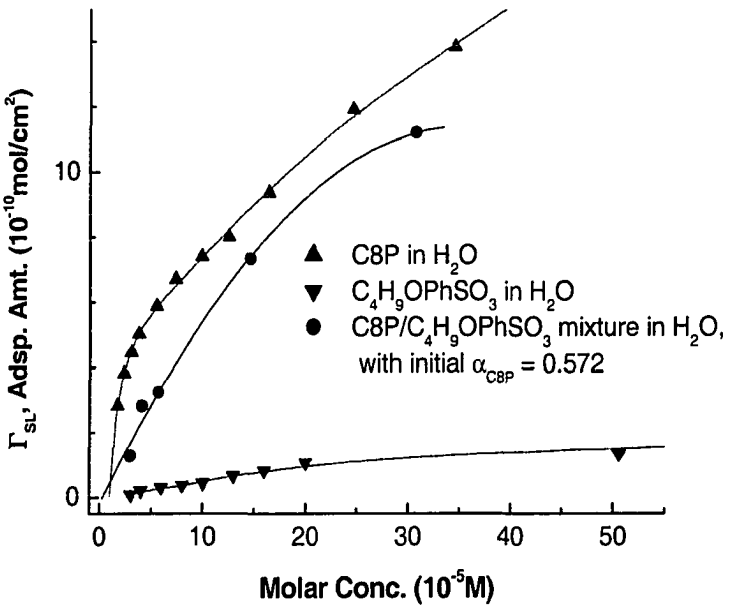

Figure 53. Adsorption isotherms of $C_4H_9OPhSO_3Na$, C8P and their mixture onto purified polyethylene powder in quartz-condensed water.

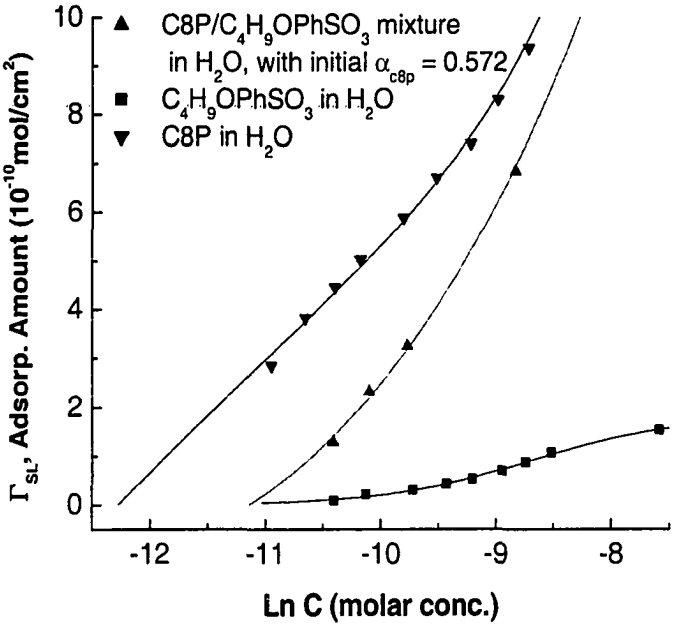

Figure 54. Plots of adsorption amount, Γ_{SL}, vs. LnC for C8P, $C_4H_9OPhSO_3Na$ and their mixture in quartz-condensed water. Concentration, C, is in mol/L.

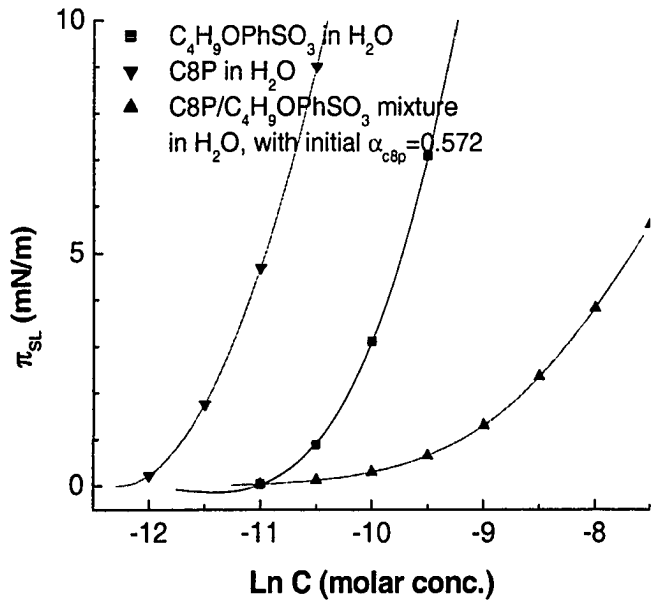

Figure 55. Plots of interfacial pressure, π_{SL}, at purified polyethylene powder / aqueous solution interface vs. LnC for C8P, $C_4H_9OPhSO_3Na$ and their mixture in quartz-condensed water. Concentration, C, is in mol/L.

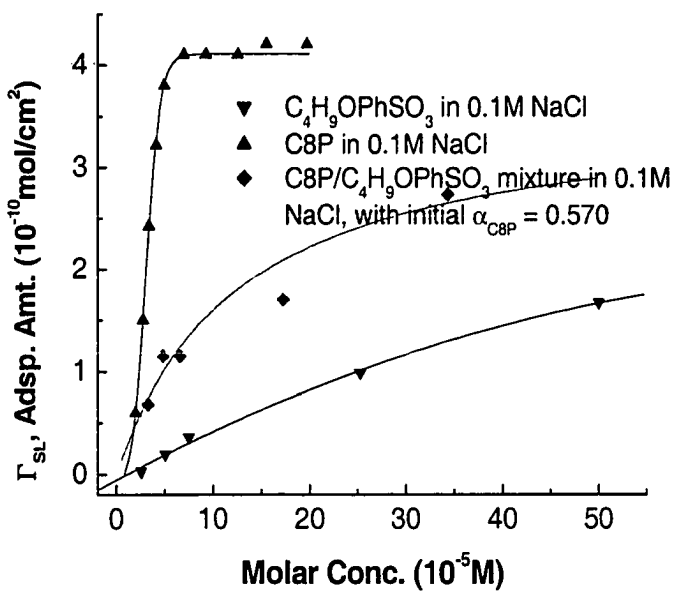

Figure 56. Adsorption isotherms of $C_4H_9OPhSO_3Na$, C8P and their mixture onto purified polyethylene powder in 0.1M NaCl.

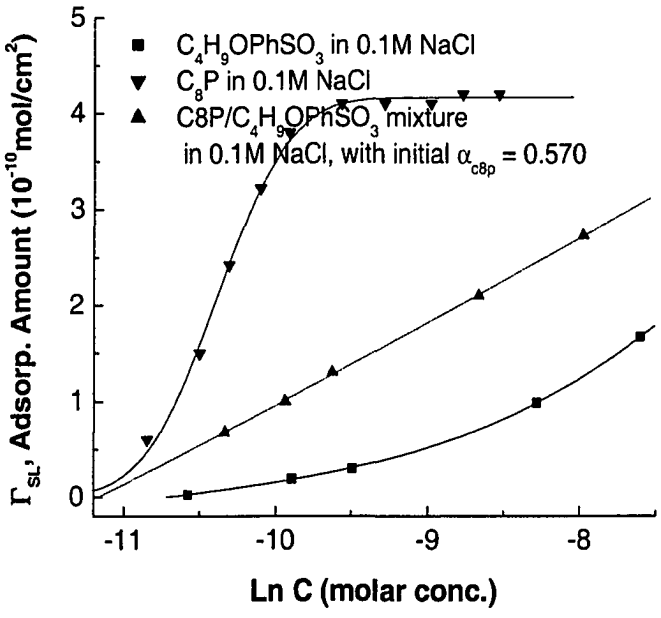

Figure 57. Plots of adsorption amount, Γ_{SL}, vs. LnC for C8P, $C_4H_9OPhSO_3Na$ and their mixture in 0.1M NaCl. Concentration, C, is in mol/L.

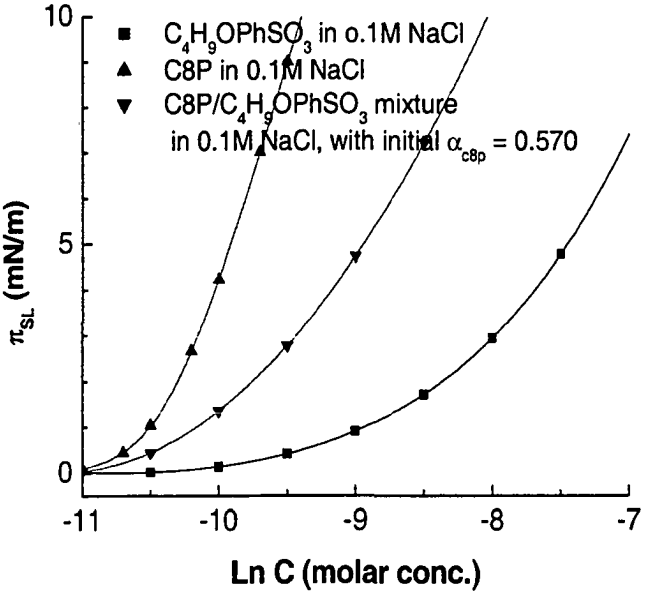

Figure 58. Plots of interfacial pressure, π_{SL}, at purified polyethylene powder / aqueous solution interface vs. LnC for C8P, $C_4H_9OPhSO_3Na$ and their mixture in 0.1M NaCl. Concentration, C, is in mol/L.

Table 22 shows the interaction parameters at the purified polyethylene powder / aqueous solution interface (β_{SL}^{σ}) for C12P/n-C_4H_9OphSO_3Na mixtures in both 0.1M NaCl and H_2O media. The adsorption isotherms for surfactants C12P, n-C_4H_9OphSO_3Na and their mixtures, and the corresponding plots of adsorption vs. LnC and interfacial pressure (π) vs. LnC for both individual and mixtures are shown in Figures 59 – 64. In contrast to C8P/n-C_4H_9OphSO_3Na mixtures, negative interaction parameters (β_{SL}^{σ}) are observed at the polyethylene powder / aqueous solution interface in C12P/n-C_4H_9OphSO_3Na mixtures, both in 0.1M NaCl and H_2O media. Also, as in the C8P/CA-520 mixtures, strong attractive interaction after mixing C12P and n-C_4H_9OphSO_3Na only occurred at the polyethylene powder/aqueous solution interface, and weak surfactant molecular interactions were observed at the air / aqueous solution interface. The net "attractive" interaction at the polyethylene powder/aqueous solution interface after mixing, compared to the weak interaction at the air / aqueous solution interface, results in spreading enhancement in the mixtures, compared to either of the individual components.

Table 22. Interaction Parameters at Purified Polyethylene Powder / Aqueous Solution Interface for C12P/n-C_4H_9OphSO_3Na Mixture, with Fixed Initial α_{C12P}

initial α_{C12P}	medium	π (mN/m)	equilibium α_{C12P}	equilibium X_{C12P}	β_{SL}^{σ}	β_{LA}^{σ}
0.604	H_2O	5	0.20	0.72	-4.4	-0.40
0.604	0.1M NaCl	5	0.25	0.73	-4.5	-0.42

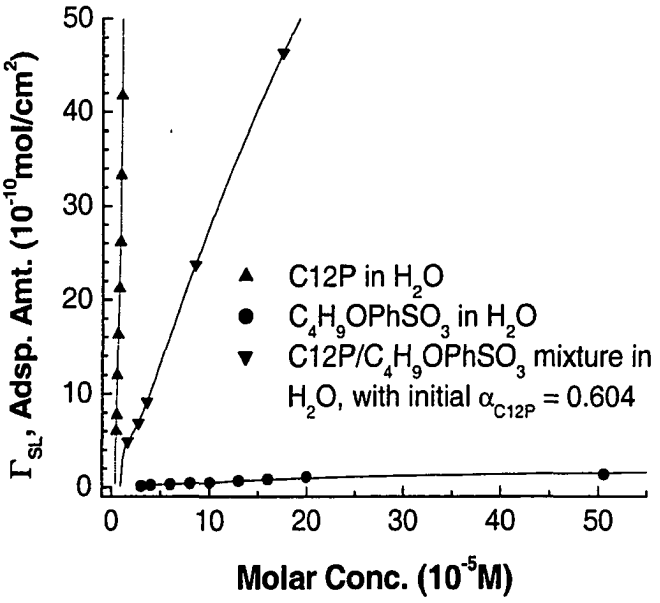

Figure 59. Adsorption isotherms of $C_4H_9OPhSO_3Na$, C12P and their mixture onto purified polyethylene powder in quartz-condensed water.

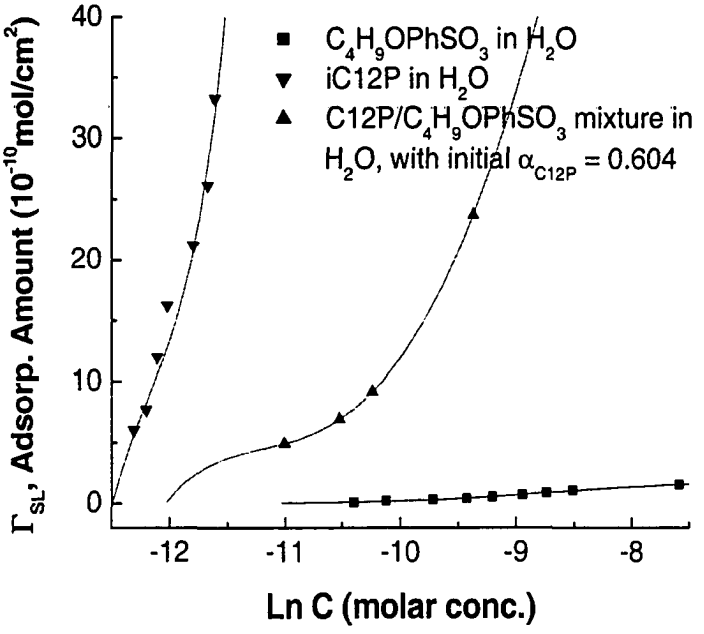

Figure 60. Plots of adsorption amount, Γ_{SL}, vs. LnC for $C_4H_9OPhSO_3Na$, C12P and their mixture in quartz-condensed water. Concentration, C, is in mol/L.

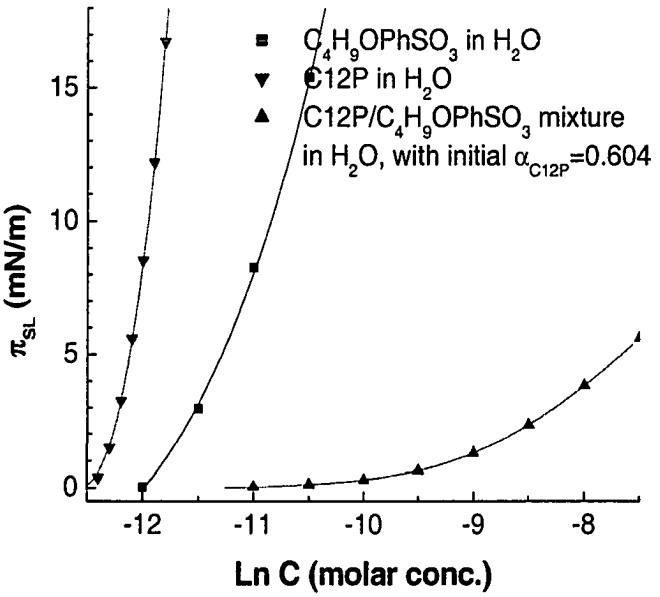

Figure 61. Plots of interfacial pressure, π_{SL}, at purified polyethylene powder / aqueous solution interface vs. LnC for C12P, $C_4H_9OPhSO_3Na$ and their mixture in quartz-condensed water. Concentration, C, is in mol/L.

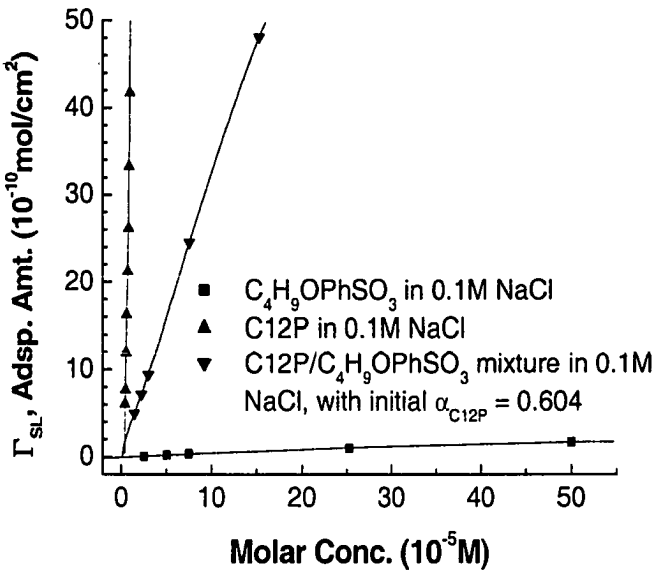

Figure 62. Adsorption isotherms of $C_4H_9OPhSO_3Na$, C12P and their mixture onto purified polyethylene powder in 0.1M NaCl.

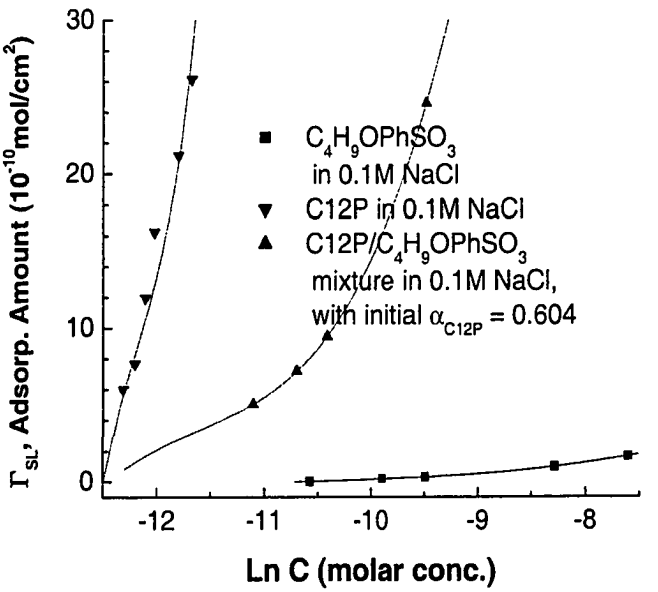

Figure 63. Plots of adsorption amount, Γ_{SL}, vs. LnC for $C_4H_9OPhSO_3Na$, C12P and their mixture in 0.1M NaCl. Concentration, C, is in mol/L.

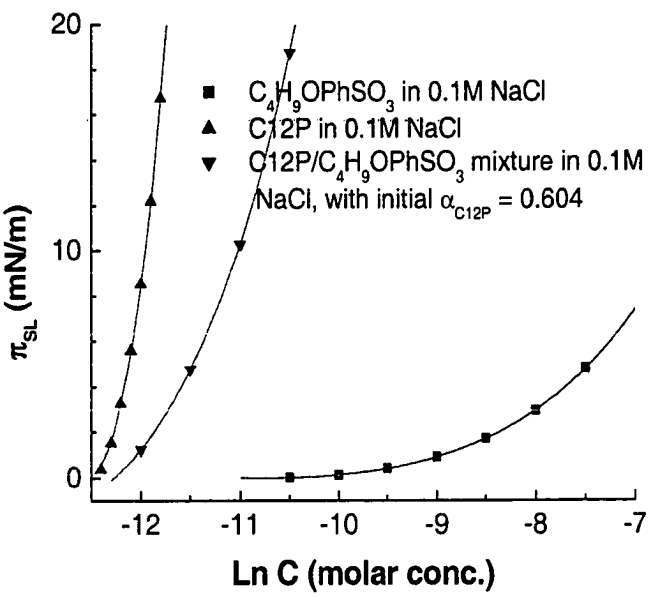

Figure 64. Plots of interfacial pressure, π_{SL}, at purified polyethylene powder / aqueous solution interface vs. LnC for C12P, $C_4H_9OPhSO_3Na$ and their mixture in 0.1M NaCl. Concentration, C, is in mol/L.

5.5 Conclusions

Spreading enhancement has been observed in some of the pyrrolidone – containing mixed surfactant systems on hydrophobic polyethylene film. Along with the spreading enhancement in the mixed surfactant systems, strong net "attractive" interactions occur only at the polyethylene powder / aqueous solution interface after mixing, as indicated by the negative β_{SL}^{σ} values, with only weak interaction occurring at the air / aqueous solution interface, as indicated by the small negative β_{LA}^{σ} values.

Lower dynamic contact angles in the mixture than in either of the components, caused by adsorption enhancement and faster adsorption at the solid / aqueous solution interface after mixing, imply spreading enhancement for the mixture, presumably by increasing the spreading coefficients at the solid / aqueous solution interface ($S_{L/S}$) and producing sharper surfactant concentration and surface tension gradients in the precursor film of the solution droplet of the mixture.

When there is no adsorption enhancement at the solid / aqueous solution interface from the mixed surfactant solution, no lower dynamic contact results and no spreading enhancement occurs for the mixture. And calculated molecular interaction parameters at the solid / aqueous solution interface (β_{SL}^{σ}) are not more negative than interaction parameters at the air / aqueous solution interface (β_{LA}^{σ}).

Appendix A.

Surface Tension Data for Studied Surfactants and Mixtures at 25.0°C and Neutral pH Conditions.

Table A1. Lauroyl n-Propyl Glycine in 0.1M NaCl

C (M)	Log C	γ_2(dyn/cm)
4.82×10^{-3}	-2.317	34.70
1/2 C_1	-2.618	34.81
1/4 C_1	-2.919	34.93
1/8 C_1	-3.220	39.45
1/16 C_1	-3.521	43.92
1/32 C_1	-3.822	49.88
1/64 C_1	-4.123	54.71

Table A2. $C_{12}EO_6$ in 0.1M NaCl

C (M)	Log C	γ(dyn/cm)
6.36×10^{-4}	-3.197	30.22
1/2 C_1	-3.498	30.29
1/4 C_1	-3.799	30.24
1/8 C_1	-4.100	30.52
1/16 C_1	-4.401	35.74
1/32 C_1	-4.702	41.70
1/64 C_1	-5.003	47.45
1/128 C_1	-5.304	52.52

Table A3. $C_{12}EO_6$ / Lauroyl N-Propyl Glycine Mixture in 0.1M NaCl, with $\alpha_{non} = 0.11$

C (M)	Log C	γ(dyn/cm)
5.32×10^{-3}	-2.274	34.31
1/4 C_1	-2.876	34.18
1/8 C_1	-3.177	33.19
1/10 C_1	-3.274	32.89
1/16 C_1	-3.478	33.14
1/32 C_1	-3.779	38.98
1/64 C_1	-4.080	44.45
1/128 C_1	-4.381	49.41
1/256 C_1	-4.682	53.99

Table A4. $C_{12}EO_6$ / Lauroyl N-Propyl Glycine Mixture in 0.1M NaCl, with α_{non} = 0.072

C (M)	Log C	γ(dyn/cm)
1.63×10^{-3}	-2.788	34.45
1/2 C_1	-3.089	33.71
1/4 C_1	-3.390	33.84
1/8 C_1	-3.691	39.35
1/16 C_1	-3.992	44.73
1/32 C_1	-4.293	49.46
1/64 C_1	-4.594	54.22

Table A5. Lauroyl N-Methoxypropyl Glycine in 0.1M NaCl

C (M)	Log C	γ(dyn/cm)
9.84×10^{-3}	-2.007	38.15
1/4 C_1	-2.609	38.42
1/8 C_1	-2.910	41.29
1/16 C_1	-3.211	46.33
1/32 C_1	-3.512	51.12
1/64 C_1	-3.813	54.96

Table A6. Lauroyl N-Methoxypropyl Glycine / $C_{12}EO_6$ Mixture in 0.1M NaCl, with α_{non}=0.0481

C (M)	Log C	γ(dyn/cm)
6.20×10^{-3}	-2.208	37.50
½ C_1	-2.509	37.23
¼ C_1	-2.810	35.60
1/8 C_1	-3.111	34.10
1/16 C_1	-3.412	38.80
1/32 C_1	-3.713	44.04
1/64 C_1	-4.014	49.25
1/128 C_1	-4.315	52.87

Table A7. n-$C_{12}E_2S$ in 0.1M NaCl

C (M)	Log C	γ(dyn/cm)
2.202×10^{-3}	-2.6572	35.16
1/2 C_1	-2.9582	35.08
1/4 C_1	-3.2592	35.27
1/8 C_1	-3.5603	36.38
1/16 C_1	-3.8613	42.65
1/32 C_1	-4.1623	48.58
1/64 C_1	-4.4634	53.91

Table A8. TMN-6 in 0.1M NaCl

C (M)	Log C	γ(dyn/cm)
7.430×10^{-3}	-2.1290	26.16
$C_1=1.622\times10^{-3}$	-2.7899	25.75
1/2 C_1	-3.0910	27.41
1/4 C_1	-3.3920	29.01
1/8 C_1	-3.6930	32.26
1/16 C_1	-3.9941	38.70
1/32 C_1	-4.2951	43.91
1/64 C_1	-4.5961	48.87
1/128 C_1	-4.8972	52.66

Table A9. $C_{12}E_2S$ / TMN-6 Mixture in 0.1M NaCl, with $\alpha_{TMN\text{-}6}=0.6$

C (M)	Log C	γ(dyn/cm)
4.117×10^{-3}	-2.3854	27.80
1/2 C_1	-2.6864	28.20
1/4 C_1	-2.9875	28.86
1/8 C_1	-3.2885	29.20
1/16 C_1	-3.5895	30.38
1/32 C_1	-3.8906	35.03
1/64 C_1	-4.1916	40.38
1/128 C_1	-4.4926	46.03
1/256 C_1	-4.7937	51.62

Table A10. n-$C_{12}E_2S$ /$C_{12}EO_6$ Mixture in 0.1M NaCl, with α_{non}=0.2

C (M)	Log C	γ(dyn/cm)
1.10×10^{-3}	-2.959	33.52
1/2 C_1	-3.260	33.53
1/4 C_1	-3.561	33.44
1/8 C_1	-3.862	33.45
1/16 C_1	-4.163	38.13
1/32 C_1	-4.464	43.95
1/64 C_1	-4.765	49.25
1/128 C_1	-5.066	54.48

Table A11. Lauroyl N-Methoxypropyl Glycine / TMN-6 Mixture in 0.1M NaCl, with α_{non}=0.208

C (M)	Log C	γ(dyn/cm)
6.21×10^{-3}	-2.207	31.85
1/2 C_1	-2.508	31.10
1/4 C_1	-2.809	29.78
1/8 C_1	-3.110	31.53
1/16 C_1	-3.411	36.92
1/32 C_1	-3.712	43.71
1/64 C_1	-4.013	47.42
1/128 C_1	-4.314	51.47

Table A12. Sodium Diamyl Sulfosuccinate (AAY) in 0.1M NaCl

C (M)	Log C	γ(dyn/cm)
1.176×10^{-1}	-0.9296	28.73
1/4 C_1	-1.5317	28.71
1/8 C_1	-1.8327	30.04
1/10 C_1	-1.9296	30.51
1/16 C_1	-2.1337	31.09
1/20 C_1	-2.2306	34.13
1/32 C_1	-2.4347	37.63
1/64 C_1	-2.7358	41.38
1/128 C_1	-3.0368	45.65
1/256 C_1	-3.3378	50.76

Table A13. Sodium Dioctyl Sulfosuccinate (AOT) in 0.1M NaCl

C (M)	Log C	γ(dyn/cm)
4.940×10^{-4}	-2.3063	25.42
1/4 C_1	-2.9083	25.45
1/8 C_1	-3.2094	25.64
1/16 C_1	-3.5104	26.92
1/32 C_1	-3.8114	31.33
1/64 C_1	-4.1125	34.89
1/128 C_1	-4.4135	39.05
1/256 C_1	-4.7145	42.72
1/512 C_1	-5.0155	47.23

Table A14. AOT / $C_{12}EO_6$ Mixture in 0.1M NaCl, with α_{non}=0.162

C (M)	Log C	γ(dyn/cm)
1.474×10^{-3}	-2.8315	25.93
1/4 C_1	-3.4336	26.55
1/8 C_1	-3.7346	27.78
1/16 C_1	-4.0356	31.03
1/32 C_1	-4.3367	36.07
1/64 C_1	-4.6377	40.01
1/128 C_1	-4.9387	44.75
1/256C_1	-5.2397	49.20

Table A15. AOT / $C_{12}EO_6$ Mixture in 0.1M NaCl, with α_{non}=0.245

C (M)	Log C	γ(dyn/cm)
1.07×10^{-3}	-2.971	26.12
1/2 C_1	-3.272	26.47
1/4 C_1	-3.573	27.20
1/8 C_1	-3.874	28.50
1/10 C_1	-3.971	29.35
1/16 C_1	-4.175	32.36
1/20 C_1	-4.272	33.93
1/32 C_1	-4.476	37.17
1/64C_1	-4.777	41.72

Table A16. AOT /TMN-6 Mixture in 0.1M NaCl, with α_{non} = 0.523

C (M)	Log C	γ(dyn/cm)
$C_1=3.10\times10^{-3}$	-2.509	25.52
1/4 C_1	-3.111	25.73
1/8 C_1	-3.412	26.49
1/16 C_1	-3.713	29.96
1/32 C_1	-4.014	34.40
1/64 C_1	-4.315	38.48
1/128 C_1	-4.616	42.10
1/256C_1	-4.917	46.41

Table A17. Sodium Dicyclohexyl Sulfosuccinate (AA-196) in 0.1M NaCl

C (M)	Log C	γ(dyn/cm)
0.191	-0.719	37.02
0.132	-0.879	37.43
5.04×10^{-2}	-1.298	38.74
2.52×10^{-2}	-1.599	41.37
$C_5=1.05\times10^{-2}$	-1.979	45.32
1/2 C_5	-2.280	48.66
1/4 C_5	-2.581	51.96

Table A18. AA-196 / TMN-6 Mixture in 0.1M NaCl, with α_{non}= 0.00949

C (M)	Log C	γ(dyn/cm)
$C_1=7.71\times10^{-2}$	-1.113	34.94
1/2 C_1	-1.414	32.01
1/4 C_1	-1.715	34.21
1/8 C_1	-2.016	38.34
1/16 C_1	-2.317	41.96
1/32 C_1	-2.618	45.70
1/64 C_1	-2.919	48.40

Table A19. AA-196 / $C_{12}EO_6$ Mixture in 0.1M NaCl, with α_{non}=0.00166

C (M)	Log C	γ(dyn/cm)
$C_1=7.65\times10^{-2}$	-1.116	37.76
1/2 C_1	-1.417	35.61
1/4 C_1	-1.718	34.61
1/8 C_1	-2.019	37.78
1/16 C_1	-2.320	42.57
1/32 C_1	-2.621	46.07
1/64 C_1	-2.923	50.19

Table A20. Sodium Diamyl Sulfosuccinate (AAY) in 1.0M NaCl

C (M)	Log C	γ(dyn/cm)
1.058×10^{-1}	-0.9755	24.84
1/4 C_1	-1.5776	25.01
1/8 C_1	-1.8786	25.09
1/16 C_1	-2.1796	26.63
1/32 C_1	-2.4806	31.94
1/64 C_1	-2.7817	36.34
1/128 C_1	-3.0827	40.68
1/256 C_1	-3.3837	44.37

Table A21. $C_{12}EO_6$ in 1.0M NaCl

C (M)	Log C	γ(dyn/cm)
6.332×10^{-4}	-3.1985	29.60
1/4 C_1	-3.8005	30.02
1/16 C_1	-4.4026	30.32
1/32 C_1	-4.7036	34.62
1/64 C_1	-5.0046	40.47
1/128 C_1	-5.3057	47.09
1/256 C_1	-5.6067	52.42

Table A22. TMN-6 in 1.0M NaCl

C (M)	Log C	γ(dyn/cm)
5.49×10^{-3}	-2.260	25.95
1/4 C_1	-2.862	26.16
1/8 C_1	-3.164	26.16
1/16 C_1	-3.465	28.72
1/32 C_1	-3.766	33.40
1/64 C_1	-4.067	37.65
1/128 C_1	-4.368	42.40
1/256 C_1	-4.669	46.45

Table A23. AAY / TMN-6 Mixture in 1.0M NaCl, with α_{non}=0.0566

C (M)	Log C	γ(dyn/cm)
$C_1=4.365\times10^{-2}$	-1.3600	25.11
1/2 C_1	-1.6610	25.31
1/4 C_1	-1.9621	25.77
1/8 C_1	-2.2631	26.03
1/16 C_1	-2.5641	28.46
1/32 C_1	-2.8651	33.08
1/64 C_1	-3.1662	37.30
1/128 C_1	-3.4672	41.39
1/256C_1	-3.7682	45.18

Table A24. AAY / $C_{12}EO_6$ Mixture in 1.0M NaCl, α_{non}=0.0114

C (M)	Log C	γ(dyn/cm)
$C_1=3.332\times10^{-2}$	-1.4773	25.07
1/2 C_1	-1.7783	25.29
1/4 C_1	-2.0794	27.19
1/8 C_1	-2.3804	28.36
1/16 C_1	-2.6814	29.15
1/32 C_1	-2.9824	32.92
1/64 C_1	-3.2835	37.65
1/128 C_1	-3.5845	42.40
1/256C_1	-3.8855	47.86

Table A25. AAY / $C_{12}EO_6$ Mixture in 1.0M NaCl, α_{non}=0.00358

C (M)	Log C	γ(dyn/cm)
C_1=3.716x10^{-2}	-1.4299	25.00
1/2 C_1	-1.7310	25.14
1/4 C_1	-2.0320	26.36
1/8 C_1	-2.3330	27.89
1/16 C_1	-2.6340	31.72
1/32 C_1	-2.9351	36.06
1/64 C_1	-3.2361	40.07
1/128 C_1	-3.5371	44.24

Table A26. Lauroyl N-propyl Glycine / TMN-6 Mixture in 0.1M NaCl, α_{non}=0.299

C (M)	Log C	γ(dyn/cm)
C_1=6.12x10^{-3}	-2.213	29.56
1/2 C_1	-2.514	29.38
1/4 C_1	-2.815	28.68
1/8 C_1	-3.116	28.80
1/16 C_1	-3.417	32.38
1/32 C_1	-3.718	36.87
1/64 C_1	-4.019	43.75
1/128 C_1	-4.320	48.12

Table A27. 1,2–C_{10} diol in 0.1M NaCl

C (M)	Log C	γ(dyn/cm)
C_1=4.310x10^{-3}	-2.3655	22.34
4/5 C_1	-2.4624	22.53
3/5 C_1	-2.5874	22.86
1/2 C_1	-2.6666	24.18
2/5 C_1	-2.7635	28.15
1/4 C_1	-2.9676	37.20
1/5 C_1	-3.0645	39.72
1/8 C_1	-3.2686	46.99
1/10 C_1	-3.3655	49.27
1/16 C_1	-3.5696	55.68

Table A28. 1,2–C_{10} diol / n-$C_{12}E_2S$ Mixture in 0.1M NaCl, α_{non}=0.866

C (M)	Log C	γ(dyn/cm)
C_1=3.290x10^{-3}	-2.483	24.51
1/2 C_1	-2.784	24.37
3/10 C_1	-3.006	28.20
1/4 C_1	-3.085	30.99
1/5 C_1	-3.182	33.99
1/8 C_1	-3.386	40.14
1/10 C_1	-3.483	42.60
1/16 C_1	-3.687	47.61
1/25 C_1	-3.881	52.29

Table A29. 1,2–C_{10} diol / $C_{12}SO_3Na$ Mixture in 0.1M NaCl, α_{non}= 0.614

C (M)	Log C	γ(dyn/cm)
C_1=4.002x10^{-3}	-2.3977	22.95
4/5 C_1	-2.4946	23.32
3/5 C_1	-2.6196	23.47
1/2 C_1	-2.6988	23.69
1/4C_1	-2.9998	30.21
0.9/5 C_1	-3.1425	35.41
1/8C_1	-3.3008	40.26
1/10 C_1	-3.3977	43.60
1/16 C_1	-3.6018	49.51
1/32 C_1	-3.9229	57.65

Table A30. C_{12}-XA (N-methyl Glycamide) in 0.1M NaCl

C (M)	Log C	γ(dyn/cm)
C_1=7.75x10^{-4}	-3.111	28.03
3/5 C_1	-3.333	27.75
1/2 C_1	-3.412	27.71
2/5 C_1	-3.509	30.34
1/4 C_1	-3.713	35.71
1/5 C_1	-3.810	37.83
1/8 C_1	-4.014	42.31
1/10 C_1	-4.111	45.34
1/16 C_1	-4.315	50.31

Table A31. $C_{12}NCl$ (pyridium) / $C_{12}EO_6$ Mixture in 0.1M NaCl, α_{non}=0.0146

C (M)	Log C	γ(dyn/cm)
C_1=1.095×10^{-2}	-1.960	39.40
4/5 C_1	-2.057	39.05
1/2 C_1	-2.261	37.75
2/5 C_1	-2.358	36.17
1/4C_1	-2.562	34.21
1/5 C_1	-2.659	33.62
1/8C_1	-2.863	35.81
1/10 C_1	-2.960	37.68
1/16 C_1	-3.164	40.97
1/20 C_1	-3.261	42.04
1/32 C_1	-3.465	44.73
1/40 C_1	-3.562	46.45

Table A32. $C_{12}NCl$ (pyridium) / $C_{12}EO_6$ Mixture in 0.1M NaCl, α_{non}=0.0110

C (M)	Log C	γ(dyn/cm)
C_1=1.457×10^{-2}	-1.837	39.61
4/5 C_1	-1.934	39.64
1/2 C_1	-2.138	39.20
2/5 C_1	-2.235	38.46
1/4C_1	-2.439	35.45
1/5 C_1	-2.536	34.54
1/8C_1	-2.740	34.64
1/10 C_1	-2.837	37.00
1/16 C_1	-3.041	40.33
1/20 C_1	-3.138	41.55
1/32 C_1	-3.342	43.98
1/40 C_1	-3.439	46.31
1/64 C_1	-3.643	48.62

Table A33. C_{16}TMC in 0.1M NaCl

C (M)	Log C	γ(dyn/cm)
C_1=1.294×10^{-3}	-2.888	37.00
1/4 C_1	-3.490	37.25
1/10 C_1	-3.888	37.33
1/16 C_1	-4.092	37.90
1/20 C_1	-4.189	38.65
1/32 C_1	-4.393	43.26
1/40 C_1	-4.490	45.15
1/64 C_1	-4.694	48.98
1/80 C_1	-4.791	50.87
1/128 C_1	-4.995	55.29

Table A34. C_{16}TMAC / $C_{12}EO_6$ Mixture in 0.1M NaCl, α_{non}=0.419

C (M)	Log C	γ(dyn/cm)
C_1=4.451×10^{-4}	-3.352	31.63
2/5 C_1	-3.750	32.00
1/4C_1	-3.954	32.00
1/5 C_1	-4.051	31.99
1/8C_1	-4.255	32.4
1/10 C_1	-4.352	32.87
1/16 C_1	-4.556	36.96
1/20 C_1	-4.653	39.61
1/32 C_1	-4.857	44.17
1/40 C_1	-4.954	45.49
1/64 C_1	-5.158	50.82
1/80 C_1	-5.255	52.99

Table A35. C_{12}-GA (N-methyl Glycamide) in 0.1M NaCl

C (M)	Log C	γ(dyn/cm)
C_1=6.94×10^{-4}	-3.159	30.22
4/5 C_1	-3.256	30.18
3/5 C_1	-3.380	30.52
1/2 C_1	-3.460	32.85
2/5 C_1	-3.557	35.26
1/4 C_1	-3.761	39.74
1/5 C_1	-3.858	41.99
1/8 C_1	-4.062	46.33
1/16 C_1	-4.363	52.81

Table A36. C_{11}-GA (N-methyl Glycamide) in 0.1M NaCl

C (M)	Log C	γ(dyn/cm)
C_1=4.119x10^{-3}	-2.385	30.63
1/2 C_1	-2.686	30.91
2/5 C_1	-2.783	31.35
1/4 C_1	-2.987	35.81
1/5 C_1	-3.084	38.06
1/8 C_1	-3.288	41.98
1/10 C_1	-3.385	44.82
1/16 C_1	-3.589	49.40
1/20 C_1	-3.686	51.35

Table A37. C_{12}-GA / $C_{12}E_2S$ Mixture in 0.1M NaCl, α_{non}=0.490

C (M)	Log C	γ(dyn/cm)
C_1=1.19x10^{-3}	-2.924	31.62
1/2 C_1	-3.225	31.76
1/4C_1	-3.526	31.76
1/5 C_1	-3.623	32.91
1/8C_1	-3.828	37.57
1/10 C_1	-3.924	40.28
1/16 C_1	-4.129	44.24
1/32 C_1	-4.430	51.10

Table A38. C_{11}-GA / $C_{12}E_2S$ Mixture in 0.1M NaCl, α_{non}=0.806

C (M)	Log C	γ(dyn/cm)
C_1=3.222x10^{-3}	-2.492	31.60
1/2 C_1	-2.793	32.10
1/4C_1	-3.094	32.30
1/5 C_1	-3.191	32.65
1/8C_1	-3.395	37.98
1/16 C_1	-3.696	44.95
1/32 C_1	-3.997	51.47

Table A39. $C_{12}SO_3Na$ in H_2O

C (M)	Log C	γ(dyn/cm)
$C_1=2.00\times10^{-2}$	-1.70	38.89
1.60×10^{-2}	-1.80	39.05
1.20×10^{-2}	-1.92	39.51
1.00×10^{-2}	-2.00	38.78
8.00×10^{-3}	-2.10	40.97
6.00×10^{-3}	-2.22	44.97
5.00×10^{-3}	-2.30	48.33
4.00×10^{-3}	-2.40	49.84
3.00×10^{-3}	-2.52	53.88
1.50×10^{-3}	-2.82	61.42

Table A40. $C_{12}SO_3Na$ in H_2O, at pH = 2.7

C (M)	Log C	γ(dyn/cm)
$C_1=2.022\times10^{-2}$	-1.694	37.81
4/5 C_1	-1.791	38.09
3/4 C_1	-1.819	38.18
1/2 C_1	-1.995	37.78
2/5 C_1	-2.092	35.06
3/10 C_1	-2.217	32.50
1/5 C_1	-2.393	31.29
1/10C_1	-2.694	35.34

Table A41. $C_{12}SO_3Na$ in 0.1MNaCl, pH = 2.7

C (M)	Log C	γ(dyn/cm)
$C_1=3.10\times10^{-3}$	-2.509	35.00
4/5 C_1	-2.606	35.05
34/50 C_1	-2.676	34.95
1/2 C_1	-2.810	37.64
2/5 C_1	-2.907	39.51
1/4 C_1	-3.111	45.15
1/5 C_1	-3.208	47.73
1/8C_1	-3.412	52.45
1/10C_1	-3.509	54.19

Table A42. $C_{12}SO_3Na$ in 0.1MNaCl, pH = 9.1

C (M)	Log C	γ(dyn/cm)
$C_1=2.944\times10^{-3}$	-2.531	35.29
4/5 C_1	-2.628	35.45
14/25 C_1	-2.783	37.20
1/5 C_1	-3.230	48.34

The surface tension curves of $C_{12}SO_3Na$ in 0.1M NaCl, at pH = 2.7, pH neutral or pH = 9.1 almost overlap, except the γ_{CMC} is a little bit higher at pH = 9.1 ($\Delta \approx 0.3$).

Table A43. $C_{12}EO_7$ in H_2O

C (M)	Log C	γ(dyn/cm)
$C_1=1.902\times10^{-3}$	-2.721	31.53
1/10 C_1	-3.721	31.85
1/20 C_1	-4.022	31.96
1/40 C_1	-4.323	36.86
1/50 C_1	-4.420	38.94
1/80 C_1	-4.624	41.85
1/100 C_1	-4.721	44.45
1/160 C_1	-4.925	48.22
1/320 C_1	-5.226	52.81

Table A44. $C_{12}EO_7$ in H_2O, pH = 2.7

C (M)	Log C	γ(dyn/cm)
$C_1=3.804\times10^{-4}$	-3.420	31.49
1/4 C_1	-4.022	31.35
1/5 C_1	-4.119	31.06
1/8 C_1	-4.323	35.03
1/10 C_1	-4.420	36.85
1/16 C_1	-4.624	40.57
1/32 C_1	-4.925	46.34
1/40 C_1	-5.022	47.90
1/64 C_1	-5.226	52.08

Table A45. $C_{12}EO_7$ in 0.1MNaCl

C (M)	Log C	γ(dyn/cm)
$C_1=3.804\times10^{-4}$	-3.420	31.52
1/2 C_1	-3.721	31.47
1/4 C_1	-4.022	31.44
1/8 C_1	-4.323	35.55
1/16 C_1	-4.624	40.71
1/32 C_1	-4.925	46.86
$C_2=9.51\times10^{-5}$	-4.022	31.22*
1/4 C_2	-4.624	41.00*

*: check two points for $C_{12}EO_7$ in 0.1M NaCl at pH = 2.7; $C_{12}EO_7$ in 0.1M NaCl at pH = 2.7 and pH neutral have the same surface tension curves.

Table A46. $C_{12}EO_7$ in 0.1MNaCl, pH = 9.1

C (M)	Log C	γ(dyn/cm)
$C_1=2.50\times10^{-4}$	-3.602	32.36
1/2 C_1	-3.903	32.44
1/4 C_1	-4.204	34.30
1/8 C_1	-4.505	39.32
1/16 C_1	-4.806	44.57
1/32 C_1	-5.107	49.93

Table A47. $C_{12}SO_3Na$ / $C_{12}EO_7$ Mixture in H_2O, α_{non}= 0.0104

C (M)	Log C	γ(dyn/cm)
$C_1=1.826\times10^{-2}$	-1.738	38.14
3/5 C_1	-1.960	37.61
1/2 C_1	-2.039	36.87
2/5 C_1	-2.136	36.61
1/4 C_1	-2.340	36.77
1/5 C_1	-2.437	36.11
1/8 C_1	-2.642	37.52
1/10 C_1	-2.738	40.30
1/16 C_1	-2.943	44.22
1/20 C_1	-3.039	46.31
1/32 C_1	-3.244	49.79
1/40 C_1	-3.340	51.03

Table A48. $C_{12}SO_3Na$ / $C_{12}EO_7$ Mixture in 0.1MNaCl, α_{non}= 0.0381

C (M)	Log C	γ(dyn/cm)
C_1=2.995x10^{-3}	-2.524	33.52
4/5 C_1	-2.621	33.54
1/2 C_1	-2.825	33.86
2/5 C_1	-2.922	33.88
1/4 C_1	-3.126	34.22
1/5 C_1	-3.223	34.48
1/8 C_1	-3.427	38.26
1/10 C_1	-3.524	39.35
1/16 C_1	-3.728	44.27
1/20 C_1	-3.825	45.65
1/32 C_1	-4.029	50.37
1/40 C_1	-4.126	51.45

Table A49. $C_{12}SO_3Na$ / $C_{12}EO_7$ Mixture in 0.1MNaCl at pH = 2.7, α_{non}= 0.0378

C (M)	Log C	γ(dyn/cm)
C_1=3.016x10^{-3}	-2.521	33.09
1/2 C_1	-2.822	33.17
1/4 C_1	-3.123	33.52
1/5 C_1	-3.220	33.74
1/8 C_1	-3.424	37.59
1/10 C_1	-3.521	39.90
1/16 C_1	-3.725	43.85
1/32 C_1	-4.026	49.77

Table A50. $C_{12}SO_3Na$ / $C_{12}EO_7$ Mixture in 0.1MNaCl at pH = 9.1, α_{non}= 0.0376

C (M)	Log C	γ(dyn/cm)
C_1=3.326x10^{-3}	-2.478	33.87
1/2 C_1	-2.779	34.06
1/4 C_1	-3.080	34.56
1/5 C_1	-3.177	34.93
1/8 C_1	-3.381	37.75
1/10 C_1	-3.478	39.85
1/16 C_1	-3.682	43.77
1/20 C_1	-3.779	45.65
1/32 C_1	-3.983	49.67

Table A51. $C_{12}EO_7$ in 0.05M NaCl

C (M)	Log C	γ(dyn/cm)
$C_1=9.585\times10^{-5}$	-4.018	31.86
1/2 C_1	-4.319	36.05
1/4 C_1	-4.620	41.80
1/8 C_1	-4.921	47.33

Table A52. $C_{12}EO_7$ in 0.2M NaCl

C (M)	Log C	γ(dyn/cm)
$C_1=9.585\times10^{-5}$	-4.018	31.66
1/2 C_1	-4.319	35.27
1/4 C_1	-4.620	40.75
1/8 C_1	-4.921	46.37

Table A53. $C_{12}SO_3Na$ in 0.05M NaCl

C (M)	Log C	γ(dyn/cm)
$C_1=5.64\times10^{-3}$	-2.249	36.08
3/4 C_1	-2.374	36.24
$C_2=3.38\times10^{-3}$	-2.471	36.35
3/8 C_1	-2.675	39.93
1/2 C_2	-2.772	43.27
3/16 C_1	-2.976	47.80
1/4 C_2	-3.073	49.50
3/32 C_1	-3.277	53.91

Table A54. $C_{12}SO_3Na$ / $C_{12}EO_7$ Mixture in 0.05M NaCl, α_{non}= 0.0368

C (M)	Log C	γ(dyn/cm)
$C_1=3.12\times10^{-3}$	-2.506	34.63
1/2 C_1	-2.807	34.95
1/4 C_1	-3.108	35.17
3/16 C_1	-3.234	37.27
1/8 C_1	-3.409	40.50
3/32 C_1	-3.535	42.53
1/16 C_1	-3.710	45.88
1/32 C_1	-4.011	51.28

Table A55. $C_{12}SO_3Na$ in 0.2M NaCl

C (M)	Log C	γ(dyn/cm)
$C_1=2.256\times10^{-3}$	-2.647	33.76
4/5 C_1	-2.744	33.74
$C_2=1.504\times10^{-3}$	-2.823	33.87
4/5 C_2	-2.920	34.59
2/5 C_1	-3.045	38.22
2/5 C_2	-3.221	41.69
1/5 C_1	-3.346	45.44
1/5 C_2	-3.522	49.61
1/10 C_1	-3.647	51.93

Table A56. $C_{12}SO_3Na$ / $C_{12}EO_7$ Mixture in 0.2M NaCl, α_{non}= 0.0599

C (M)	Log C	γ(dyn/cm)
$C_1=1.60\times10^{-3}$	-2.796	32.51
1/2 C_1	-3.097	32.92
1/4 C_1	-3.398	33.60
3/16 C_1	-3.523	35.78
1/8 C_1	-3.699	39.43
3/32 C_1	-3.824	41.79
1/16 C_1	-4.000	45.37
1/32 C_1	-4.301	50.79
3/128C_1	-4.426	52.92

Table A57. $C_{12}SO_3Na$ in 0.1M KCl

C (M)	Log C	γ(dyn/cm)
$C_1=3.008\times10^{-3}$	-2.522	33.77
3/4 C_1	-2.647	34.01
1/2 C_1	-2.823	35.56
3/8 C_1	-2.948	39.02
1/4 C_1	-3.124	43.64
3/16 C_1	-3.249	46.47
1/8 C_1	-3.425	50.94

Table A58. $C_{12}SO_3Na$ / $C_{12}EO_7$ Mixture in 0.1M KCl, α_{non}= 0.0413

C (M)	Log C	γ(dyn/cm)
C_1=1.88×10^{-3}	-2.726	32.14
1/2 C_1	-3.027	32.89
7/20 C_1	-3.182	33.28
1/4 C_1	-3.328	34.69
7/40 C_1	-3.483	38.16
1/8 C_1	-3.629	41.10
1/16 C_1	-3.930	47.21

Table A59. $C_{14}EO_8$ in 0.1M NaCl

C (M)	Log C	γ(dyn/cm)
C_1=4.227×10^{-5}	-4.374	35.19
1/2 C_1	-4.675	35.22
1/4 C_1	-4.976	36.20
1/8 C_1	-5.277	39.89
1/16 C_1	-5.578	45.82
1/32 C_1	-5.879	50.33

Table A60. $C_{12}SO_3Na$ / C_{12}-GA Mixture in 0.1M NaCl, α_{non}= 0.213

C (M)	Log C	γ(dyn/cm)
C_1=3.058×10^{-3}	-2.515	30.09
1/2 C_1	-2.816	29.74
7/20 C_1	-2.970	29.61
1/4 C_1	-3.117	29.56
7/40 C_1	-3.271	33.03
1/8 C_1	-3.418	36.60
7/80 C_1	-3.572	40.55
1/16 C_1	-3.719	44.16
7/160 C_1	-3.873	48.20

Table A61. $C_{12}SO_3Na$ / $C_{14}EO_8$ Mixture in 0.1M NaCl, α_{non}= 0.007

C (M)	Log C	γ(dyn/cm)
C_1=1.818x10^{-3}	-2.740	34.93
1/2 C_1	-3.041	35.70
7/20 C_1	-3.196	36.53
1/4 C_1	-3.342	37.13
7/40 C_1	-3.497	39.71
1/8 C_1	-3.643	42.91
7/80 C_1	-3.798	45.63
1/16 C_1	-3.944	48.11

Table A62. $C_{12}SO_3Na$ / TMN-6 Mixture in 0.1M NaCl, α_{non}= 0.201

C (M)	Log C	γ(dyn/cm)
C_1=3.012x10^{-3}	-2.521	28.96
1/2 C_1	-2.822	28.49
1/4 C_1	-3.123	29.43
7/40 C_1	-3.278	31.38
1/8 C_1	-3.424	34.89
7/80 C_1	-3.579	39.14
1/16 C_1	-3.725	41.57
7/160 C_1	-3.880	44.26

Table A63. AOT / 1,2--C_{10} diol Mixture in 0.1M NaCl, α_{non}= 0.838

C (M)	Log C	γ(dyn/cm)
C_1=3.847x10^{-3}	-2.415	23.71
1/2 C_1	-2.716	24.33
¼ C_1	-3.017	25.00
7/40 C_1	-3.172	27.85
1/8 C_1	-3.318	30.56
7/80 C_1	-3.473	33.15
1/16 C_1	-3.619	35.61
7/160 C_1	-3.774	38.01
1/32 C_1	-3.920	40.47
1/64 C_1	-4.221	45.13

Table A64. AOT / C_{12}-GA Mixture in 0.1M NaCl, α_{non}= 0.531

C (M)	Log C	γ(dyn/cm)
C_1=1.772×10^{-3}	-2.752	25.30
1/2 C_1	-3.053	25.39
1/4 C_1	-3.354	25.40
7/40 C_1	-3.508	25.46
1/8 C_1	-3.655	26.63
7/80 C_1	-3.809	29.35
1/16 C_1	-3.956	32.16
7/160 C_1	-4.110	34.64
1/32 C_1	-4.257	37.25

Table A65. AOT / $C_{14}EO_8$ Mixture in 0.1M NaCl, α_{non}= 0.0248

C (M)	Log C	γ(dyn/cm)
C_1=8.517×10^{-4}	-3.070	25.25
1/2 C_1	-3.371	25.31
2/5 C_1	-3.468	25.60
¼ C_1	-3.672	27.17
7/40 C_1	-3.827	28.74
1/8 C_1	-3.973	29.87
1/16 C_1	-4.274	33.92
7/160 C_1	-4.429	36.41
1/32 C_1	-4.575	38.51
1/64 C_1	-4.876	42.83
7/640 C_1	-5.031	45.09

Table A66. AOT / $C_{14}EO_8$ Mixture in 0.1M NaCl, α_{non}= 0.0407

C (M)	Log C	γ(dyn/cm)
C_1=8.052×10^{-4}	-3.094	25.2
1/2 C_1	-3.395	25.4
¼ C_1	-3.696	27.3
1/8 C_1	-3.997	29.8
1/16 C_1	-4.298	32.9
1/32 C_1	-4.599	37.9
1/64 C_1	-4.900	42.7
1/128 C_1	-5.201	47.0

Table A67. Surfynol 465 in 0.1M NaCl

C (M)	Log C	γ(dyn/cm)
2.5 C_1	-1.598	29.30
$C_1=1.009\times10^{-2}$	-1.996	29.13
2.5/4 C_1	-2.200	30.56
1/2 C_1	-2.297	31.82
1/4 C_1	-2.598	35.33
1/8 C_1	-2.899	39.06
1/16 C_1	-3.200	42.42
1/32 C_1	-3.501	46.26
1/64 C_1	-3.802	49.25

Table A68. Surfynol 440 in 0.1M NaCl

C (M)	Log C	γ(dyn/cm)
$C_1=1.064\times10^{-2}$	-1.973	27.03
3/4 C_1	-2.098	27.34
1/2 C_1	-2.274	28.56
1/4 C_1	-2.575	32.27
1/8 C_1	-2.876	36.02
1/10 C_1	-2.973	37.34
1/16 C_1	-3.177	39.88
1/32 C_1	-3.478	43.61
1/64 C_1	-3.779	47.16

Table A69. Surfynol 465 / $C_{12}SO_3Na$ Mixture in 0.1M NaCl, α_{non}= 0.812

C (M)	Log C	γ(dyn/cm)
$C_1=2.486\times10^{-2}$	-1.604	30.04
1/2 C_1	-1.905	30.46
¼ C_1	-2.207	31.00
1/8 C_1	-2.508	31.39
1/16 C_1	-2.809	34.61
1/32 C_1	-3.110	39.46
1/64 C_1	-3.411	43.61
1/128 C_1	-3.712	47.43

Table A70. Surfynol 440 / $C_{12}SO_3Na$ Mixture in 0.1M NaCl, α_{non}= 0.772

C (M)	Log C	γ(dyn/cm)
C_1=1.025x10^{-2}	-1.989	26.30
1/2 C_1	-2.290	27.25
7/20 C_1	-2.445	27.71
¼ C_1	-2.591	28.32
1/8 C_1	-2.892	33.21
1/16 C_1	-3.193	38.23
1/32 C_1	-3.494	42.81
1/64 C_1	-3.795	47.01

Table A71. Surfynol 104 in 0.1M NaCl

C (M)	Log C	γ(dyn/cm)
C_2=3.735x10^{-3}	-2.428	32.70
C_3=2.73x10^{-3}	-2.564	34.99
C_1=1.48x10^{-3}	-2.830	38.75
1/2 C_1	-3.131	43.02
1/4 C_1	-3.432	47.08
1/8 C_1	-3.733	50.94

Table A72. Surfynol 104 / $C_{12}SO_3Na$ Mixture in 0.1M NaCl, α_{non}= 0.751

C (M)	Log C	γ(dyn/cm)
C_2=8.059x10^{-3}	-2.094	25.19
C_1 = 7/10 C_2	-2.249	25.81
1/2 C_1	-2.550	27.88
¼ C_1	-2.851	34.02
1/8 C_1	-3.152	39.80
1/16 C_1	-3.453	44.73
1/32 C_1	-3.754	49.64

Table A73. Surfynol 465 / $C_{12}E_2S$ Mixture in 0.1M NaCl, α_{non}= 0.959

C (M)	Log C	γ(dyn/cm)
$C_1=1.053\times10^{-2}$	-1.978	29.62
1/2 C_1	-2.279	30.64
¼ C_1	-2.580	31.43
7/40 C_1	-2.735	32.98
1/8 C_1	-2.881	35.00
1/16 C_1	-3.182	39.78
1/32 C_1	-3.483	44.00
1/64 C_1	-3.784	47.64

Table A74. Surfynol 440 / $C_{12}E_2S$ Mixture in 0.1M NaCl, α_{non}= 0.950

C (M)	Log C	γ(dyn/cm)
$C_1=8.645\times10^{-3}$	-2.063	25.90
1/2 C_1	-2.364	27.50
¼ C_1	-2.665	29.23
7/40 C_1	-2.820	31.52
1/8 C_1	-2.966	34.10
1/16 C_1	-3.267	38.75
1/32 C_1	-3.568	43.19
1/64 C_1	-3.869	47.27

Table A75. $C_{14}EO_4$ in 0.1M NaCl

C (M)	Log C	γ(dyn/cm)
$C_1=7.22\times10^{-5}$	-4.141	28.91
1/2 C_1	-4.442	28.93
¼ C_1	-4.744	29.01
1/8 C_1	-5.045	30.09
1/16 C_1	-5.346	32.99
7/160 C_1	-5.500	37.35
1/32 C_1	-5.647	41.78
1/64 C_1	-5.948	48.03

Table A76. $C_{14}EO_4$ / $C_{12}SO_3Na$ Mixture in 0.1M NaCl, α_{non}= 0.00632

C (M)	Log C	γ(dyn/cm)
$C_1=2.707\times10^{-3}$	-2.568	33.62
1/2 C_1	-2.869	32.07
¼ C_1	-3.170	30.96
7/40 C_1	-3.324	32.68
1/8 C_1	-3.471	36.15
7/80 C_1	-3.625	39.77
1/16 C_1	-3.772	43.13
1/32 C_1	-4.073	50.96

Table A77. $C_{12}TMC$ in 0.1M NaCl

C (M)	Log C	γ(dyn/cm)
$C_1=1.98\times10^{-2}$	-1.703	39.95
1/2 C_1	-2.004	41.36
7/20 C_1	-2.159	41.32
¼ C_1	-2.305	43.71
7/40 C_1	-2.460	46.01
1/8 C_1	-2.606	48.32
7/80 C_1	-2.761	51.39
1/16 C_1	-2.907	53.99

Table A78. $C_{12}EO_7$ / $C_{12}TMAC$ Mixture in 0.1M NaCl, α_{non}= 0.0119

C (M)	Log C	γ(dyn/cm)
$C_1=8.02\times10^{-3}$	-2.096	37.64
1/2 C_1	-2.397	35.29
7/20 C_1	-2.552	34.68
¼ C_1	-2.698	36.18
7/40 C_1	-2.853	39.38
1/8 C_1	-2.999	41.89
7/80 C_1	-3.154	44.31
1/16 C_1	-3.300	47.22
1/32 C_1	-3.601	52.20

Table A79. $C_{14}EO_8$ / C_{12}TMAC Mixture in 0.1M NaCl, α_{non}= 0.00256

C (M)	Log C	γ(dyn/cm)
$C_1=7.94\times10^{-3}$	-2.100	39.60
1/2 C_1	-2.401	37.77
7/20 C_1	-2.556	37.91
¼ C_1	-2.702	38.11
7/40 C_1	-2.857	39.93
1/8 C_1	-3.003	42.16
7/80 C_1	-3.158	44.26
1/16 C_1	-3.304	45.51
1/32 C_1	-3.605	50.51

Table A80. 5, 6 -- C_{10}diol in 0.1M NaCl

C (M)	Log C	γ(dyn/cm)
$C_1=2.327\times10^{-3}$	-2.633	51.69
7/10 C_1	-2.788	54.31
1/2 C_1	-2.934	56.72
7/20 C_1	-3.089	59.12

Table A81. 4, 5 -- C_{10}diol in H_2O

C (M)	Log C	γ(dyn/cm)
$C_1=2.995\times10^{-3}$	-2.524	49.19
7/10 C_1	-2.679	51.91
1/2 C_1	-2.825	54.25
1/4 C_1	-3.126	59.34
4.00×10^{-3}	-2.398	47.13
$C_3=1.509\times10^{-3}$	-2.821	53.99**
1/2 C_3	-3.122	59.07**

**: check two points for 4, 5--C_{10}diol in 0.1M NaCl medium. Almost the same curve for 4, 5--C_{10}diol in both H_2O and 0.1M NaCl media.

Table A82. $C_{12}SO_3Na$ / 4, 5 -- C_{10}diol Mixture in 0.1M NaCl, α_{non}= 0.655

C (M)	Log C	γ(dyn/cm)
C_1=6.39×10^{-3}	-2.194	28.43
C_2=4.87×10^{-3}	-2.312	28.83
7/10 C_2	-2.467	31.26
7/20 C_2	-2.768	39.04
7/40 C_2	-3.069	45.26
7/80 C_2	-3.370	53.04
7/160 C_2	-3.671	58.06

Table A83. $C_{12}SO_3Na$ / 5, 6 -- C_{10}diol Mixture in 0.1M NaCl, α_{non}= 0.638

C (M)	Log C	γ(dyn/cm)
C_1= 4.69×10^{-3}	-2.329	29.0
1/2 C_1	-2.630	35.44
7/20 C_1	-2.785	39.10
1/4 C_1	-2.931	43.04
1/8 C_1	-3.232	49.86
1/16 C_1	-3.533	56.50

Table A84. TM 15-S-7 in 0.1M NaCl

C (M)	Log C	γ(dyn/cm)
5 C_1	-2.961	28.34
C_1=2.188×10^{-4}	-3.660	28.49
1/2 C_1	-3.961	28.93
1/4 C_1	-4.262	30.47
1/8 C_1	-4.563	35.40
1/16 C_1	-4.864	40.71
1/32 C_1	-5.165	46.07
1/64 C_1	-5.466	50.91

Table A85. $C_{12}SO_3Na$ / TM 15-S-7 Mixture in 0.1M NaCl, α_{non}= 0.0342

C (M)	Log C	γ(dyn/cm)
C_1=2.558x10^{-3}	-2.592	31.50
1/2 C_1	-2.893	31.14
1/4 C_1	-3.194	32.14
1/8 C_1	-3.495	36.23
1/16 C_1	-3.796	42.90
1/32 C_1	-4.097	48.53
1/64 C_1	-4.398	54.20

Table A86. C_{12}TMC in 0.5M NaCl

C (M)	Log C	γ(dyn/cm)
C_1=2.00x10^{-2}	-1.699	38.93
1/2 C_1	-2.000	39.10
¼ C_1	-2.301	39.25
1/8 C_1	-2.602	39.47
1/16 C_1	-2.903	44.52
1/32 C_1	-3.204	50.04
1/64 C_1	-3.505	55.80

Table A87. $C_{12}EO_7$ in 0.5M NaCl

C (M)	Log C	γ(dyn/cm)
C_1=3.55x10^{-4}	-3.450	29.56
¼ C_1	-4.052	29.67
1/8 C_1	-4.353	32.31
1/16 C_1	-4.654	37.43
1/32 C_1	-4.955	43.39
1/64 C_1	-5.256	48.73
1/128 C_1	-5.557	54.34

Table A88. $C_{12}EO_7$ / $C_{12}TMC$ Mixture in 0.5M NaCl, α_{non}= 0.0259

C (M)	Log C	γ(dyn/cm)
C_1=1.027×10^{-2}	-1.988	37.01
1/2 C_1	-2.289	36.54
¼ C_1	-2.590	34.50
1/8 C_1	-2.891	32.70
1/16 C_1	-3.192	35.99
1/32 C_1	-3.493	41.81
1/64 C_1	-3.794	47.23
1/128 C_1	-4.096	51.61

Table A89. $C_{12}TMC$ in 0.2M NaCl

C (M)	Log C	γ(dyn/cm)
C_1=2.00×10^{-2}	-1.699	40.09
1/2 C_1	-2.000	40.10
¼ C_1	-2.301	40.18
1/8 C_1	-2.602	44.29
1/16 C_1	-2.903	50.02
1/32 C_1	-3.204	55.47
1/64 C_1	-3.505	59.93

Table A90. $C_{12}EO_7$ / $C_{12}TMAC$ Mixture in 0.2M NaCl, α_{non}= 0.0174

C (M)	Log C	γ(dyn/cm)
C_1=1.527×10^{-2}	-1.816	38.42
1/2 C_1	-2.117	37.40
¼ C_1	-2.418	34.41
1/8 C_1	-2.719	32.46
1/16 C_1	-3.020	37.61
1/32 C_1	-3.321	44.03
1/64 C_1	-3.622	49.32
1/128 C_1	-3.923	54.39

Table A91. $C_{12}TMC$ in 0.05M NaCl

C (M)	Log C	γ(dyn/cm)
$C_1=2.55\times10^{-2}$	-1.593	41.63
7/10 C_1	-1.748	41.58
7/20 C_1	-2.049	41.83
7/40 C_1	-2.350	47.02
7/80 C_1	-2.651	52.54
7/160 C_1	-2.952	57.99

Table A92. $C_{12}EO_7$ / $C_{12}TMAC$ Mixture in 0.05M NaCl, α_{non}= 0.00965

C (M)	Log C	γ(dyn/cm)
$C_1=2.57\times10^{-2}$	-1.589	39.93
1/2 C_1	-1.890	37.97
¼ C_1	-2.191	34.60
7/40 C_1	-2.346	33.17
1/8 C_1	-2.492	33.51
1/16 C_1	-2.793	39.45
1/32 C_1	-3.094	45.27
1/64 C_1	-3.395	50.93

Table A93. $C_{12}EO_7$ in 0.1M NH_4Cl, no pH adjustment

C (M)	Log C	γ(dyn/cm)
$C_1=1.964\times10^{-4}$	-3.707	29.76
1/2 C_1	-4.008	30.07
¼ C_1	-4.309	34.16
1/8 C_1	-4.610	40.53
1/16 C_1	-4.911	45.76
1/32 C_1	-5.212	51.42
4 C_1	-3.105	29.38

Table A94. $C_{12}EO_7$ in 0.1M LiCl

C (M)	Log C	γ(dyn/cm)
$C_1=1.964\times10^{-4}$	-3.707	29.76
1/2 C_1	-4.008	30.07
¼ C_1	-4.309	34.16
1/8 C_1	-4.610	40.53
1/16 C_1	-4.911	45.76
1/32 C_1	-5.212	51.42

Table A95. $C_{12}SO_3Na$ in 0.1M LiCl

C (M)	Log C	γ(dyn/cm)
$C_1=7.489\times10^{-3}$	-2.126	37.12
1/2 C_1	-2.427	37.06
¼ C_1	-2.728	39.69
7/40 C_1	-2.883	43.95
1/8 C_1	-3.029	47.46
7/80 C_1	-3.184	49.84
7/160 C_1	-3.485	55.97

Table A96. $C_{12}EO_7$ / $C_{12}SO_3Na$ Mixture in 0.1M LiCl, α_{non}= 0.0311

C (M)	Log C	γ(dyn/cm)
$C_1=4.122\times10^{-3}$	-2.385	35.05
1/2 C_1	-2.686	34.15
¼ C_1	-2.987	33.66
1/8 C_1	-3.288	36.42
7/80 C_1	-3.443	39.70
1/16 C_1	-3.589	42.54
1/32 C_1	-3.890	48.47
1/64 C_1	-4.191	53.93

Table A97. $C_{12}SO_3Na$ in 0.1M NH_4Cl, no pH adjustment

C (M)	Log C	γ(dyn/cm)
C_1=7.489×10^{-3}	-2.126	33.50
1/2 C_1	-2.427	33.58
¼ C_1	-2.728	33.86
7/40 C_1	-2.883	37.14
1/8 C_1	-3.029	41.09
7/80 C_1	-3.184	44.63
1/16 C_1	-3.330	48.24
7/160 C_1	-3.485	51.35

Table A98. $C_{12}EO_7$ / $C_{12}SO_3Na$ Mixture in 0.1M NH_4Cl, no pH Adjustment, α_{non}= 0.0378

C (M)	Log C	γ(dyn/cm)
C_1=4.151×10^{-3}	-2.382	32.21
1/2 C_1	-2.683	31.72
¼ C_1	-2.984	31.89
1/8 C_1	-3.285	33.54
1/16 C_1	-3.586	39.74
1/32 C_1	-3.887	46.50
1/64 C_1	-4.188	51.74

Table A99. $C_{14}EO_8$ / $C_{12}SO_3Na$ Mixture in 0.1M NH_4Cl, no pH Adjustment, α_{non}= 0.00598

C (M)	Log C	γ(dyn/cm)
C_1=2.925×10^{-3}	-2.534	33.10
1/2 C_1	-2.835	33.02
1/4 C_1	-3.136	35.05
1/8 C_1	-3.437	37.68
1/16 C_1	-3.738	43.18
1/32 C_1	-4.039	~ 49
1/64 C_1	-4.340	~ 55.6

Table A100. $C_{14}EO_8$ / $C_{12}SO_3Na$ Mixture in 0.1M LiCl, α_{non}= 0.00598

C (M)	Log C	γ(dyn/cm)
$C_1=2.925\times10^{-3}$	-2.534	36.37
1/2 C_1	-2.835	36.33
1/4 C_1	-3.136	36.87
1/8 C_1	-3.437	39.21
7/80 C_1	-3.592	41.97
1/16 C_1	-3.738	44.70
1/32 C_1	-4.039	51.79

Table A101. $C_{14}EO_8$ in 0.1M NH_4Cl, no pH adjustment

C (M)	Log C	γ(dyn/cm)
$C_1=4.37\times10^{-5}$	-4.360	34.67
1/2 C_1	-4.661	34.99
1/4 C_1	-4.962	35.91
1/8 C_1	-5.263	38.88
1/16 C_1	-5.564	44.36
1/32 C_1	-5.865	49.47
1/64 C_1	-6.166	54.87
$C_2=4.37\times10^{-5}$	-4.360	34.76*
1/4 C_2	-4.962	36.22*
1/16 C_2	-5.564	44.56*

*: check 3 points for $C_{14}EO_8$ in 0.1M LiCl, the same result as in 0.1M NH_4Cl.

Table A102. $C_{14}EO_8$ / $C_{12}SO_3Na$ Mixture in 0.1M NH_4Cl, no pH adjustment, α_{non}= 0.00795

C (M)	Log C	γ(dyn/cm)
$C_1=2.892\times10^{-3}$	-2.539	33.21
1/2 C_1	-2.840	33.54
1/4 C_1	-3.141	35.05
7/40 C_1	-3.296	34.65
1/8 C_1	-3.442	36.86
7/80 C_1	-3.597	38.42
1/16 C_1	-3.743	42.28
7/160 C_1	-3.898	44.40
1/32 C_1	-4.044	47.05

Table A103. $C_{12}EO_4$ / $C_{12}SO_3Na$ Mixture in 0.1M NaCl, α_{non}= 0.0254

C (M)	Log C	γ(dyn/cm)
C_1=2.983x10^{-3}	-2.525	32.13
1/2 C_1	-2.826	30.89
1/4 C_1	-3.127	30.84
7/40 C_1	-3.282	33.84
1/8 C_1	-3.428	37.30
7/80 C_1	-3.583	40.73
1/16 C_1	-3.729	44.47
1/32 C_1	-4.030	50.30

Table A104. $C_{12}EO_4$ / $C_{12}SO_3Na$ Mixture in 0.1M NH_4Cl, no pH adjustment, α_{non}= 0.0255

C (M)	Log C	γ(dyn/cm)
C_1=3.001x10^{-3}	-2.523	31.47
1/2 C_1	-2.824	29.44
7/20 C_1	-2.979	29.35
1/4 C_1	-3.125	29.93
7/40 C_1	-3.280	32.29
1/8 C_1	-3.426	35.86
7/80 C_1	-3.581	39.39
1/16 C_1	-3.727	43.48
1/32 C_1	-4.028	50.30

Table A105. $C_{12}EO_4$ in 0.1M NaCl

C (M)	Log C	γ(dyn/cm)
C_1=3.785x10^{-4}	-3.422	28.29
1/2 C_1	-3.724	28.63
1/4 C_1	-4.025	29.63
1/8 C_1	-4.326	31.34
1/16 C_1	-4.627	36.33
7/160 C_1	-4.782	39.82
1/32 C_1	-4.928	43.40
1/64 C_1	-5.229	49.70

Table A106. $C_{12}EO_4$ / $C_{12}SO_3Na$ Mixture in 0.1M LiCl, α_{non}= 0.0232

C (M)	Log C	γ(dyn/cm)
C_1=2.994×10^{-3}	-2.524	33.60
1/2 C_1	-2.825	31.22
1/4 C_1	-3.126	32.07
7/40 C_1	-3.281	34.66
1/8 C_1	-3.427	38.43
7/80 C_1	-3.582	41.80
1/16 C_1	-3.728	44.80
1/32 C_1	-4.029	51.57

Table A107. $C_{14}EO_4$ in 0.1M LiCl

C (M)	Log C	γ(dyn/cm)
C_1=5.90×10^{-5}	-4.229	28.64
1/2 C_1	-4.530	28.73
1/4 C_1	-4.831	29.23
1/8 C_1	-5.132	30.71
1/16 C_1	-5.433	33.14
1/32 C_1	-5.734	42.3
1/64 C_1	-6.035	52.0

Table A108. $C_{14}EO_4$ / $C_{12}SO_3Na$ Mixture in 0.1M NH_4Cl, no pH adjustment, α_{non}= 0.00499

C (M)	Log C	γ(dyn/cm)
C_1=4.409×10^{-3}	-2.356	33.17
1/2 C_1	-2.657	32.45
1/4 C_1	-2.958	31.58
7/40 C_1	-3.113	31.16
1/8 C_1	-3.259	32.59
7/80 C_1	-3.414	33.65
1/16 C_1	-3.560	37.09
7/160 C_1	-3.715	41.59
1/32 C_1	-3.861	47.19

Table A109. $C_{14}EO_4$ / $C_{12}SO_3Na$ Mixture in 0.1M LiCl, α_{non}= 0.00404

C (M)	Log C	γ(dyn/cm)
C_1=2.919×10^{-3}	-2.535	35.72
1/2 C_1	-2.836	33.32
1/4 C_1	-3.137	33.05
1/8 C_1	-3.438	38.20
1/16 C_1	-3.739	47.54
1/32 C_1	-4.040	54.44

Table A110. $C_{14}EO_4$ / $C_{12}SO_3Na$ Mixture in 0.1M NH_4Cl, no pH adjustment, α_{non}= 0.00792

C (M)	Log C	γ(dyn/cm)
C_1=2.892×10^{-3}	-2.539	32.78
1/2 C_1	-2.840	31.13
7/20 C_1	-2.995	31.01
1/4 C_1	-3.141	30.94
1/8 C_1	-3.442	33.47
7/80 C_1	-3.597	34.48
1/16 C_1	-3.743	39.54
1/32 C_1	-4.044	48.23

Table A111. $C_{12}EO_7$ in 0.05M $CaCl_2$

C (M)	Log C	γ(dyn/cm)
C_1=4.829×10^{-4}	-3.316	29.41
1/4 C_1	-3.918	29.35
1/8 C_1	-4.219	31.95
1/16 C_1	-4.520	37.74
1/32 C_1	-4.821	43.54
1/64 C_1	-5.122	49.15

Table A112. $C_{12}E_2S$ in 0.05M $CaCl_2$

C (M)	Log C	γ(dyn/cm)
$C_1=6.525\times10^{-4}$	-3.185	31.25
1/2 C_1	-3.486	31.43
1/4 C_1	-3.787	31.53
7/40 C_1	-3.942	33.81
1/8 C_1	-4.088	37.16
7/80 C_1	-4.243	40.62
1/16 C_1	-4.390	43.97
1/32 C_1	-4.691	50.40

Table A113. $C_{12}EO_7$ / $C_{12}E_2S$ Mixture in 0.05M $CaCl_2$, α_{non}= 0.358

C (M)	Log C	γ(dyn/cm)
$C_1=1.016\times10^{-3}$	-2.993	29.47
1/2 C_1	-3.294	29.64
1/4 C_1	-3.595	29.87
1/8 C_1	-3.896	30.02
1/16 C_1	-4.197	32.88
7/160 C_1	-4.352	36.59
1/32 C_1	-4.498	39.87
1/64 C_1	-4.799	46.09
1/128 C_1	-5.100	51.61

Table A114. $C_{12}EO_4$ / $C_{12}E_2S$ Mixture in 0.05M $CaCl_2$, α_{non}= 0.250

C (M)	Log C	γ(dyn/cm)
$C_1=6.96\times10^{-4}$	-3.157	28.55
1/2 C_1	-3.458	28.38
1/4 C_1	-3.759	28.26
1/8 C_1	-4.060	29.09
7/80 C_1	-4.215	32.08
1/16 C_1	-4.362	35.03
7/160 C_1	-4.516	39.74
1/32 C_1	-4.663	43.16
7/320 C_1	-4.817	46.87
1/64 C_1	-4.964	50.05

Table A115. $C_{12}E_2S$ in 0.033M $CaCl_2$

C (M)	Log C	γ(dyn/cm)
$C_1=9.986\times10^{-4}$	-3.001	31.61
1/4 C_1	-3.603	31.71
1/8 C_1	-3.904	34.02
1/16 C_1	-4.205	40.95
1/32 C_1	-4.506	47.65
1/64 C_1	-4.807	53.46

Table A116. $C_{12}EO_7$ / $C_{12}E_2S$ Mixture in 0.033M $CaCl_2$, α_{non}= 0.343

C (M)	Log C	γ(dyn/cm)
$C_1=7.60\times10^{-4}$	-3.119	29.80
1/2 C_1	-3.420	29.83
1/4 C_1	-3.721	29.86
1/8 C_1	-4.022	30.40
7/80 C_1	-4.177	33.89
1/16 C_1	-4.323	36.36
7/160 C_1	-4.478	40.22
1/32 C_1	-4.624	43.04
1/64 C_1	-4.925	49.19

Table A117. $C_{12}EO_7$ / $C_{12}E_2S$ Mixture in 0.1M NaCl, α_{non}= 0.198

C (M)	Log C	γ(dyn/cm)
$C_1=6.225\times10^{-4}$	-3.206	33.05
1/2 C_1	-3.507	32.65
1/4 C_1	-3.808	32.42
7/40 C_1	-3.963	34.18
1/8 C_1	-4.109	37.23
1/16 C_1	-4.410	43.54
1/32 C_1	-4.711	49.74

Table A118. $C_{12}EO_4$ / $C_{12}E_2S$ Mixture in 0.033M $CaCl_2$, α_{non}= 0.246

C (M)	Log C	γ(dyn/cm)
$C_1=6.62\times10^{-4}$	-3.179	28.48
1/4 C_1	-3.781	28.08
1/8 C_1	-4.082	30.13
7/80 C_1	-4.237	33.23
1/16 C_1	-4.383	36.73
7/160 C_1	-4.538	40.33
1/32 C_1	-4.684	43.84
1/64 C_1	-4.985	50.75

Table A119. $C_{12}EO_4$ / $C_{12}E_2S$ Mixture in 0.1M NaCl, α_{non}= 0.149

C (M)	Log C	γ(dyn/cm)
$C_1=6.577\times10^{-4}$	-3.182	31.50
1/2C_1	-3.483	30.90
1/4 C_1	-3.784	30.39
1/8 C_1	-4.085	35.27
7/80 C_1	-4.240	39.27
1/16 C_1	-4.386	41.96
7/160 C_1	-4.541	46.23
1/32 C_1	-4.687	49.19

Table A120. $C_{12}EO_4$ / $C_{12}TMC$ Mixture in 0.1M NaCl, α_{non}= 0.00793

C (M)	Log C	γ(dyn/cm)
$C_1=1.61\times10^{-2}$	-1.793	39.08
1/2C_1	-2.094	35.62
1/4 C_1	-2.395	32.33
7/40 C_1	-2.550	32.73
1/8 C_1	-2.696	35.13
1/16 C_1	-2.997	39.84
7/160 C_1	-3.152	44.4
1/32 C_1	-3.298	47.2
7/320 C_1	-3.453	50.2
1/64 C_1	-3.599	52.85

Table A121. $C_{12}EO_4$ / $C_{12}TMC$ Mixture in 0.1M NaCl, α_{non}= 0.0198

C (M)	Log C	γ(dyn/cm)
C_1=1.02x10^{-2}	-1.991	36.36
1/2C_1	-2.292	31.60
7/20 C_1	-2.447	30.86
1/4 C_1	-2.593	30.21
1/8 C_1	-2.894	33.10
7/80 C_1	-3.049	36.07
1/16 C_1	-3.196	39.21
7/160 C_1	-3.350	42.57
1/32 C_1	-3.497	46.14
1/64 C_1	-3.798	52.33

Table A122. $C_{12}EO_4$ / $C_{12}TMC$ Mixture in 0.1M NaCl, α_{non}= 0.00402

C (M)	Log C	γ(dyn/cm)
C_1=1.506x10^{-2}	-1.822	40.00
1/2C_1	-2.123	35.56
7/20 C_1	-2.278	34.04
1/4 C_1	-2.424	33.47
7/40 C_1	-2.579	37.01
1/8 C_1	-2.725	39.93
7/80 C_1	-2.880	43.55
1/16 C_1	-3.026	46.39
1/32 C_1	-3.327	52.73

Table A123. $C_{12}EO_4$ / $C_{12}SO_3Na$ Mixture in 0.1M NaCl, α_{non}= 0.0603

C (M)	Log C	γ(dyn/cm)
C_1=3.683x10^{-3}	-2.434	30.72
1/2 C_1	-2.735	29.53
1/4 C_1	-3.036	29.06
7/40 C_1	-3.191	28.84
1/8 C_1	-3.337	30.25
7/80 C_1	-3.492	33.54
1/16 C_1	-3.638	36.92
7/160 C_1	-3.793	40.26
1/32 C_1	-3.939	44.03
1/64 C_1	-4.240	51.39

Table A124. $C_{12}EO_4$ / $C_{12}SO_3Na$ Mixture in 0.1M NaCl, α_{non}= 0.0100

C (M)	Log C	γ(dyn/cm)
C_1=3.495x10^{-3}	-2.457	33.39
1/2 C_1	-2.758	31.15
7/20 C_1	-2.912	31.21
1/4 C_1	-3.059	32.96
7/40 C_1	-3.213	36.97
1/8 C_1	-3.360	40.21
7/80 C_1	-3.515	44.00
1/16 C_1	-3.661	47.27
7/160 C_1	-3.816	52.00

Table A125. 1,2–C_{10} diol / $C_{12}SO_3Na$ Mixture in 0.1M NaCl, α_{non}= 0.805

C (M)	Log C	γ(dyn/cm)
C_1=4.304x10^{-3}	-2.366	22.86
1/2 C_1	-2.667	22.88
7/20 C_1	-2.822	24.70
1/4C_1	-2.968	30.18
7/40 C_1	-3.123	35.09
1/8C_1	-3.269	40.15
7/80 C_1	-3.424	44.99

Table A126. 1,2–C_{10} diol / $C_{12}SO_3Na$ Mixture in 0.1M NaCl, α_{non}= 0.256

C (M)	Log C	γ(dyn/cm)
C_1=4.06x10^{-3}	-2.391	23.96
1/2 C_1	-2.692	23.69
7/20 C_1	-2.847	27.65
1/4C_1	-2.994	32.62
7/40 C_1	-3.148	37.90
1/8C_1	-3.295	42.36
7/80 C_1	-3.449	47.22
1/16 C_1	-3.596	51.23

Table A127. $C_{12}SO_3Na$ / C_{12}-GA Mixture in 0.1M NaCl, α_{non}= 0.567

C (M)	Log C	γ(dyn/cm)
C_1=2.40×10^{-3}	-2.620	28.95
1/2 C_1	-2.921	28.95
1/4 C_1	-3.222	29.07
7/40 C_1	-3.377	30.05
1/8 C_1	-3.523	34.06
7/80 C_1	-3.678	38.00
1/16 C_1	-3.824	41.76
1/32 C_1	-4.125	48.88

Table A128. $C_{12}SO_3Na$ / C_{12}-GA Mixture in 0.1M NaCl, α_{non}= 0.0533

C (M)	Log C	γ(dyn/cm)
C_1=3.820×10^{-3}	-2.418	32.44
1/2 C_1	-2.719	31.26
7/20 C_1	-2.874	30.70
1/4 C_1	-3.020	33.07
7/40 C_1	-3.175	36.79
1/8 C_1	-3.321	41.34
7/80 C_1	-3.476	44.49
1/16 C_1	-3.622	49.01

Table A129. C8P in H_2O

C (M)	Log C	γ(dyn/cm)
C_1=5.22×10^{-3}	-2.282	28.27
1/2 C_1	-2.583	35.63
7/20 C_1	-2.738	39.36
1/4 C_1	-2.884	43.13
7/40 C_1	-3.039	46.80
1/8 C_1	-3.185	50.34
1/16 C_1	-3.486	57.40

Table A130. Igepal CA-520 in H_2O

C (M)	Log C	γ(dyn/cm)
$C_1=1.49\times10^{-3}$	-2.827	27.94
1/4 C_1	-3.429	27.95
1/8 C_1	-3.730	27.89
1/16 C_1	-4.031	31.18
7/160 C_1	-4.186	34.66
1/32 C_1	-4.332	37.45
7/320 C_1	-4.487	41.34
1/64 C_1	-4.633	44.15
1/128 C_1	-4.934	50.19

Table A131. C8P / Igepal CA-520 Mixture in H_2O, α_{C8P}= 0.900

C (M)	Log C	γ(dyn/cm)
$C_1=2.14\times10^{-3}$	-2.670	27.34
1/2 C_1	-2.971	27.95
7/20 C_1	-3.126	31.35
1/4 C_1	-3.272	34.28
7/40 C_1	-3.427	38.27
1/8 C_1	-3.573	41.10
1/16 C_1	-3.874	47.63

Table A132. C8P / Igepal CA-520 Mixture in H_2O, α_{C8P}= 0.763

C (M)	Log C	γ(dyn/cm)
$C_1=1.51\times10^{-3}$	-2.821	27.56
1/2 C_1	-3.122	27.68
7/20 C_1	-3.277	28.01
1/4 C_1	-3.423	30.83
7/40 C_1	-3.578	34.23
1/8 C_1	-3.724	37.30
1/16 C_1	-4.025	43.99
1/32 C_1	-4.326	50.11

Table A133. $C_{12}EO_4$ / $C_{14}EO_8$ Mixture in 0.1M NaCl, α_{C14}= 0.164

C (M)	Log C	γ(dyn/cm)
C_1=2.40×10^{-4}	-3.620	28.13
1/2 C_1	-3.921	28.72
1/4 C_1	-4.222	29.55
1/8 C_1	-4.523	31.81
1/16 C_1	-4.824	36.48
7/160 C_1	-4.979	40.06
1/32 C_1	-5.125	43.88
1/64 C_1	-5.426	48.81

Appendix B.

Equilibrium Contact Angle Results for Surfactants Studied and Mixtures in 0.1M NaCl and 25.0°C, at Neutral pH Condition. Solid Substrate is Parafilm Without Any Pretreatment

$C_{12}EO_4$ in 0.1M NaCl, and θ on Parafilm (no pretreatment)

C (M)	Log C	γ(dyn/cm)	θ	γ·cosθ
$C_1=5.74\times10^{-4}$	-3.241	28.2	31.5	24.1
$1/2C_1$	-3.542	28.3	40.5	21.5
$1/4\ C_1$	-3.843	28.4	40.6	21.6
$1/8\ C_1$	-4.144	28.4	50.1	18.22
$1/16\ C_1$	-4.445	35.2	69.9	11.1
$1/32\ C_1$	-4.746	42.6	90.3	-0.23
$1/64\ C_1$	-5.047	50.0	98-90	

$C_{14}EO_8$ in 0.1M NaCl, and θ on Parafilm (no pretreatment)

C (M)	Log C	γ(dyn/cm)	θ	γ·cosθ
$C_1=6.55\times10^{-4}$	-4.184	34.74	56.3	19.5
$1/2C_1$	-4.485	34.75	58.0	18.7
$1/4\ C_1$	-4.786	34.88	73.0	10.3
$1/8\ C_1$	-5.087	36.68	91.5	-0.9
$1/16\ C_1$	-5.388	39.60		
$1/32\ C_1$	-5.689	44.03	98.1	-6.6
$1/64\ C_1$	-5.990	53.77		

$C_{12}E_2S$ in 0.1M NaCl, and θ on Parafilm (no pretreatment)

C (M)	Log C	γ(dyn/cm)	θ	γ·cosθ
$C_1=3.323\times10^{-3}$	-2.478	35.00	60.9	17.1
$1/2C_1$	-2.779	35.00	60.2	17.4
$1/4\ C_1$	-3.080	35.00	61.5	16.7
$1/8\ C_1$	-3.381	35.20	60.1	17.5
$1/16\ C_1$	-3.683	38.4	70.6	12.8
$1/32\ C_1$	-3.984	42.4	80.2	7.2
$1/64\ C_1$	-4.285	50.8	92.7	-2.4
	-4.586	57.4	97.5	-7.5

C_{12}TMAC in 0.1M NaCl, and θ on Parafilm (no pretreatment)

C (M)	Log C	γ(dyn/cm)	θ	γ·cosθ
$C_1=2.0\times10^{-2}$	-1.699	40.0	65.8	16.4
7/10 C_1	-1.854	40.0	65.8	16.4
1/2C_1	-2.00	40.0	69.9	13.8
1/4 C_1	-2.301	43.6	77.9	9.2
1/8 C_1	-2.602	48.6	84.3	4.8
1/16 C_1	-2.903	53.6	92.8	-2.6
1/32 C_1	-3.204	58.8	101.1	-11.3

$C_{12}EO_4$ / $C_{14}EO_8$ in 0.1M NaCl, and θ on Parafilm (no pretreatment) α_{C14}= 0.164

C (M)	Log C	γ(dyn/cm)	θ	γ·cosθ
$C_1=2.40\times10^{-4}$	-3.620	28.13	39.0	21.9
1/2C_1	-3.921	28.72	39.8	22.0
1/4 C_1	-4.222	29.55	49.5	19.2
1/8 C_1	-4.523	31.81	74.4	8.6
1/16 C_1	-4.824	36.48	89.3	0.5
7160C_1	-4.979	40.06	93.0	-2.1
1/32 C_1	-5.125	43.88		
1/64 C_1	-5.426	48.81	96.2	-5.4

$C_{12}EO_4$ / $C_{12}E_2S$ in 0.1M NaCl, and θ on Parafilm (no pretreatment) α_{non}= 0.149

C (M)	Log C	γ(dyn/cm)	θ	γ·cosθ
$C_1=9.64\times10^{-4}$	-3.016	31.8	50.0	20.4
1/2C_1	-3.317	31.3	48.7	20.7
1/4 C_1	-3.618	30.7	48.6	20.3
1/8 C_1	-3.919	31.3	61.5	14.9
1/16 C_1	-4.220	38.5	68.6	14-11.3
1/32 C_1	-4.521	45.7	81.7	6.6
1/64 C_1	-4.822	52.8	90.6	-0.6

$C_{14}EO_8$ / $C_{12}E_2S$ in 0.1M NaCl, and θ on Parafilm (no pretreatment) α_{non}= 0.05

C (M)	Log C	γ(dyn/cm)	θ	γ·cosθ
C_1=5.0×10^{-4}	-3.301	35.3	58.0	18.7
1/2C_1	-3.602	35.33	58.7	18.4
1/4 C_1	-3.903	35.6	63.6	15.9
1/8 C_1	-4.204	37.46	82.0	5.2
7/80 C_1	-4.359	40.74	87.4	1.9
1/16 C_1	-4.505	42.54	91.8	-1.4
1/32 C_1	-4.806	48.38	100.2	-8.5

$C_{14}EO_8$ / C_{12}TMAC in 0.1M NaCl, and θ on Parafilm (no pretreatment) α_{non}= 0.00256

C (M)	Log C	γ(dyn/cm)	θ	γ·cosθ
C_1=1.20×10^{-2}	-1.921	40.6	68.8	14.7
1/2C_1	-2.222	38.8	69.0	13.9
1/4 C_1	-2.523	37.9	71.9	11.8
1/8 C_1	-2.824	39.6	84.0	4.1
1/16 C_1	-3.125	43.9	92.7	-2.1
1/32 C_1	-3.426	48.2	97.1	-6.0
1/64 C_1	-3.727	52.4	101.7	-10.6

$C_{12}EO_4$ / C_{12}TMAC in 0.1M NaCl, and θ on Parafilm (no pretreatment) α_{non}= 0.00793

C (M)	Log C	γ(dyn/cm)	θ	γ·cosθ
C_1=1.21×10^{-2}	-1.917	37.7	63.6	16.8
1/2C_1	-2.218	34.4	61.0	16.7
1/4 C_1	-2.519	31.9	74.3	8.6
1/8 C_1	-2.820	37.8	88.5	1.1
1/16 C_1	-3.121	43.7	93.9	-3.0
1/32 C_1	-3.422	49.6	99.7	-8.4

Bibliography

1. Thomas, S.; Ali, S. M. Farouq. *J. Canadian Petroleum Technology* **2001**, 40, 46.

2. Austad, Tor; Milter, Jess. *Surfactants* **2000**, 203.

3. Al-Sabagh, A. M. *Polym. Adv. Technol.* **2000**, 11, 48.

4. Qiao, Wei-hong; Zhang, Shu-biao; Wang, Shao-hui; Wu, Tao; Li, Zong-shi *Jingxi Huagong* **1999,** 16, 71.

5. Bergeron, V.; Hanssen, Jan Erik; Shoghl, F. N. *Colloids Surf., A* **1997**, 123, 609.

6. Borchardt, John K. *Preprints - Am. Chem. Soc. Div. Petro. Chem.* **1993,** 38, 108.

7. Celik, M. S.; Hancer, M.; Miller, J. D. *J. Colloid Interface Sci.* **2002,** 256, 121.

8. Moudgil, Brij M.; Singh, Pankaj K.; Adler, Joshua J. In *Handbook of Applied Surface and Colloid Chemistry* **2002,** 1, 219-249.

9. Xu, Qun; Somasundaran, P. *Publications of the Australasian Institute of Mining and Metallurgy* **1993,** 3/93, 601.

10. Dobias, Bohuslav. *Surfactant Sci. Ser.* **1993**, 47, 539.

11. Fuerstenau, D. W.; Herrera-Urbina, Ronaldo *Surfactant Sci. Ser.* **1991**, 37, 407.

12. Jain, Vivek; Demond, Avery H. *Environ. Sci. Technol.* **2002**, 36, 5434.

13. Ko, Seok-Oh; Schlautman, Mark A.; Carraway, Elizabeth R. *Environ. Sci. Technol.* **1999,** 33, 2765.

14. Harwell, J. H.; Knox, R. C.; Sabatini, D. A. *Annual Surfactants Review* **1998,** 1, 30.

15. Mosler, Randi; Hatton, T. Alan *Current Opinion in Colloid & Interface Sci.* **1996,** 1, 540.

16. Aratono, Makoto; Kawagoe, Hiroaki; Toyomasu, Takayuki; Ikeda, Norihiro; Takiue, Takanori; Matsubara, Hiroki. *Langmuir* **2001**, 17, 7344.

17. Hauthal, Hermann G.; Jurges, Peter; Mohle, Lothar; Ohlerich, Udo. *J. Surfactants and Detergents* **1999**, 2, 175.

18. Rosen, Milton J.; Song, Li D. *Langmuir* **1996**, 12, 4945.

19. Somasundaran, P.; Krishnakumar, S. *Colloids Surf., A* **1994**, 93, 79.

20. Rosen, Milton J.; Zhu, Zhen Huo. *J. Am. Oil Chem. Soc.* **1993**, 70, 65.

21. Gau, Churn Shiouh; Zograft, George *J. Colloid Interface Sci.* **1990**, 140, 1.

22. Kilau, Howard W.; Pahlman, John E. *Colloids Surf.* **1987**, 26, 217.

23. Glanville, James O.; Haley, Leighton H. *Colloids Surf.* **1982**, 4, 213.

24. Cohen, A. W.; Rosen, M. J. *J. Am. Oil Chem. Soc.* **1981**, 58, 1062.

25. Norenberg, R.; Oetter, G. *Tenside, Surfactants, Detergents* **2001**, 38, 356.

26. Wei, Xiao-Fang; Liu, Hui-Zhou *J. Surfactants and Detergents* **2000**, 3, 491.

27. Szafranski, R.; Lawson, J. B.; Hirasaki, G. J.; Miller, C. A.; Akiya, N.; King, S.; Jackson, R. E.; Meinardus, H.; Londergan, J. *Progr. Colloid Polym. Sci.* **1998**, 111, 162

28. Rieger, Martin *Surfactant Sci. Ser.* **1996**, 57, 381.

29. Varadaraj, Ramesh; Bock, Jan; Valint, Paul, Jr.; Zushma, Stephen; Brons, Neil. *J. Colloid Interface Sci.* **1990**, 140, 31.

30. Rosen, Milton J. *J. Am. Oil Chem. Soc.* **1972**, 49, 293.

31. Miller, Clarence A. *J. Cosmetic Sci.* **2001**, 52, 144.

32. Tong, Jihong; Nakajima, Mitsutoshi; Nabetani, Hiroshi; Kikuchi, Yuji. *J. Surfactants and Detergents* **2000,** 3, 285.

33. Rocha, Sandro R. P. da; Harrison, Kristi L.; Johnston, Keith P. *Langmuir* **1999**, 15, 419.

34. Rang, M. J.; Miller, C. A. *Progr. Colloid Polym. Sci.* **1998**, 109, 101.

35. Ruths, Marina; Granick, Steve. *Langmuir* **1998**, 14, 1804.

36. Zelenev, Andrei; Matijevic, Egon. *Colloids Surf., A* **1997**, 125, 171.

37. Miller, Clarence A. *Handbook of Surface and Colloid Chemistry,* 2nd ed.; 2003, 511.

38. Robb, I. D.; Stevenson, P. S. *Langmuir* **2000**, 16, 7939.

39. Weiss, Jochen; McClements, D. Julian. *Langmuir* **2000**, 16, 5879.

40. Linden, Mika; Aagren, Patrik; Karlsson, Stefan; Bussian, Patrick; Amenitsch, Heinz. *Langmuir* **2000**, 16, 5831.

41. Huibers, Paul D. T.; Shah, Dinesh O. *Langmuir* **1997**, 13, 5762.

42. Summers, Mark; Eastoe, Julian; Davis, Sean. *Langmuir* **2002**, 18, 5023.

43. Eastoe, Julian; Paul, Alison; Downer, Adrian; Steytler, David C.; Rumsey, Emily. *Langmuir* **2002**, 18, 3014.

44. Silas, James A.; Kaler, Eric W. *J. Colloid Interface Sci.* **2001**, 243, 248.

45. Lee, C. T., Jr.; Psathas, P. A.; Ziegler, K. J.; Johnston, K. P.; Dai, H. J.; Cochran, H. D.; Melnichenko, Y. B.; Wignall, G. D. *J. Phys. Chem., B* **2000**, 104, 1094.

46. Li, X.; Washenberger, R. M.; Scriven, L. E.; Davis, H. T.; Hill, Randal M. *Langmuir* **1999**, 15, 2267.

47. Ferreira Marques, M. F.; Burrows, H. D.; da Graca Miguel, M.; de Lima, A. P.; Lopes gil, C.; Duplatre, G. *J. Chem. Soc., Faraday Trans.* **1997**, 93, 3827.

48. Klier, J.; Suarez, R. S.; Green, D. P.; Kumar, A. M.; Hoffman, M.; Tucker, C. J.; Landes, B.; Redwine, D. *J. Am. Oil Chem. Soc.* **1997**, 74, 861.

49. Abe, Masahiko. *Surfactant Sci. Ser.* **1997**, 66, 279.

50. Gibbs, J. W. *The Collected Works of J. W. Gibbs*, Longmans, Green, London, 1928, Vol. I, p. 119.

51. Rosen, M. J. *Surfactants and Interfacial Phenomena,* 2nd ed.; Wiley-Interscience; New York, 1989; (a) pp. 65-68, (b) pp. 44–46, (c) pp. 393, (d) pp. 404-409, (e) pp. 394-401, (f) pp. 397, (g) pp. 143-148.

52. Regev, O.; Leaver, M. S.; Zhou, R.; Puntambekar, S. *Langmuir* **2001**, 17, 5141.

53. Ashbaugh, Henry S.; Piculell, Lennart; Lindman, Bjoern. *Langmuir* **2000**, 16, 2529.

54. Bossev, Dobrin Petrov; Matsumoto, Mutsuo; Nakahara, Masaru. *J. Phys. Chem., B* **1999**, 103, 8251.

55. Lesemann, Markus; Thirumoorthy, Kanthimathi; Kim, Yoo Joong; Jonas, Jiri; Paulaitis, Michael E. *Langmuir* **1998**, 14, 5339.

56. Cerichelli, Giorgio; Mancini, Giovanna. *Current Opinion in Colloid & Interface Sci.* **1997**, 2, 641.

57. Quist, Per-Ola; Sooederlind, Erik. *J. Colloid Interface Sci.* **1995**, 172, 510.

58. Menger, F. M.; Littau, C. A. *J. Am. Chem. Soc.* **1993**, 115, 10083.

59. Lindman, Bjoern; Soederman, Olle; Wennerstroem, Haakan. *Surfactant Sci. Ser.* **1987**, 22, 295.

60. Wennerstroem, Haakan; Lindman, Bjoern; Soederman, Olle; Drakenberg, Torbjoern; Rosenholm, Jarl B. *J. Am. Chem. Soc.* **1979**, 101, 6860.

61. Persson, Bert Ove; Drakenberg, Torbjoern; Lindman, Bjoern. *J. Phys. Chem.* **1979**, 83, 3011.

62. Esmer, Kadir; Tarcan, Erdogan *Spectroscopy Lett.* **2001**, 34, 443.

63. El Seoud, Omar A.; Correa, N. Mariano; Novaki, Luzia P. *Langmuir* **2001**, 17, 1847.

64. Novaki, Luzia P.; Correa, N. Mariano; Silber, Juana J.; El Seoud, Omar A. *Langmuir* **2000**, 16, 5573.

65. Almanza-Workman, A. Marcia; Raghavan, Srini; Sperline, Roger P. *Langmuir* **2000**, 16, 3636.

66. Mueller, Martin; Grosse, Ingrid; Jacobasch, Hans-Joerg; Sams, Philip *Tenside, Surfactants, Detergents* **1998**, 35, 354.

67. Wong, Tuck C.; Wong, Ning Bew; Tanner, Peter A. *J. Colloid Interface Sci.* **1997**, 186, 325.

68. Baden, Naoki; Kajimoto, Okitsugu; Hara, Kimihiko *J. Phys. Chem. B* **2002**, 106, 8621.

69. Alami, E.; Kamenka, N.; Raharimihamina, A.; Zana, R. *J. Colloid Interface Sci.* **1993**, 158, 342.

70. Frindi, M.; Michels, B.; Zana, R. *J. Phys. Chem.* **1992**, 96, 6095.

71. Malliaris, Angelos; Lang, Jacques; Zana, Raoul *J. Phys. Chem.* **1986**, 90, 655.

72. Turro, Nicholas J.; Kuo, Ping Lin. *J. Phys. Chem.* **1986**, 90, 837.

73. Lianos, Panagiotis; Lang, Jacques; Zana, Raoul *J. Colloid Interface Sci.* **1983**, 91, 276.

74. Bonini, Celine; Heux, Laurent; Cavaille, Jean-Yves; Lindner, Peter; Dewhurst, Charles; Terech, Pierre *Langmuir* **2002**, 18, 3311.

75. Bergstroem, Magnus; Pedersen, Jan Skov. *J. Phys. Chem., B* **2000**, 104, 4155.

76. Dupuy, C.; Auvray, X.; Petipas, C.; Anthore, R.; Rico-Lattes, I.; Lattes, A. *Langmuir* **1998**, 14, 91.

77. Wong, K.; Cabane, B.; Duplessix, R.; Somasundaran, P. *Langmuir* **1989**, 5, 1346.

78. Berr, Stuart S.; Jones, Richard R. M. *J. Phys. Chem.* **1989**, 93, 2555.

79. Cabane, Bernard. *Surfactant Sci. Ser.* **1987**, 22, 57.

80. Holland, P. M.; Rubingh, D.N. In *Mixed Surfactant Systems*; Holland, P. M., Rubingh, D.N., Eds.; ACS Symposium Series 501; American Chemical Society: Washington, DC, 1992; p 1.

81. Holland, P. M. In *Mixed Surfactant Systems*; Holland, P. M., Rubingh, D.N., Eds.; ACS Symposium Series 501; American Chemical Society: Washington, DC, 1992; p 31.

82. Rosen, M. J. *J. Am. Oil Chem. Soc.* **1989**, 66, 1840.

83. Rosen, M. J. In *Phenomena in Mixed Surfactant Systems*; Scamehorn, J.F., Ed.; ACS Symposium Series 311; American Chemical Society: Washington, DC, 1986; p 144.

84. Scamehorn, J.F. In *Phenomena in Mixed Surfactant Systems*; Scamehorn, J.F., Ed.; ACS Symposium Series 311; American Chemical Society: Washington, DC, 1986; p 1.

85. Shiloach, A.; Blankschtein, D. *Langmuir* **1998**, 14, 1618.

86. Bergström, M.; Eriksson, J. C. *Langmuir* **2000**, 16, 7173.

87. Nagarajan, R. In *Mixed Surfactant Systems*; Holland, P. M., Rubingh, D. N., Eds.; ACS Symposium Series 501; American Chemical Society: Washington, DC, 1992; p 54.

88. Matsubara, H.; Ohta, A.; Kameda, M.; Ikeda, N.; Aratono, M. *Langmuir* **2000**, 16, 7589.

89. Li, F.; Rosen, M. J.; Sulthana, S. B. *Langmuir* **2001**, 17, 1037.

90. Zhao, G-X.; Ding, F-X.; Zhu, B-Y. *Colloids Surf., A* **1998**, 132, 1.

91. Saiyad, A. H.; Bhat, S. G. T.; Rakshit, A. K. *Colloid Polym. Sci.* **1998**, 276, 913.

92. Filipovic-Vincekovic, N.; Juranovic, I.; Grahek, Z. *Colloids Surf., A* **1997**, 125, 115

93. Siddiqui, F. A.; Franses, E. I. *Langmuir* **1996**, 12, 354.

94. Anand, K.; Yadav, O. P.; Singh, P. P. *Colloids Surf., A* **1993**, 75, 21.

95. Hua, X. Y.; Rosen, M. J. *J. Colloid Interface Sci.* **1982**, 90, 212.

96. Wu, Y. F. *PhD Thesis*; The City University of New York, 2002.

97. Rosen, M. J.; Zhao, F. *J. Colloid Interface Sci.* **1983**, 95, 443.

98. Gu, B.; Rosen, M. J. *J. Colloid Interface Sci.* **1989**, 129, 537.

99. Rosen, M. J. *Langmuir* **1991**, 7, 885.

100. Liu, L.; Rosen, M. J. *J. Colloid Interface Sci.* **1996**, 179, 454.

101. Rosen, M. J.; Hua, X. Y. *J. Colloid Interface Sci.* **1982**, 86, 164.

102. Rubingh, D. N. In *Solution Chemistry of Surfactants* Vol. 1; Mittal, K. L. Ed.; Plenum: New York, 1979; pp. 337-354.

103. Góralczyk, D. *J. Colloid Interface Sci.* **1996**, 184, 139.

104. Rosen, M. J.; Zhu, Z. H. *J. Am. Oil Chem. Soc.* **1988**, 65, 663.

105. Hua, X. Y.; Rosen, M. J. *J. Colloid Interface Sci.* **1988**, 125, 730.

106. Kwan, C., Rosen, M. J. *J. Phys. Chem.* **1980**, 84, 547.

107. Swern, D.; Billen, G. N.; Scanlan, J. T. *J. Am. Chem. Soc.* **1946**, 68, 1504.

108. Rosen, M. J. *J. Colloid Interface Sci.* **1981**, 79, 587; **1982**, 86, 587.

109. Reid, V. W., Longman, G. F., and Heinerth, E. *Tenside* **1967**, 4, 292.

110. Skoog, D. A.; Leary, J. *Principles of Instrumental Analysis*, 4th ed.; Harcourt Brace College Publishing; New York, 1992; p.127.

111. Rosen, M. J.; Zhu, B. Y. *J. Colloid Interface Sci.* **1984**, 99, 427.

112. Rosen, M. J.; Friedman, D.; Gross, M. J. *J. Phys. Chem.* **1964**, 68, 3219.

113. Rosen, M. J.; Sulthana, Shireen B. *J. Colloid Interface Sci.* **2001**, 239, 528.

114. Rosen, M. J.; Gao, T.; Nakatsuji, Y.; Masuyama, A. *Colloids Surf.*, A **1994**, 88, 1.

115. Zhao, G-X; Chan, Y. Z.; Ou, J. G.; Tien, B. X. and Huang, Z. M. *Hua Hsueh Hsueh Pao* (*Acta Chimica Sinica*) **1980**, 38, 409.

116. Lucassen-Reynders, E. H. *J. Colloid Interface Sci.* **1981**, 81, 150.

117. Tajima, K.; Nakamura, A. *Bull. Chem. Soc. Japan* **1979**, 52, 2060.

118. Rosen, M. J.; Zhu, Z. H. *J. Colloid Interface Sci.* **1989**, 133, 473.

119. Nagarajan, R. In *New Horizons: Detergents for the New Millennium Conference Invited Papers*; American Oil Chemists Society and Consumer Specialty Products Association: Fort Myers, Florida, 2001.

120. Nagarajan, R.; Kalpakci, B. *Polym. Prepr. Am. Chem. Soc. Div. Polym.* **1982**, 23, 41.

121. Matsubara, H.; Muroi, S.; Kameda, M.; Ikeda, N.; Ohta, A.; Aratono, M. *Langmuir* **2001**, 17, 7752.

122. Rosen, M. J.; Zhou, Q. *Langmuir* **2001**, 17, 3532.

123. Wu, Y. F.; Rosen, M. J. *Langmuir* **2002**, 18, 2205.

124. Marangoni, C. G. M. *Annln Phys.* (Poggendrof), **1871**, 143, 337.

125. Rosen, M. J.; Wu, Y. F. *Langmuir* **2001**, 17, 7296.